3D Geomodeling for Europe
Project number: GeoE.171.005

Deliverable 3.8

Harmonized depth models and structural framework of the NL-GER-DK North Sea

Authors and affiliation:
Hauke Thöle
Fabian Jähne-Klingberg
[BGR]
Hans Doornenbal
Maryke den Dulk
[TNO]
Peter Britze
Finn Jakobsen
[GEUS]

E-mail of lead author:
Hauke.Thoele@bgr.de

Version: 29-10-2021

This report is part of a project that has received funding by the European Union's Horizon 2020 research and innovation programme under grant agreement number 731166.

Deliverable Data		
Deliverable number	D3.8	
Dissemination level	Public	
Deliverable name	Harmonized depth models and Structural Framework	
Work package	WP3, North Sea area NL-DE-DK	
Lead WP/Deliverable beneficiary	BGR + TNO & GEUS (co-Lead)	
Deliverable status		
Submitted (Author(s))	29/10/2021	Hauke Thöle
Verified (WP leader)	30/10/2021	Hans Doornenbal
Approved (Project leader)	30/10/2021	Stefan Knopf (BGR)

GENERAL INTRODUCTION

The GeoERA research project ”3D Geomodeling for Europe (3DGEO-EU)”, which started in July 2018, aimed to show on the example of cross-border pilot areas, how harmonization of geological data and subsurface models can be established across political borders. One of the pilot areas selected as a showcase for harmonization and worked on in work package 3 (WP3) of the project spanned thereby the offshore cross-border North Sea area between the Netherlands, Germany and Denmark. In this region, the partners the Netherlands Organization for Applied Scientific Research (TNO, NL), the Geological Survey of Denmark and Greenland (GEUS, DK) and the Federal Institute for Geosciences and Natural Resources (BGR, GER) pursued the objective to integrate existing national (and regional) geomodels into a harmonized, consistent cross-border geomodel of the North Sea area.

The following report presents the final harmonization results of the WP3 study, including a harmonized horizon depth model of the Entenschnabel region (Chapter 3.1) and a cross-border fault model of a segment of the Coffee Soil Fault (eastern boundary of the Central Graben; Chapter 3.2). The work conducted to create the fault model is described. This includes also the steps involved in building seismic velocity volumes for time-to-depth conversion (Chapter 2). Furthermore, a harmonized, sub-regional scale Structural Framework for the area of the Dutch, German and Danish North Sea and adjacent areas is presented (Chapter 4).

TABLE OF CONTENTS

1 INTRODUCTION

The GeoERA research project ”3D Geomodeling for Europe (3DGEO-EU)”, which started in July 2018, aimed to show on the example of cross-border pilot areas (work packages 1-3), how harmonization of geological data and subsurface models can be established across political borders. The pilot area of work package 3 (WP3) spans thereby the offshore cross-border North Sea area between the Netherlands, Germany and Denmark (Figure 1). In this region, the partners, the Netherlands Organization for Applied Scientific Research (TNO, NL), the Geological Survey of Denmark and Greenland (GEUS, DK) and the Federal Institute for Geosciences and Natural Resources (BGR, GER) intended to integrate existing national (and regional) geomodels into a harmonized, consistent cross-border geomodel of the North Sea area.

The following report describes the final harmonization results and digital products of the WP3 study. Besides the presentation of a harmonized horizon depth model for the Entenschnabel region and a discussion on unresolved horizon modeling issues in this region (Chapter 3.1), D3.8 mainly focussed on various sub-aspects related to the cross-border harmonization of structural models/elements of different scales. For example, a segment of the Coffee Soil Fault (eastern boundary of the Central Graben) was modeled in detail to demonstrate how a main fault can be harmonized across borders and how uncertainties in structural interpretations can be represented in such fault models (Chapter 3.2). The implemention of a harmonized cross-border velocity model usable for time-to-depth conversion played thereby a critical role for developing a reliable cross-border fault model, as it allowed to interpret and analyze the fault segment based on depth converted seismic sections. This is crucial because angular relationships between horizons and faults or basic geometric properties, which act as indications for fault kinematics, are generally skewed in the time domain. Depth conversion allows to circumvent the structurally ambiguity inherent in time and thus to create a more realistic fault model than is possible in the time domain. The challenges associated with the depth conversion and the steps towards a velocity model which can be used to consistently transfer data to the depth domain without distortions are described in detail in Chapter 2.

Even though the offshore border region of the Dutch, German and Danish North Sea is probably one of the best studied in Europe, little has been done to categorize and harmonize the structural inventory of the subsurface across borders. One effort of WP3 was therefore to establish a harmonized, sub-regional scale Structural Framework (SF) which is presented in Chapter 4. The challenges and uncertainties associated with the creation are also discussed here using illustrative examples. Due to the enormous challenges and uncertainties associated with the harmonization of subsurface structures, however, the presented work can only be regarded as a first entry into the very work-intensive harmonization and modeling of transboundary structures. Since it was not possible to create a consistent SF for the entire region within the framework of the project, special attention was paid to introduce interested readers to the problem and providing them with the tools to work through this topic themselves. This goal is achieved by providing various digital products (Chapter 5) and comprehensive supplemental information on the region's SF in the Appendix (Chapter 8) to this report as well as in an additional report (Thöle & Jähne-Klingberg, 2021).

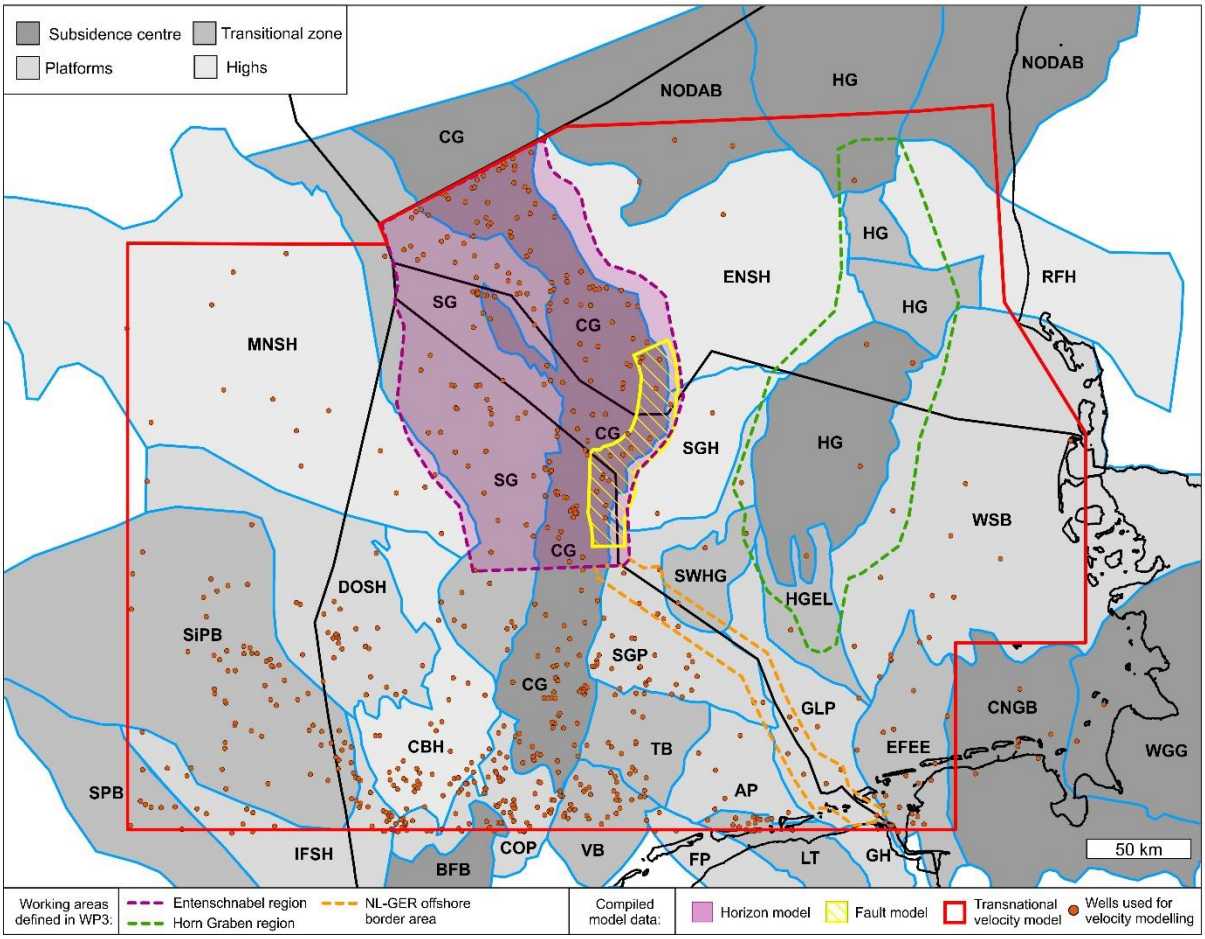

Figure 1: Structural Framework compiled within WP3 for the area of the Bristih, Dutch, German and Danish North Sea sectors. Furthermore, the extent of the transnational velocity model created in WP3 is indicated by the red polygon together with the wells used for the model construction. Also marked is the area of the Entenschnabel horizon depth model (Chapter 3.1) as well as those of the Coffee Soil Fault model presented in Chapter 3.2. Working areas initially defined in the North Sea for 3DGEO-EU WP3 are further marked by dotted lines (yellow= NL-GER offshore border area / purple = Entenschnabel region / green = Horn Graben region).

Abbreviations of main structural elements: SG = Step Graben / CG = Central Graben / ENSH = East North Sea High / HG = Horn Graben / RFH = Ringkøbing-Fyn High / MNSH = Mid North Sea High / SGH = Schillgrund High / SGP = Schillgrund Platform / SWHG = southwestern branch Horn Graben / HGEL = southern branch Horn Graben – Ems Lineament / WSB : West Schleswig Block / GLP = G- and L-Platform / EFEE = East Frisia – Ems Estuary Region / CNGB = NW part of the Central North German Basin / WGG – Western branch Glückstadt Graben / DOSH = Dogger Shelf / CBH = Cleaver Bank High / COP = Central offshore Platform / VB = Vlieland Basin / TB = Terschelling Basin / BFB = Broad Fourteens Basin / FP = Friesland Platform / AP = Ameland Platform / LT = Lauwerszee Trough / GH = Groningen High / SIPB = Silver Pit Basin / SPB = Sole Pit Basin / IFSH = Indefatigable Shelf / NODAB = Norwegian-Danish Basin.

2 VELOCITY MODELING AND TIME-TO-DEPTH CONVERSION

2.1 General introduction

Within WP3, a transnational velocity model for time-to-depth conversion was developed covering main parts of the UK, Danish, German and northern part of the Dutch North Sea (Figure 1; Doornenbal et al., 2021). Establishing this velocity model was an important step in the harmonization process in several respects. Prior to the project, velocity models for time-depth conversion were largely built separately by each partner (Arfai et al., 2014; Groß, 1986; Japsen, 1993; van Dalfsen et al., 2006) and these models differ partly considerable, especially in the deeper graben systems where the rock intervals are not constrained by drilling data. The enormous impact of differences in the former national velocity models on the time-depth conversion is highlighted in Figure 2 by the cross-border comparison of horizon models between offshore Germany and the Netherlands and impressively shows the need for harmonization. Differences in main seismic horizons observed here in the time domain (Figure 2a) partly increase or decrease after time-depth conversion (Figure 2b), depending on the differences in the national velocity models used for this conversion.

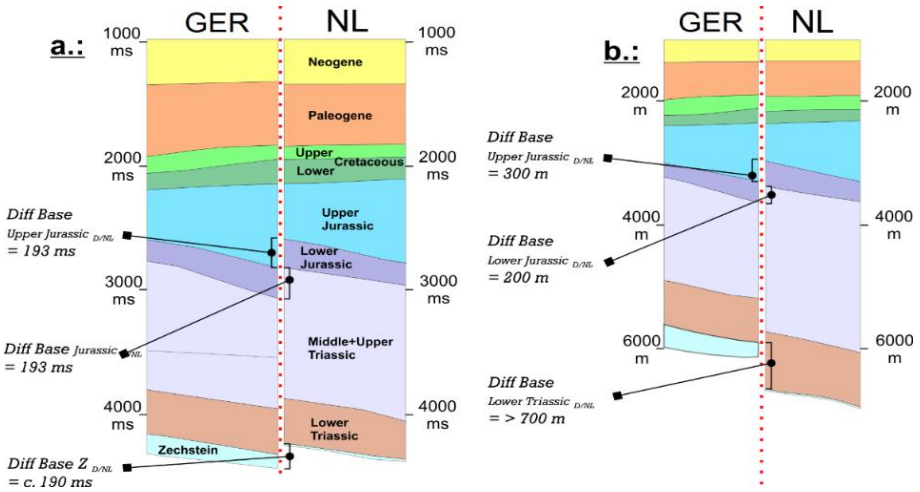

Figure 2: Cross-border comparison of horizon models between offshore GER and NL in the southeastern Entenschnabel in time (a) and depth (b) domain. (a) Differences in TWT are mainly the result of differences in seismic stratigraphic concepts or structural interpretation. Concerning the GER/NL offshore border region, major differences are visible for the Mesozoic to Paleozoic. (b) Differences observed in TWT interpretation may be increased or decreased by time-depth conversion, depending on differences in the velocity model used for conversion. Note increase in vertical difference in the Lower Triassic after depth conversion.

With the transnational velocity model established in WP3, it is now feasible to convert the seismic horizons harmonized during the project in the time domain (Thöle et al., 2021) into depth without distortions along the national borders. Beside this, the velocity model played further a critical role for developing a reliable cross-border fault model of a segment of the Central Graben main fault. This fault, often referred to as Coffee Soil Fault, was chosen in WP3 as an example for the harmonization of a main fault, and the results of this cross-border harmonization study are presented in detail in Chapter 3.2. The velocity model established was important in this case as it allows to interpret and analyze the fault segment based on depth converted seismic sections. In general, analyzing faults in depth is more reliable because seismic sections displayed in time often present structural geometries that are different from the true geometry in the subsurface due to distortions caused by lateral and vertical changes

in seismic velocity. The vast impact of varying velocities on subsurface geometries is exemplified in Figure 3, where a high-velocity body is surrounded by lower-velocity rocks. The horizontal interface at 4 km depth (green line; Figure 3a), for example, looks partly like an anticlinal structure on the time section (Figure 3b) because the sound waves travel more slowly to the 4 km interface on the right and left hand of the high velocity body than in the region of this body. In order to circumvent such structural ambiguity inherent in time and to achieve a more reliable fault model, seismic sections were converted prior to the fault interpretation from time to depth using the transnational velocity model established in WP3. A depth conversion of seismic sections, however, was not feasible with the original layer-cake velocity model compiled in Petrel (Doornebal et al., 2021) and was therefore converted for this purpose into a seismic velocity volume using Paradigm SeisEarth. The way to build such a seismic velocity volume for time-to-depth conversion and how and why the original velocity model was locally modified around salt structures will be described in Chapter 2.3. Prior to this, the transnational velocity model is briefly described in Chapter 2.2. Its limitations for the time-to-depth conversion is discussed in Chapter 2.3.1. For more details on the creation of the transnational velocity model the reader is referred to Deliverable 3.7 (Doornenbal et al., 2021).

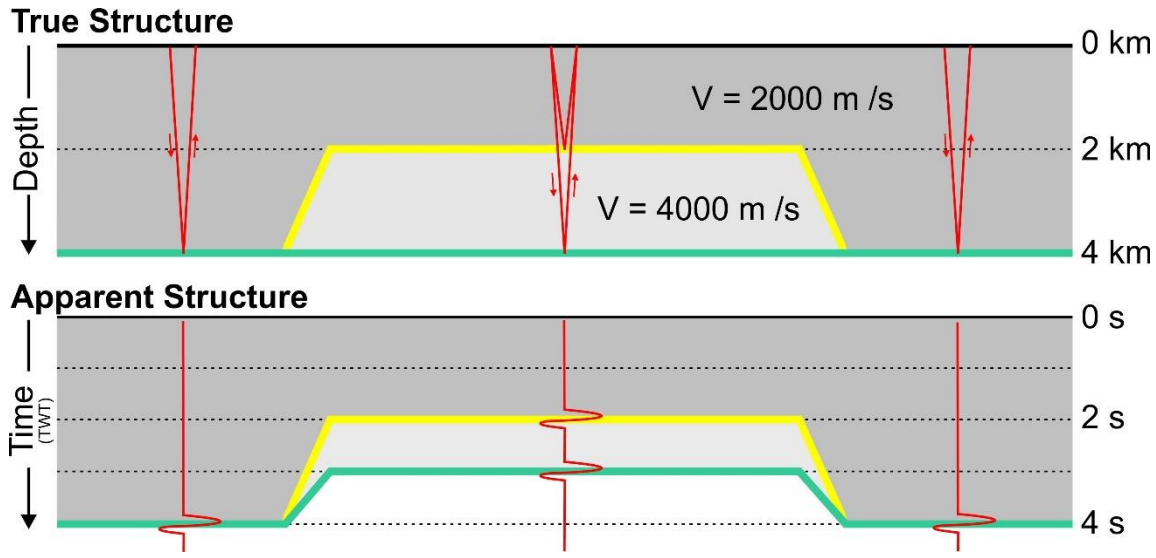

Figure 3: (a) Geologic cross-section in depth with laterally and vertical varying velocities. (b) Time section showing the distortion produced by the laterally varying velocity.

2.2 Transnational velocity model – an overview

The transnational velocity model established in WP3 for main parts of the British, Danish, German and northern part of the Dutch North Sea combines a V_0-K Layer Cake velocity model for Cenozoic and Mesozoic units with a V_{int}-DeltaT velocity model used for the Zechstein interval. In total, seven main stratigraphic layers were selected to build the velocity model, whereby the Cenozoic succession, which is divided by the Near Mid Miocene Unconformity into two parts, was modeled as one unit (Table 1). As input data for the model, velocity information from 724 wells were gathered (Figure 1), either (calibrated) sonic logs or check-shot/VSP data.

Table 1: Key stratigraphic horizons selected for harmonization in WP3 and corresponding lithostratigraphic interval codes as well as lithostratigraphic intervals and methods used for the velocity modeling.

No	Harmonized stratigraphic horizon	Code	Modeled intervals	Model type
1	Near Mid Miocene Unconformity	NU	N	V_0-K model
2	Near base Cenozoic	NLM		
3	Base Upper Cretaceous	CK	CK	V_0-K model
4	Near base Lower Cretaceous	KN	KN	V_0-K model
5	Near base Upper Jurassic	S	S	V_0-K model
6	Near base Lower Jurassic	AT	AT	V_0-K model
7	Near base Lower Triassic	TR	TR	V_0-K model
8	Base Zechstein	ZE	ZE	V_{int}-DeltaT model

A V_0-K layer cake model was used for all layers, except for the Zechstein, as it is generally assumed for these units that their acoustic velocity increases with depth under the influence of burial and compaction. The velocity of a compacting layer (at a given depth and location) can be described thereby by the following equation:

$$V(x,y,z) = V_0(x,y) + K \cdot z$$

$V(x,y,z)$ = velocity of the unit at depth z
$V_0(x,y)$ = velocity at ordnance level
K = factor determining the linear increase of velocity with depth

The model parameters V_0 and K were determined for the transnational velocity model per stratigraphic layer according to the interval velocities (V_{int}) versus mid depth (Z_{mid}) method (Robein, 2003), which was combined with a local V_0 parameter calibration at boreholes ("local V0_basefit"; see Doornenbal et al., 2021). An important aspect in determining the K-factor for a velocity model covering such a large area (Figure 1) was to evaluate whether a single K-value per lithostratigraphic unit can be regarded as valid for the whole study area or whether regionalized K-values are more suitable for the velocity model due to varying burial and compaction histories of sediments in different parts of the study area. After analyzing V_{int}–Z_{mid} relations – per modeled stratigraphic layer - for the study area as a whole or splitting it in structural elements, structural element types or combination of structural elements finally the following K-values were chosen to build the transnational velocity model:

- regionalized K values (inside / outside CG+SG) for N and CK intervals and
- global K values (whole study area) for KN, S, AT and TR intervals

The results of the V_{int} – Z_{mid} analysis for the whole study area and the regionalized results for the areas "Outside CG+SG* and "Inside CG+CG" are summarized in Table 2, and the K-values finally used for the velocity model are marked there in red. Regarding the reasons for choosing a specific K-value, the reader is referred to Deliverable 3.7 (Doornenbal et al., 2021).

Table 2: Results of V_{int}-Z_{mid} analysis for the whole study area and regionalized results for the areas "Outside CG+SG and "Inside CG+CG". The global and regionalized K-values finally used for the velocity model are marked in red. Abbreviations: CG = Central Graben; SG = Step Graben (see Figure 1 for areal extent of the structural elements).*

	Whole study area				Outside CG+SG				Inside CG+SG			
Code	K	V_0	R^2	wells	K	V_0	R^2	wells	K	V_0	R^2	wells
NU	0.35	1792	0.55	163	0.40	1777	0.39	114	0.31	1814	0.28	49
NLM	0.15	1856	0.21	244	0.24	1767	0.26	159	0.03	2019	0.01	85
N	0.16	1852	0.51	368	**0.32**	1758	0.65	211	**0.02**	2003	0.05	157
CK	0.62	2582	0.65	539	**0.91**	2216	0.78	351	**0.64**	2365	0.72	188
KN	**0.37**	2342	0.32	481	0.59	1988	0.74	340	0.20	2539	0.09	141
S	**0.09**	2769	0.03	212	0.65	1661	0.68	55	0.07	2713	0.03	157
AT	**0.35**	2129	0.62	94	0.58	1771	0.93	18	0.26	2392	0.34	76
TR	**0.42**	2721	0.54	287	0.49	2584	0.67	257	0.31	2758	0.26	30

For the construction of regional V_0 distribution maps, the V_0 results based on the Local V_0_basefit calibration were used and gridded with a kriging algoritm (simple, exponential type, sill 1, range 80 km, nugget 0.001) and a 250 x 250 m grid increment. In order to prevent unrealistic velocities in areas with very thick Triassic succession such as the Central Graben, it was decided to integrate for this interval a cap velocity of 5000 m/s into the petrel workflow used for the velocity modeling. The cap velocity is supported by the results of the $V_{int} - Z_{mid}$ analysis (see Figure 12 in Deliverable 3.7) and from other basin areas (Schnabel et al., 2021). The areas affected by the cap velocity are highlighted in Figure 4 for the Entenschnabel region, showing that mainly the deepest parts of the Central Graben are affected.

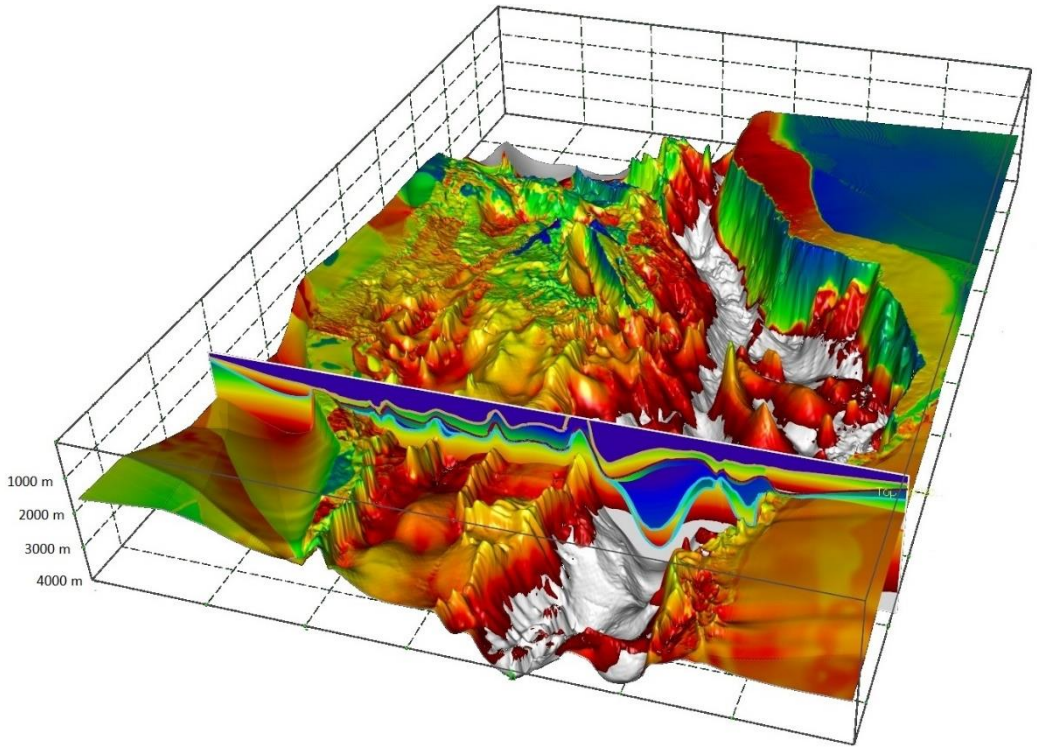

Figure 4: Base Triassic horizon of the Entenschnabel region attributed with interval velocities (V_{int}) derived from the constructed seismic velocity volume (Chapter 2.3) as well as a cross-section showing the interval velocities of the other modeled horizons. A Triassic cap velocity of 5000 m/s applies for the areas shown in white, affecting mainly the deepest parts of the Central Graben.

In contrast to the Cenozoic and Mesozoic layers, the Zechstein interval velocity is not a function of depth and compaction. The most dominant factor for the interval velocity is the lithological composition, with the proportion of halite mainly determining the interval velocity. In general, layers with limited thickness show a relative high abundance of high velocity carbonate layers, whereas in regions of high Zechstein thickness (e.g. diapirs), halite usually predominates. Therefore, the Zechstein velocities were modeled based on a simple interval velocity - thickness (or ΔT) relation (Figure 5) rather using the V_0-K approach.

- $V_{int}prov$ = 4500 m/s if ΔTZE ≥170 ms
- $V_{int}prov$ = 4950 + (450 · cos(ΔTZE + 10)) if ΔTZE <170 ms

To construct a V_{int}-grid usable for time-to-depth conversion of the Zechstein interval, a provisional grid was first generated based on the travel times from seismic interpretation and then corrected for differences at well location. For more detailed information on the workflow for creating the Zechstein V_{int}-grid, please see Deliverable 3.7 (Doornenbal et al., 2021).

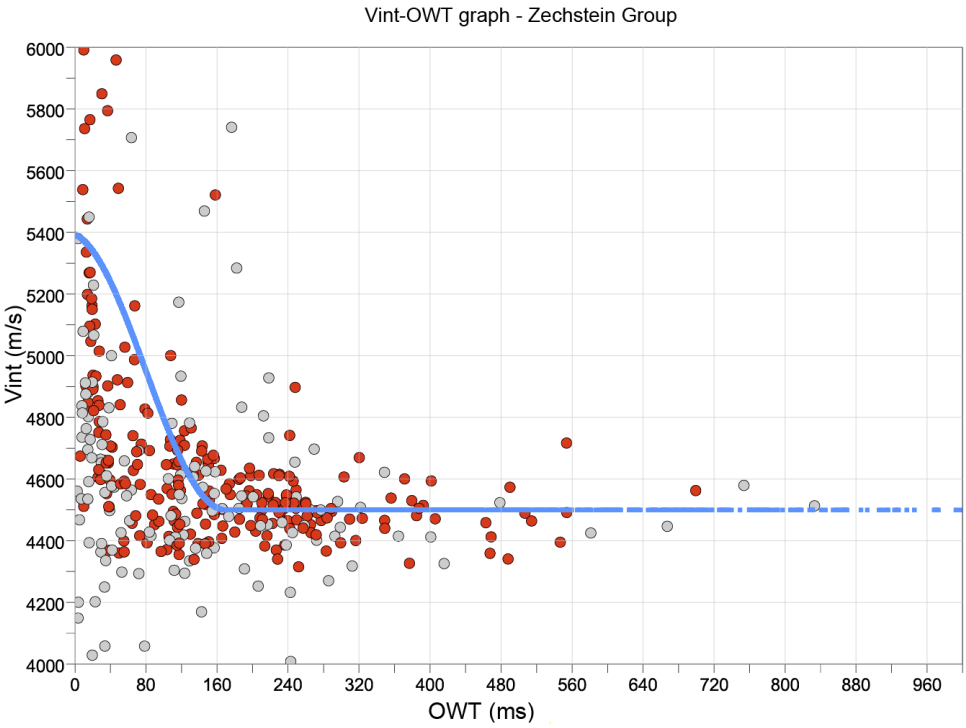

Figure 5: Interval velocity (V_{int}) in relation to thickness (ΔT-ZE in ms OWT=One-Way-Time) for the Zechstein unit. Red dots show V_{int} -values of wells selected for the creation of the Zechstein velocity grid.

2.3 Time-to-depth conversion using seismic velocity volumes

2.3.1 Layer-cake velocity model vs. seismic velocity volume

A layer-cake velocity model as it was initially constructed in WP3 with Petrel allows only a time-to-depth conversion of those horizons for which initial velocities and gradients have been defined. Other objects (e.g. horizons, faults and seismics) without own velocity information cannot be converted to depth with this type of model, as no velocity values or depth values are determined for the areas "between" the modeled horizons. But to allow this, e.g. to convert seismic sections for fault studies from time to depth, the transnational velocity model was locally converted for the working area, referred to as the Entenschnabel region (Figure 1), into a seismic velocity volume. For this purposes, a "horizon-based" Global Velocity Model (GVM) was constructed in a first step with the Paradigm SeisEarth^{TM} software. Similar to the layer-cake velocity model, a "horizon-based" GVM is defined by horizon surfaces (time or depth domain) and associated velocity information (here V_0 and K-value). However, unlike the layer-cake model, the conversion between the time and depth domains is not based solely on the horizons of the input model. Instead, in the "horizon-based" GVM, a temporal 3D volume model is generated in the course of the time-to-depth conversion. The volumes between the reference horizons are filled by volume cells and seismic propagation velocities are computed for each cell based on the input parameters V_0 and K. Simplified, this can be seen as a subdivision of the interval into a sequence of numerous smaller intervals (volume cells), for each of which individual velocities are calculated. An essential advantage of this method is the use of a volume model as a basis for the time-depth conversion. By using a volume model, where each cell contains velocity information, it is possible, in contrast to the layer-cake model, to convert also objects for which no own velocity information are defined.

Based on the temporal 3D volume of the GVM, a seismic velocity volume in the standard format for seismic data (segy) was generated in the next step. The velocity information of the GVM were transferred thereby into this volume as parameters. For each volume cell, a velocity value was calculated in form of an interval velocity. To keep the memory requirement manageable, a uniform cell size of 250 ms x 250 ms x 4 ms was chosen for the computed seismic volume. By using a seismic velocity volume, as with the "horizon-based" GVM, any data (horizons, interpretation data, seismic profiles) can be transferred from time to depth and vice versa. Due to its data format, however, the seismic velocity volume has the advantage over the temporal volume of the GVM in that it allows interoperability with other software products (e.g. Schlumberger Petrel, SKUA-GOCAD, Schlumberger Geoframe). In order to use the seismic velocity volume in SKUA-GOCAD for time-to-depth conversion, the interval velocities were finally converted to average velocities (Figure 6a).

For the pre-Zechstein interval, for which no velocity data were gathered in WP3, an initial velocity of 3200 m/s and a gradient (K-value) of 0.2 was chosen according to former studies in the region (Groß, 1986). This was done in order to convert also objects below the Base Zechstein horizon which represents the lower limit of the transnational velocity model.

2.3.2 Time-to-depth conversion around salt structures

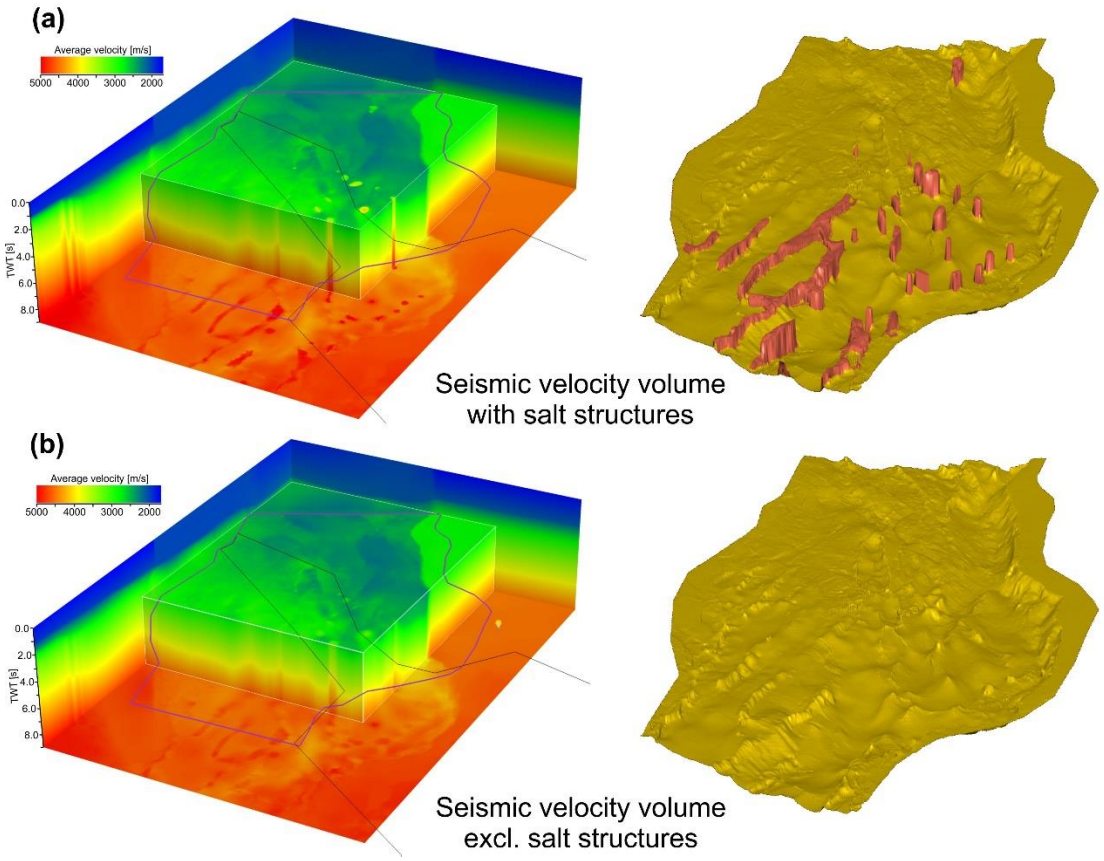

Figure 6: Two seismic velocity volumes with average velocities were generated for the Entenschnabel region. (a) One seismic velocity volume was computed with salt structures modeled as vertical shapes and (b) the other was modeled without salt structures down to the base of the Triassic.

Several large salt domes and walls, in part forming complex multi-z structures with overhang or mushroom shapes (Figure 7a), are present in the Entenschnabel region. In the Petrel workflow used to construct the transnational velocity model, these salt structures are modified to a vertical shape, generally using the maximum extent of the salt structures as a reference (Figure 7b). Due to the higher interval velocity of the Zechstein (~4500 m/s) compared to the surrounding rocks, a pull-down effect is observed in the areas of the salt dome overhangs when e.g. horizons are converted here to depth using the seismic velocity volume generated based on the transnational velocity model (Figure 7c).

To correct the pull-down effect and thus preserve the original interpretation trend, the closed grids used as input for the construction of the “horizon-based” GVM were modified around the salt structures. All salt structures initially modified to a vertical shape were discarded down to the base of the Triassic, and the resulting gaps in the horizon grids were manually adjusted and closed, generally following a smoothed trend to avoid jumps in the velocity field (Figure 8b). Based on these modified grids, a new seismic velocity volume was computed for the Entenschnabel region. Data converted from time to depth with this volume are generally less distorted in the vicinity of salt structures (Figure 8c) than is the case with the other volume (Figure 7c). Therefore, the velocity volume modeled without salt structures was used to convert the harmonized horizon of the Entenschnabel region (Chapter 3.1) as well as seismic sections for the fault study of the Coffee Soil fault (Chapter 3.2) from time to depth.

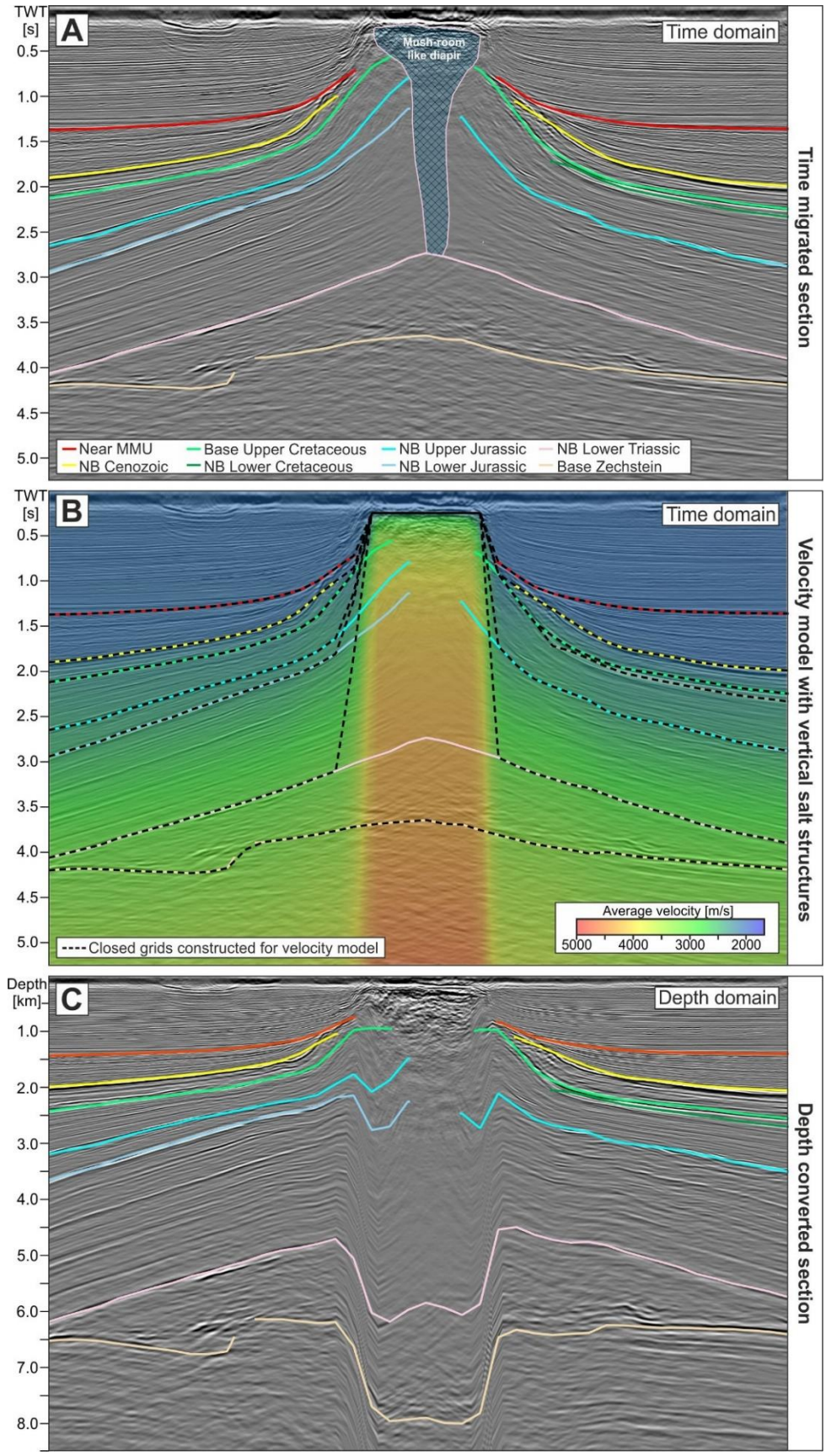

Figure 7: (A) Seismic time section with interpreted horizons around a mushroom-shaped salt diapir. (B) Same seismic time section shown together with average velocities of a seismic velocity volume generated in WP3. The salt diapir was modified here to a vertical shape for the velocity modeling (C) Depth converted seismic section and horizons showing a clear pull-down effect beneath the modeled salt diapir.

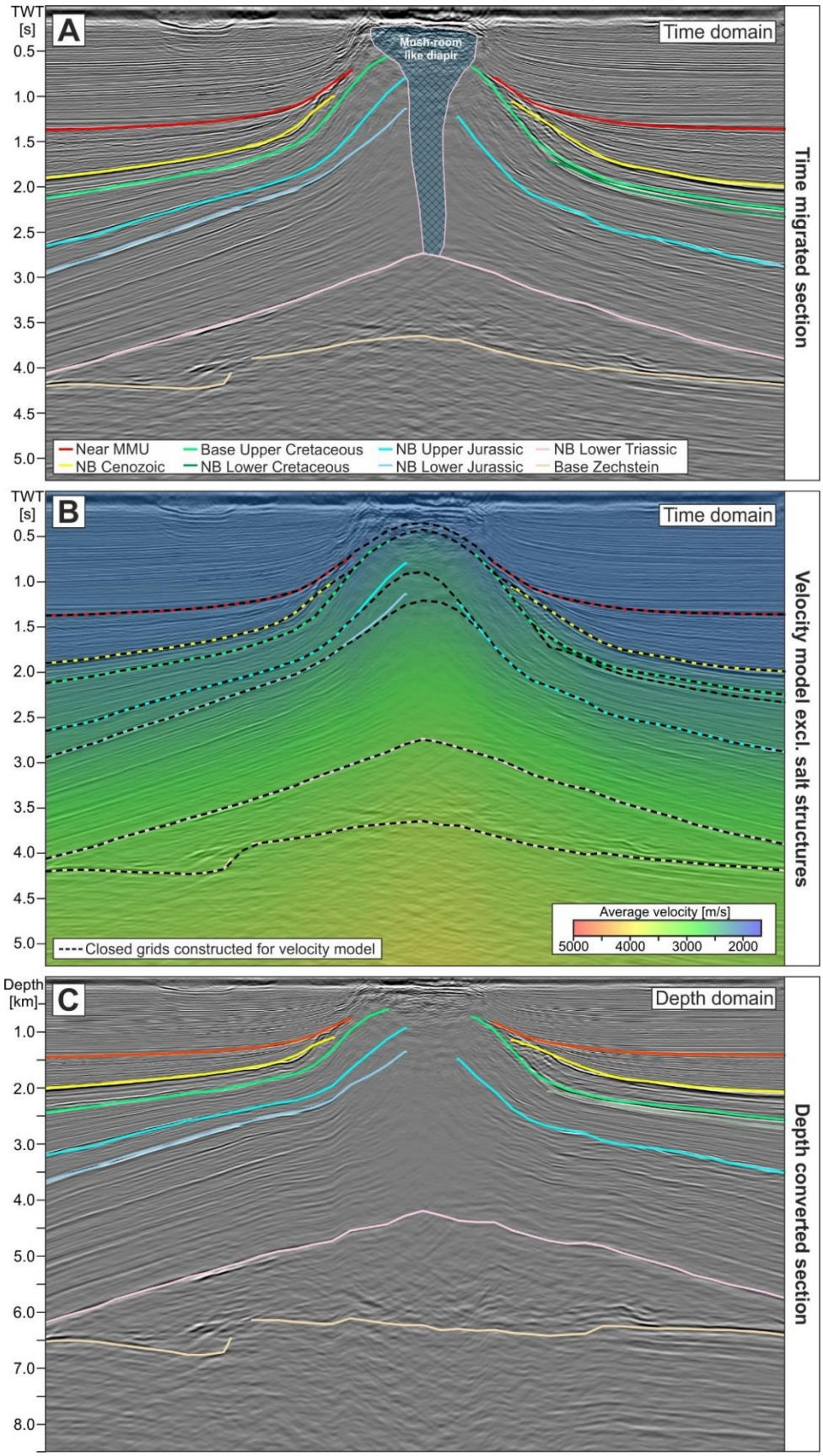

Figure 8: (A) Seismic time section with interpreted horizons around a mushroom-shaped salt diapir. (B) Same seismic time section shown together with average velocities of a seismic velocity volume generated in WP3. For velocity modeling, a layer cake horizon model without salt structures down to the base of the Triassic was used. (C) Depth converted seismic section and horizons showing no pull-down effect beneath the modeled salt diapir.

3 HARMONIZED DEPTH MODELS

Two harmonized depth models were finally created in WP3 for the offshore cross-border North Sea area between the Netherlands, Germany and Denmark and will be described in the following chapters:

- Horizon model of the Entenschnabel region (Chapter 3.1)
- Fault model of a segment of the Coffee Soil Fault (Chapter 3.2)

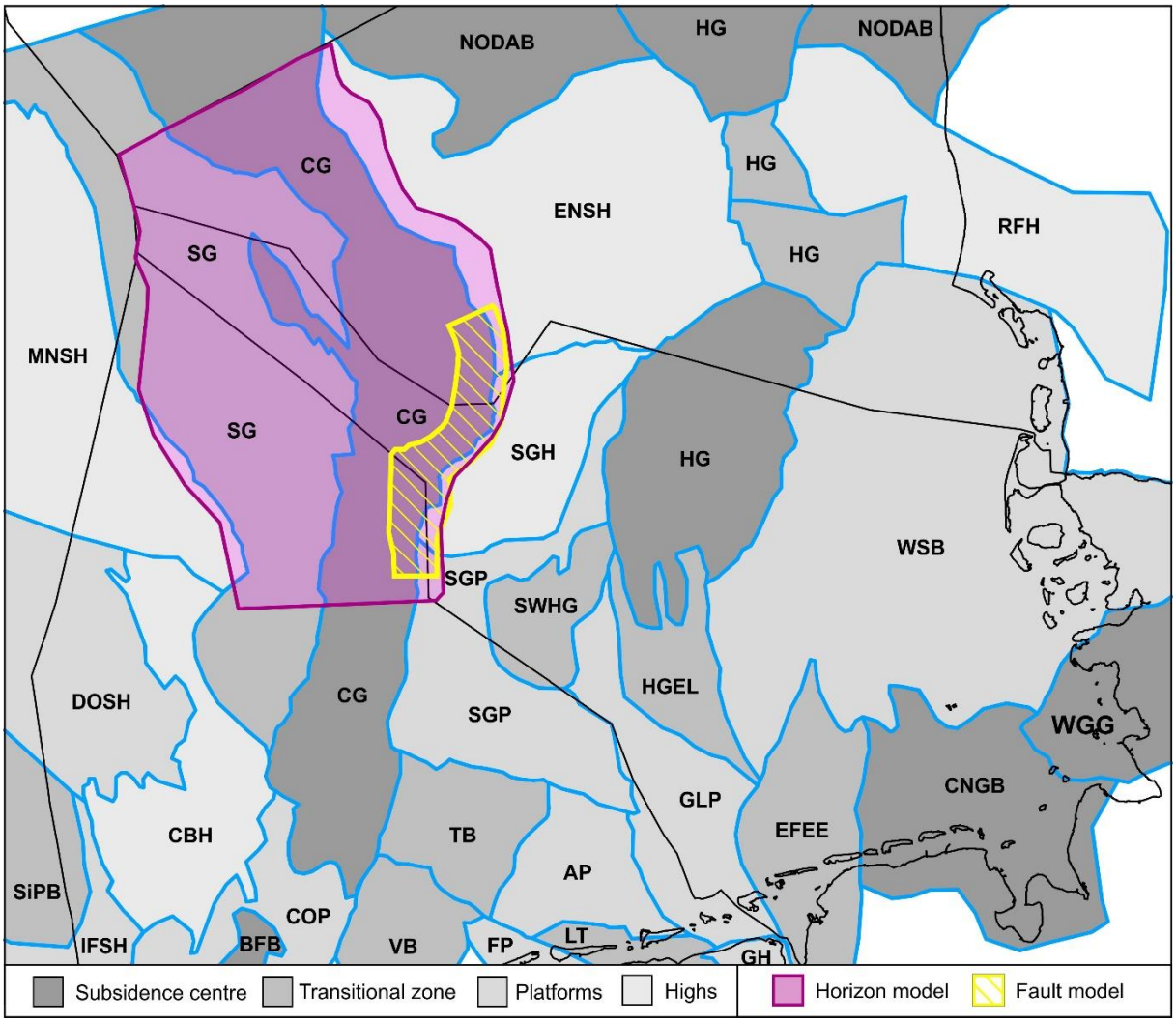

Figure 9: Map of main structural elements in the area of the Dutch, German and Danish North Sea sectors showing the location of the horizon model of the Entenschnabel region as well as the location of the fault model compiled for a segment of the Coffee Soil Fault (Central Graben main fault).

Main structural elements: SG = Step Graben / CG = Central Graben / ENSH = East North Sea High / HG = Horn Graben / RFH = Ringkøbing-Fyn High / MNSH = Mid North Sea High / SGH = Schillgrund High / SGP = Schillgrund Platform / SWHG = southwestern branch Horn Graben / HGEL = southern branch Horn Graben – Ems Lineament / WSB : West Schleswig Block / GLP = G- and L-Platform / EFEE = East Frisia – Ems Estuary Region / CNGB = NW part of the Central North German Basin / WGG – Western branch Glückstadt Graben / DOSH = Dogger Shelf / CBH = Cleaver Bank High / COP = Central offshore Platform / VB = Vlieland Basin / TB = Terschelling Basin / BFB = Broad Fourteens Basin / FP = Friesland Platform / AP = Ameland Platform / LT = Lauwerszee Trough / GH = Groningen High / SIPB = Silver Pit Basin / IFSH = Indefatigable Shelf / NODAB = Norwegian-Danish Basin.

3.1 Horizon model of the Entenschnabel region

3.1.1 Model area and selected stratigraphic horizons

The cross-border horizon model of the Entenschnabel region incorporates 8 key stratigraphic horizons from the base of the Zechstein to the Cenozoic (Table 3) and covers the northwestern part of the German North Sea sector and the adjacent areas in Denmark and the Netherlands (Figure 9). The region of the model is characterized by a complex rift-dominated structural pattern, with the Central Graben as the main structure, forming in general a half-graben system (Møller & Rasmussen, 2003). Prior to cross-border harmonization in this structurally complex region, there existed in part considerable discrepancies in the nationally-mapped horizons along the borders. These disparities were largely related to differences in the seismic picking concepts, misinterpretations of structural geometries, or the low significance of seismic data used for the horizon interpretation in certain areas. Most of the discrepancies observed in the time horizon grids initially provided for harmonization were addressed in WP3 and could be removed by seismic re-interpretation as well as to some extent by adjustments through grid mathematics. For details on the harmonization work conducted, the reader is referred to Deliverable 3.6 (Thöle et al., 2021). There, the challenges and problems encountered with the harmonization as well as the revisions made to harmonize the nationally-mapped seismic horizons across borders are described in detail.

All horizons were harmonized in the time domain (Thöle et al., 2021) and later converted to depth for the final horizon model using the compiled seismic velocity volume without salt structures (Chapter 2.3.2.). The depth and thickness maps of the harmonized horizons are displayed in Chapter 3.1.2 and unresolved harmonization issues are discussed in Chapter 3.1.3.

Table 3: Key stratigraphic horizons selected for harmonization in WP3 and corresponding lithostratigraphic interval codes.

No	Harmonized stratigraphic horizon	Code
1	Near Mid Miocene Unconformity	NU
2	Near base Cenozoic	NL-NM
3	Base Upper Cretaceous	CK
4	Near base Lower Cretaceous	KN
5	Near base Upper Jurassic	S
6	Near base Lower Jurassic	AT
7	Near base Lower Triassic	TR
8	Base Zechstein	ZE

3.1.2 Harmonized horizons

3.1.2.1 Near Mid Miocene Unconformity

Depth

2D map view

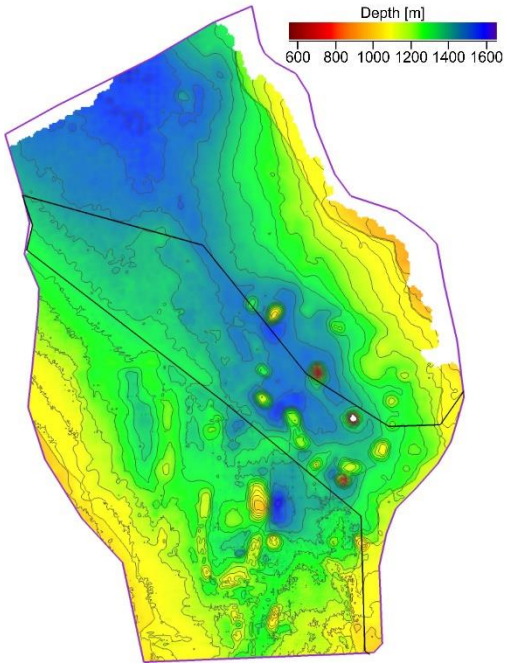

3D view from SE

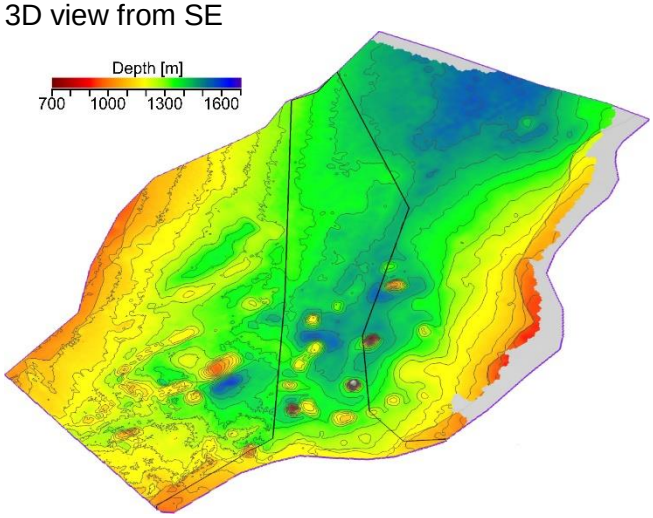

Min	566 m	Max	1604 m
25th perc.	1204 m	Median	1319 m
75th perc.	1416 m	90th perc.	1471 m

Thickness

2D map view

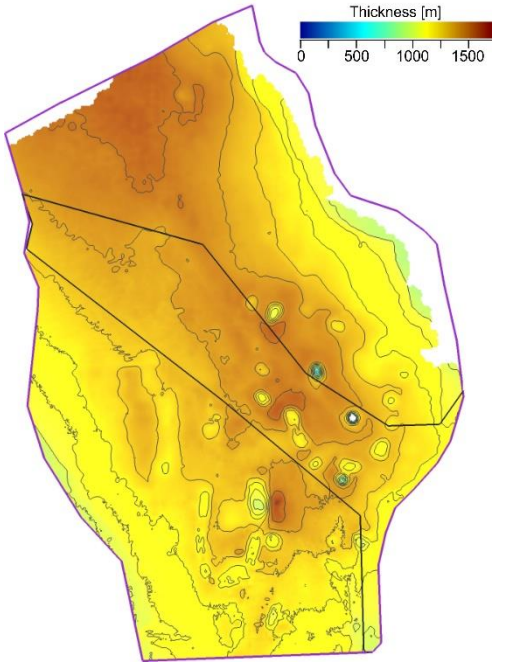

3D view from SE

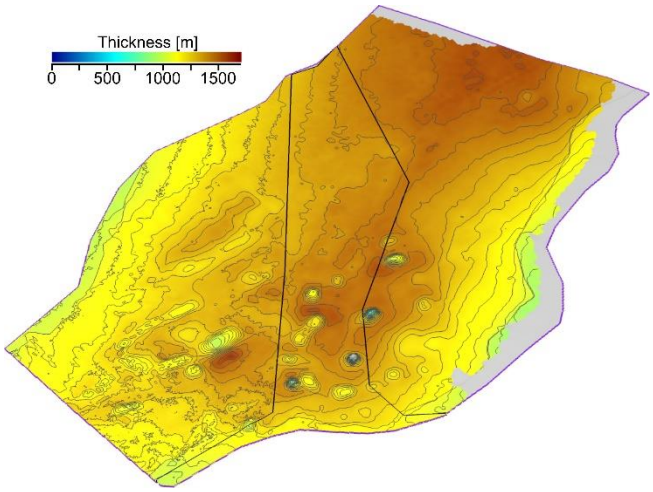

Min	566 m	Max	1604 m
25th perc.	1204 m	Median	1319 m
75th perc.	1416 m	90th perc.	1471 m

Figure 10: Depth map of the harmonized Near Mid Miocene Unconformity and thickness of the overlying Upper Cenozoic succession. Details on the revisions made to harmonize the horizon are described in detail in Deliverable 3.6 (Thöle et al., 2021).

3.1.2.2 Near base Cenozoic

Depth

2D map view

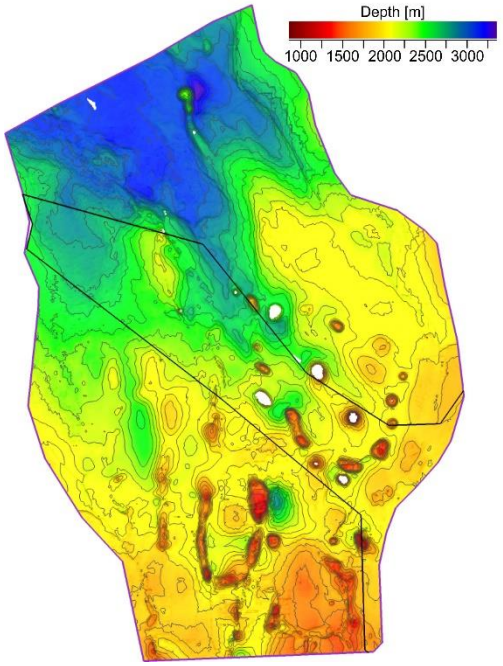

3D view from SE

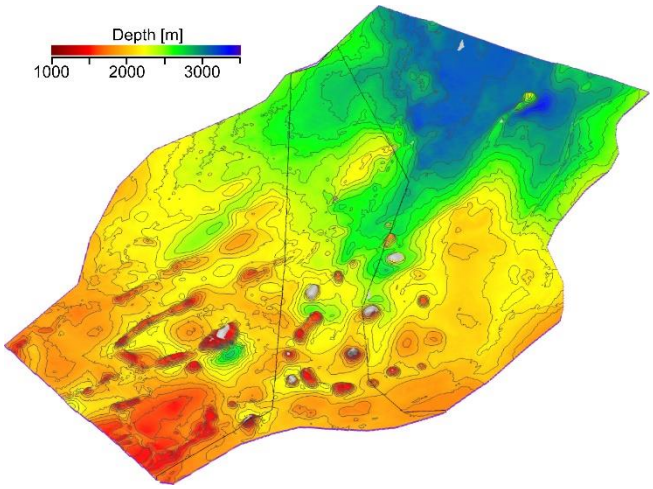

Min	850 m	Max	3331 m
25th perc.	1979 m	Median	2199 m
75th perc.	2626 m	90th perc.	2951 m

Thickness

2D map view

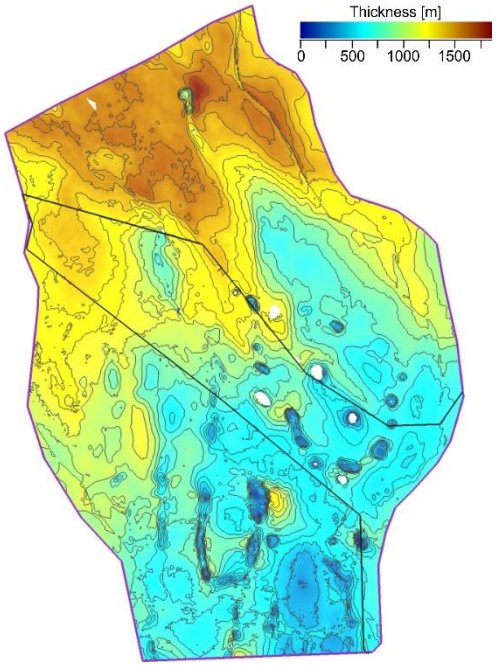

3D view from SE

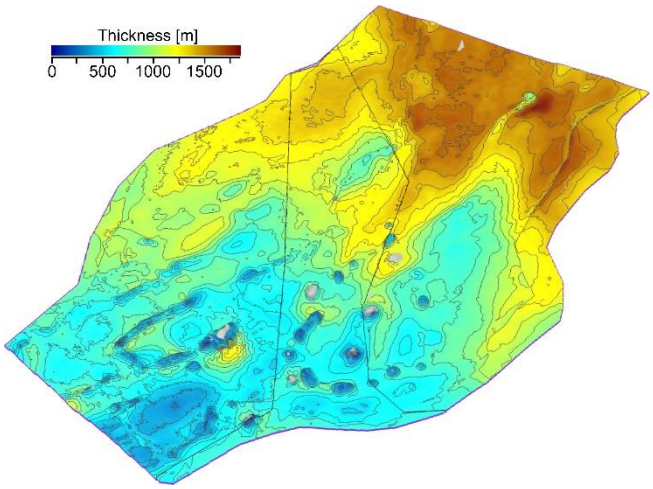

Min	0 m	Max	1819 m
25th perc.	719 m	Median	965 m
75th perc.	1290 m	90th perc.	1530 m

Figure 11: Depth map of the harmonized Near base Cenozoic and thickness of the overlying Lower Cenozoic succession. Details on the revisions made to harmonize the horizon are described in detail in Deliverable 3.6 (Thöle et al., 2021).

3.1.2.3 Base Upper Cretaceous

Depth

2D map view

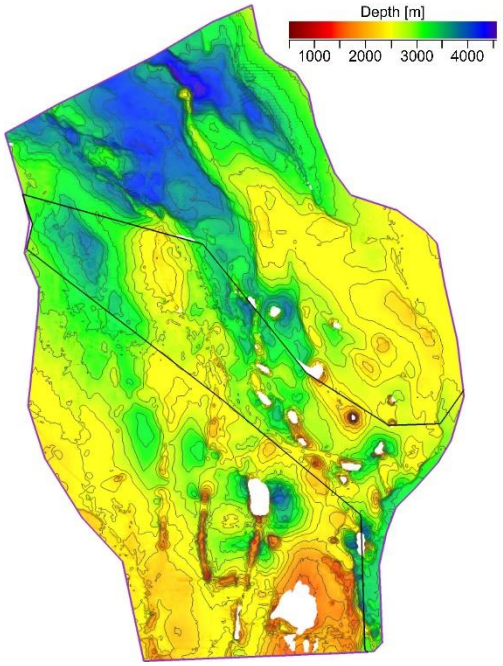

3D view from SE

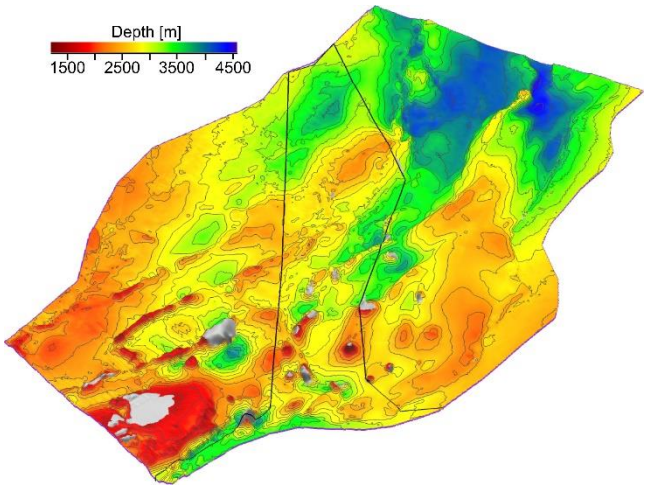

Min	533 m	Max	4542 m
25th perc.	2465 m	Median	2790 m
75th perc.	3257 m	90th perc.	3691 m

Thickness

2D map view

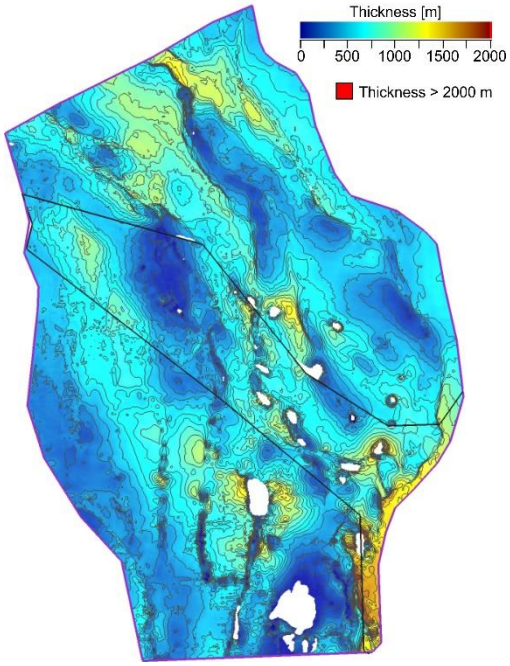

3D view from SE

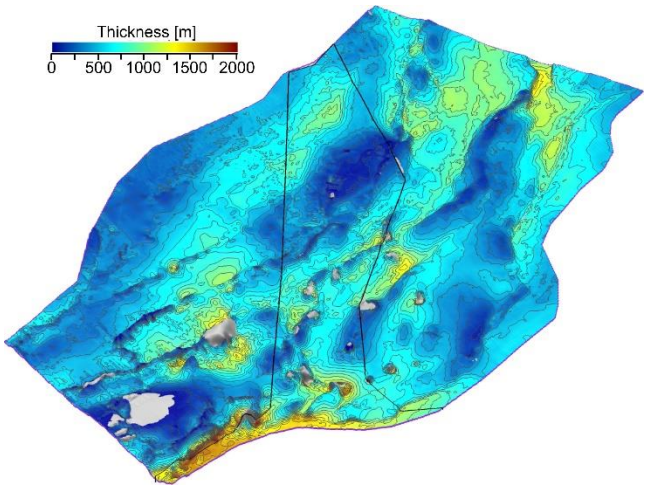

Min	0 m	Max	2489 m
25th perc.	362 m	Median	533 m
75th perc.	739 m	90th perc.	932 m

Figure 12: Depth map of the harmonized Base Upper Cretaceous and thickness of the Upper Cretaceous. Details on the revisions made to harmonize the horizon are described in detail in Deliverable 3.6 (Thöle et al., 2021).

3.1.2.4 Near base Lower Cretaceous

Depth

2D map view

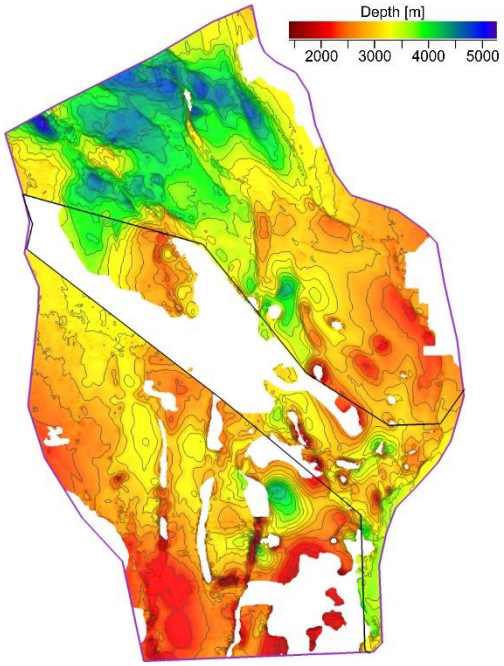

3D view from SE

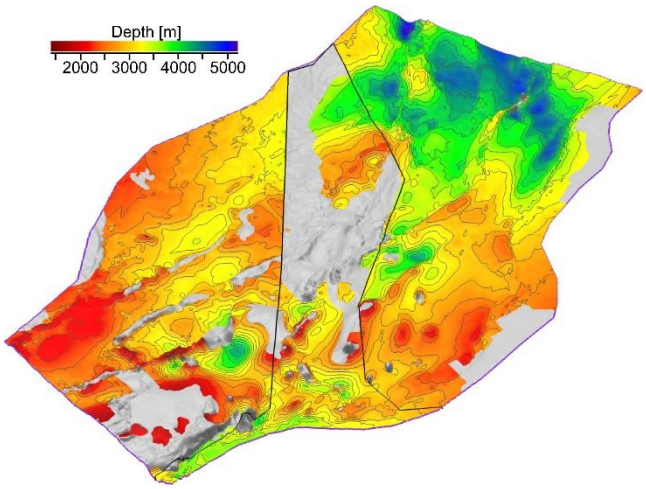

Min	1407 m	Max	5221 m
25th perc.	2638 m	Median	2983 m
75th perc.	3497 m	90th perc.	4030 m

Thickness

2D map view

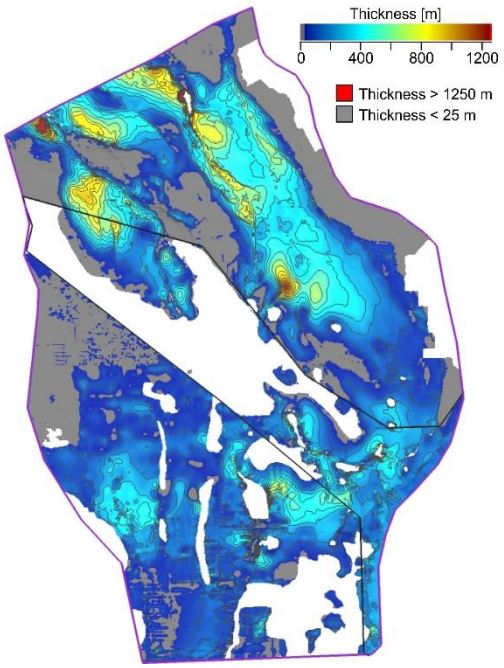

3D view from SE

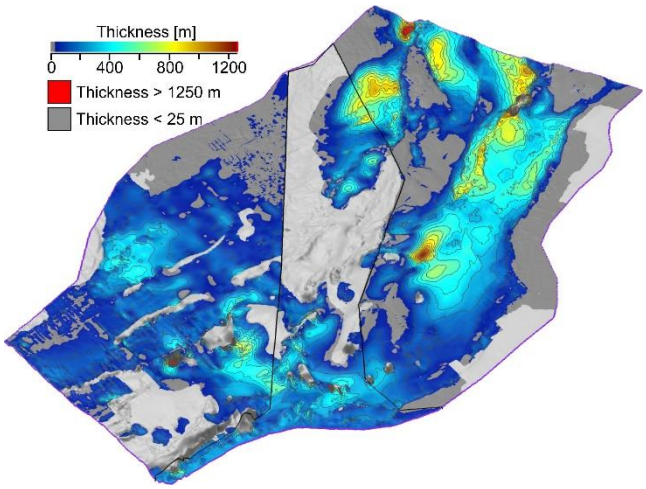

Min	0 m	Max	2309 m
25th perc.	35 m	Median	110 m
75th perc.	259 m	90th perc.	454 m

Figure 13: Depth map of the harmonized Near base Lower Cretaceous and thickness of the Lower Cretaceous. Details on the revisions made to harmonize the horizon are described in detail in Deliverable 3.6 (Thöle et al., 2021). Note the differences in the distributional pattern of the Lower Cretaceous which still exists in the harmonized grid. These discrepancies can be primarily attributed to different seismic picking concepts applied by the Geological surveys in charge. Since no national approach can be preferred, no harmonization has been made at this point (see Chapter 3.1.3). Considering only thicknesses of more than 25 m, however, the distributional pattern of the Lower Cretaceous is generally in good agreement along the national borders.

3.1.2.5 Near base Upper Jurassic

Depth

2D map view

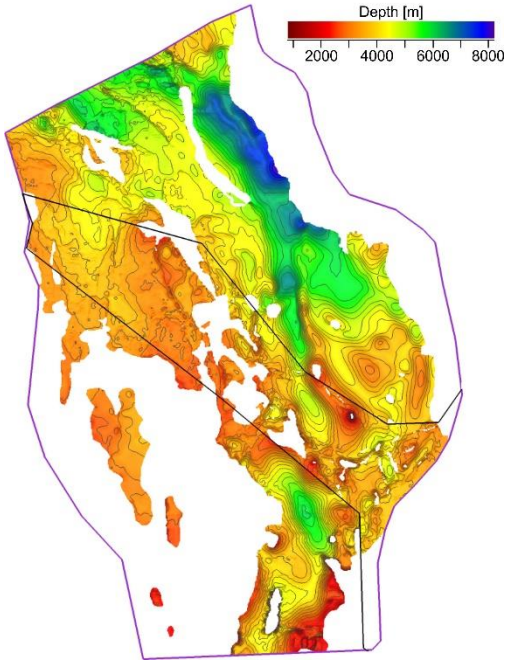

3D view from SE

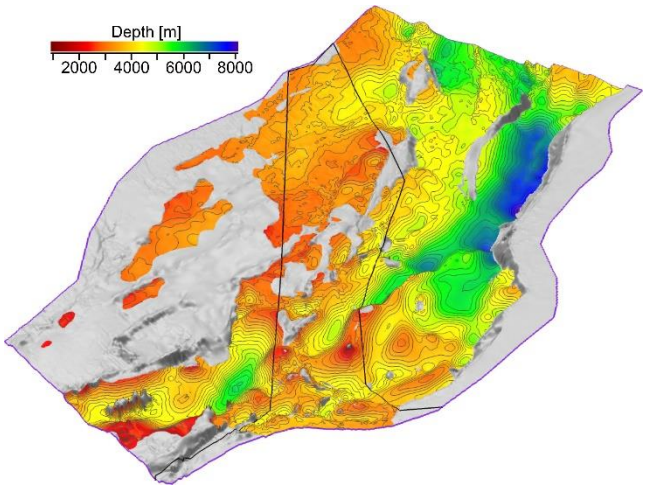

Min	871 m	Max	8188 m
25th perc.	3277 m	Median	3900 m
75th perc.	4743 m	90th perc.	5747 m

Thickness

2D map view

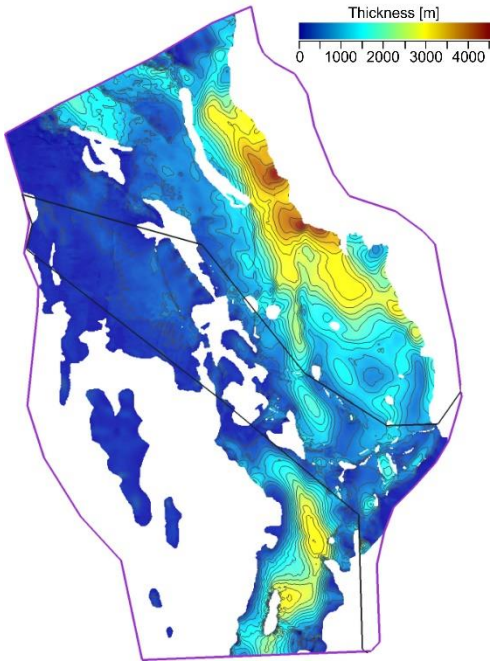

3D view from SE

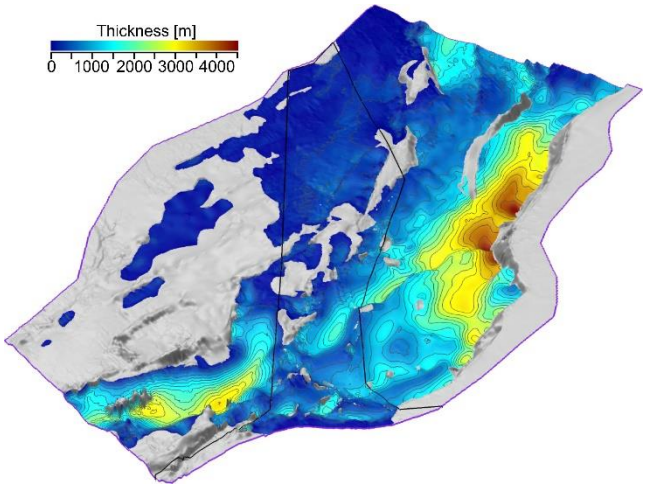

Min	0 m	Max	4508 m
25th perc.	217 m	Median	655 m
75th perc.	1409 m	90th perc.	2556 m

Figure 14: Depth map of the harmonized Near base Upper Jurassic and thickness of the Upper Jurassic. Details on the revisions made to harmonize the horizon are described in detail in Deliverable 3.6 (Thöle et al., 2021).

3.1.2.6 Near base Lower Jurassic

Depth

2D map view

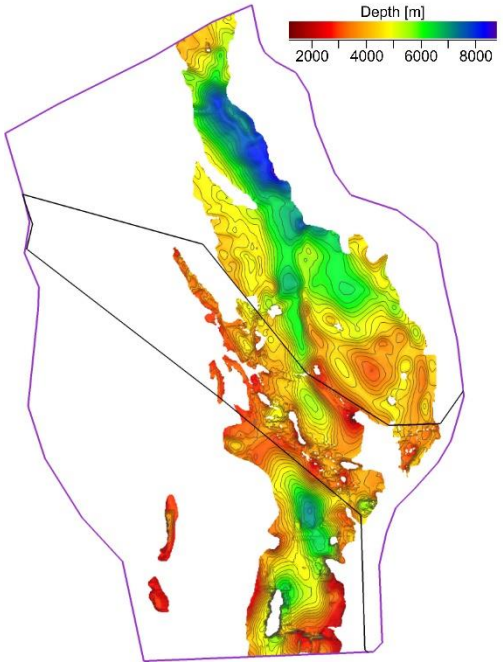

3D view from SE

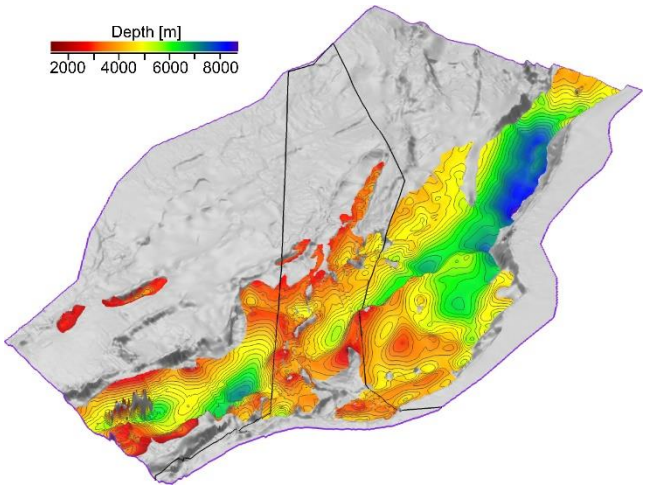

Min	112 m	Max	8719 m
25th perc.	3730 m	Median	4497 m
75th perc.	5539 m	90th perc.	6524 m

Thickness

2D map view

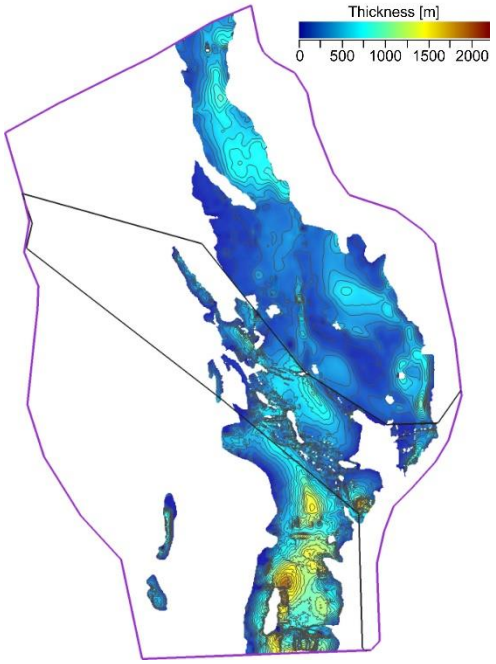

3D view from SE

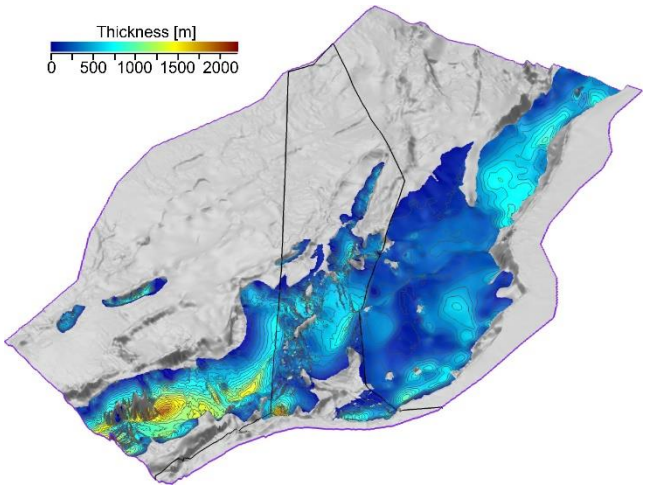

Min	0 m	Max	3860 m
25th perc.	186 m	Median	325 m
75th perc.	545 m	90th perc.	851 m

Figure 15: Depth map of the harmonized Near base Lower Jurassic and thickness of the Middle-Lower Jurassic. Details on the revisions made to harmonize the horizon are described in detail in Deliverable 3.6 (Thöle et al., 2021).

3.1.2.7 Near base Lower Triassic

Depth

2D map view

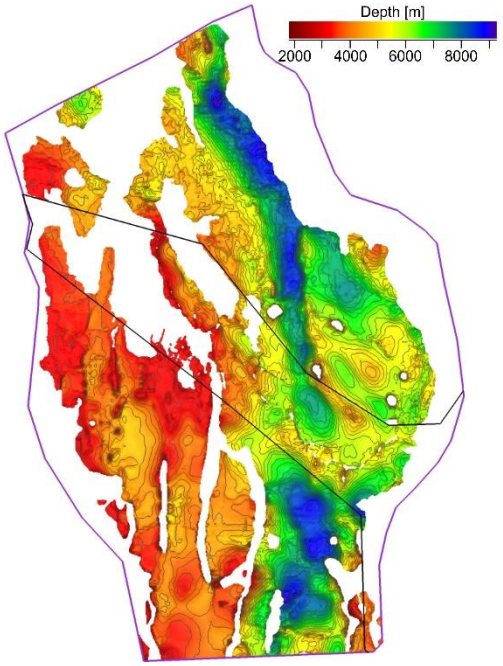

3D view from SE

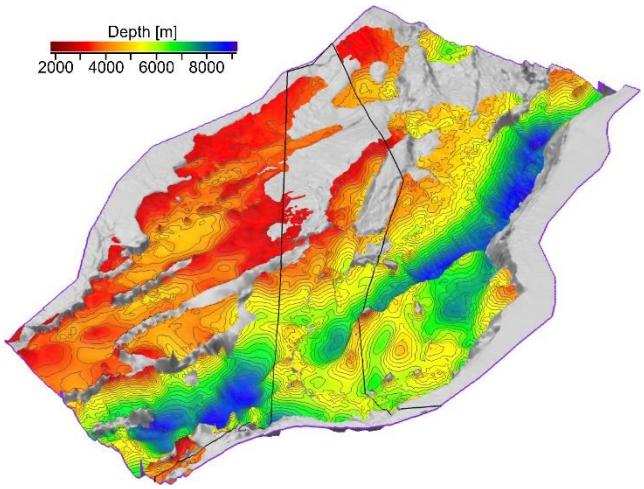

Min	1849 m	Max	9242 m
25th perc.	3881 m	Median	5004 m
75th perc.	6268 m	90th perc.	7465 m

Thickness

2D map view

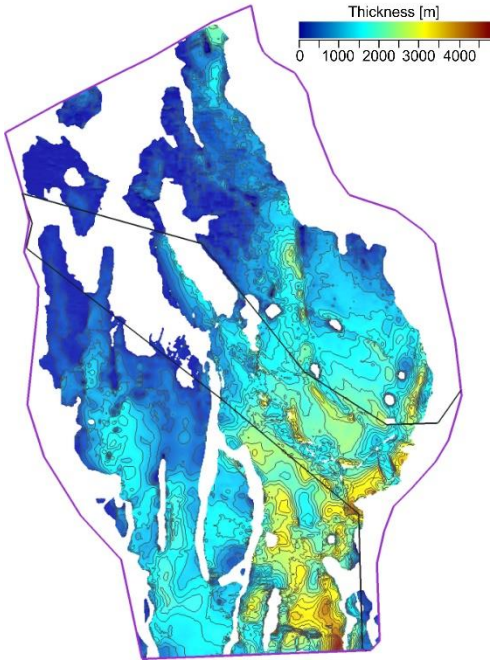

3D view from SE

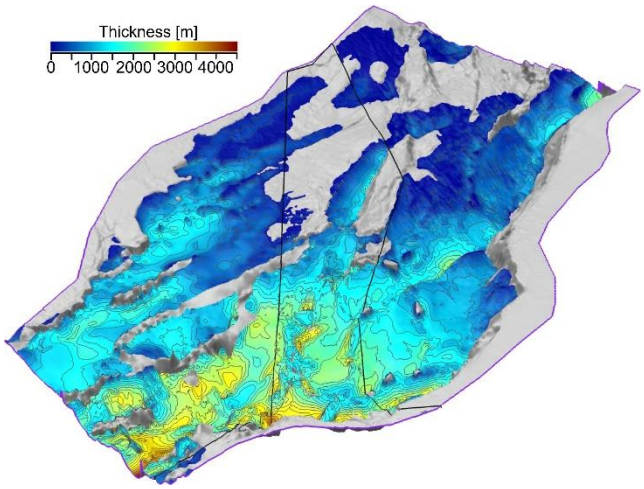

Min	0 m	Max	4782 m
25th perc.	489 m	Median	1133 m
75th perc.	1771 m	90th perc.	2415 m

Figure 16: Depth map of the harmonized Near base Lower Triassic and thickness of the Triassic. Details on the revisions made to harmonize the horizon are described in detail in Deliverable 3.6 (Thöle et al., 2021).

3.1.2.8 Base Zechstein

Depth

2D map view

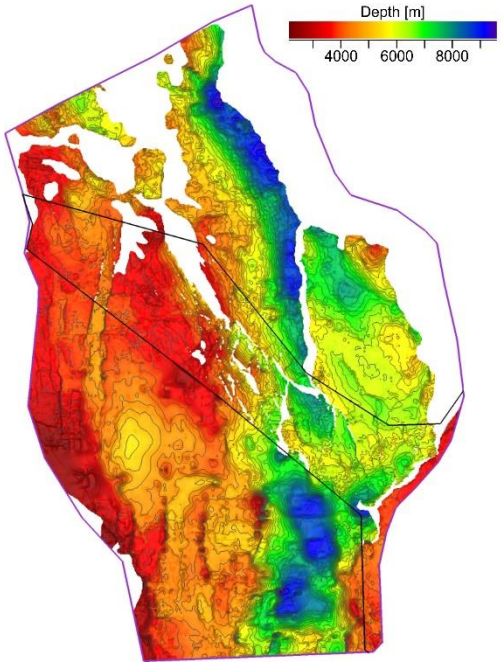

3D view from SE

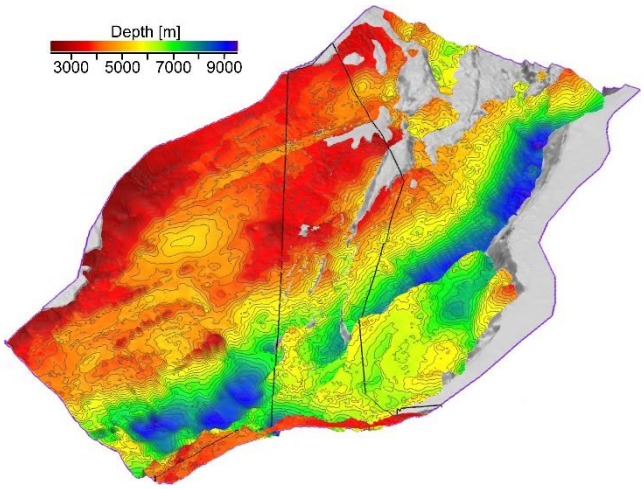

Min	2188 m	Max	9544 m
25th perc.	4016 m	Median	4870 m
75th perc.	6356 m	90th perc.	7521 m

Thickness

2D map view

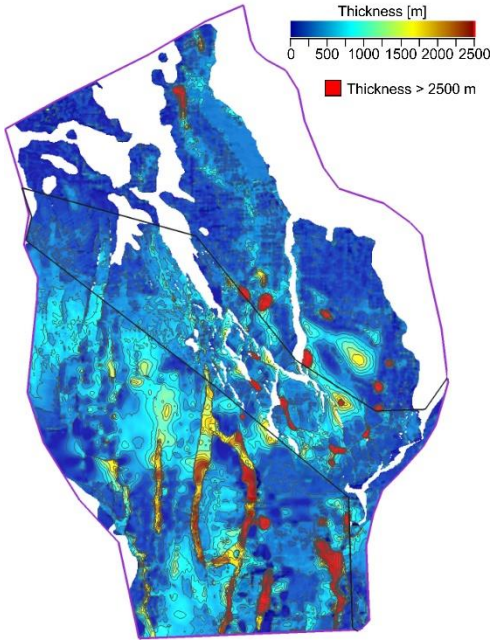

3D view from SE

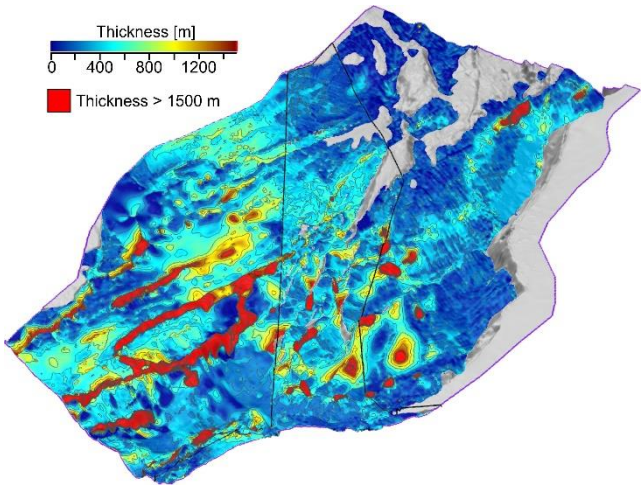

Min	0 m	Max	7236 m
25th perc.	186 m	Median	332 m
75th perc.	573 m	90th perc.	937 m

Figure 17: Depth map of the harmonized Base Zechstein and thickness of the Zechstein interval. Details on the revisions made to harmonize the horizon are described in detail in Deliverable 3.6 (Thöle et al., 2021).

3.1.3 Harmonization status and unresolved issues

Most cross-border discrepancies observed in the time horizon grids initially provided for harmonization (Thöle et al., 2019) were removed in this study by seismic re-interpretation as well as to some extent by adjustments and model generalization through grid mathematics (Thöle et al., 2021). However, there remain disparities in the national horizon models which could not be fully resolved in the timeframe of the project for various reasons.

One example of unresolved issues concerns the Near base Lower Cretaceous, which still shows considerable differences in its distributional pattern along the borders (Figure 13). Except for the Outer Rough Basin, for example, no Lower Cretaceous is present in the northern part of the German Entenschnabel, whereas in the Dutch and Danish sectors Lower Cretaceous is widely distributed. A widespread distribution of Lower Cretaceous deposits, however, cannot be verified by wells in the German Entenschnabel. Furthermore, the Lower Cretaceous is truncated here in many areas by the overlying Upper Cretaceous and seems to be absent or below seismic resolution (see e.g. Figure 25 in Deliverable D3.5; Thöle et al., 2020). Since the available well information indicate a non-distribution and the Lower Cretaceous is seismically not discernible, no Base Lower Cretaceous was therefore mapped in certain areas of the German sector. However, in the northern Dutch offshore, for example, residual Lower Cretaceous is locally confirmed by wells and it was assumed during the seismic mapping that Lower Cretaceous is at least thinly distributed throughout the area although seismically not discernible. As a consequence, the Base Lower Cretaceous was mapped here in large parts of the northern Dutch offshore sector. Both interpretation approaches can be generally regarded as appropriate, and most likely there is a transitional zone along the border between non- and residual distribution. That the discrepancies in the distributional pattern are primarily related to the different seismic picking concepts applied is also supported by the mapped thickness distribution of the Lower Cretaceous (Figure 13). Considering only thicknesses of more than 25 m, the distributional pattern of the Lower Cretaceous is generally in good agreement along the national borders. For this reason, and because both interpretation approaches can be regarded as appropriate, it was decided to leave these cross-border discrepancies for the time being and not to harmonized them.

Another unresolved issue concerns the representation of faults in the national horizons model that served as input for the harmonized model. In the German horizon model (Arfai et al., 2014), for example, most faults exhibiting horizon offsets were mapped and are represented by gaps in the horizon grids. Contrary to this, only major faults, i.e., faults with large offsets and faults that are important for the definition of structural elements, are usually considered in the Danish and Dutch horizon models. Therefore, their horizons partly coincide with fault planes and also locally e.g. with salt dome flanks. A harmonization of fault traces across borders, however, can be time-consuming and is generally hampered by the fact that most faults occur in structurally complex regions, and here the national horizons tend to be highly generalized. In light of this generalization, a re-interpretation of horizons would often be unavoidable to ensure a geologically plausible harmonization, but this is generally not feasible for the entire study area due to time constraints. To demonstrate how harmonization of faults across borders can be generally achieved, a segment of the Coffee Soil Fault (eastern boundary of the Central Graben) was chosen as an example for harmonizing a main fault zone. The results of this study are presented in the following chapter.

3.2 Fault model of the Coffee Soil Fault

3.2.1 Structural overview and modeled fault

The Southern and Central North Sea is a highly structural differentiated area with a multiphase and multidirectional extensional history. In addition, the Mesozoic and Cenozoic overburden is extensively influenced by halotectonics, which has largely affected subsidence patterns and facies distribution since the Triassic (e.g. Doornenbal and Stevens, 2020; Evans et al., 2003). Furthermore, Late Cretaceous NNE-SSW directed contraction overprinted or inverted former (Mesozoic) rift-structures and diapirs (e.g. Kley, 2018). The result is a complex and heterogeneously distributed structural pattern of crossing and interlocking structural directions (Figures 18 & 20), in particular along the Central Graben main fault (Coffee Soil Fault / Schillgrund Fault). The majority of cross-border structures are either rift-related normal/oblique faults, in parts overprinted by transpression or dip-slip inverted, or fault zones related to diapirism (e.g. crestal faults). Often both, extensional tectonics and halotectonics, are equally important for the development, kinematics and geometry of the structures.

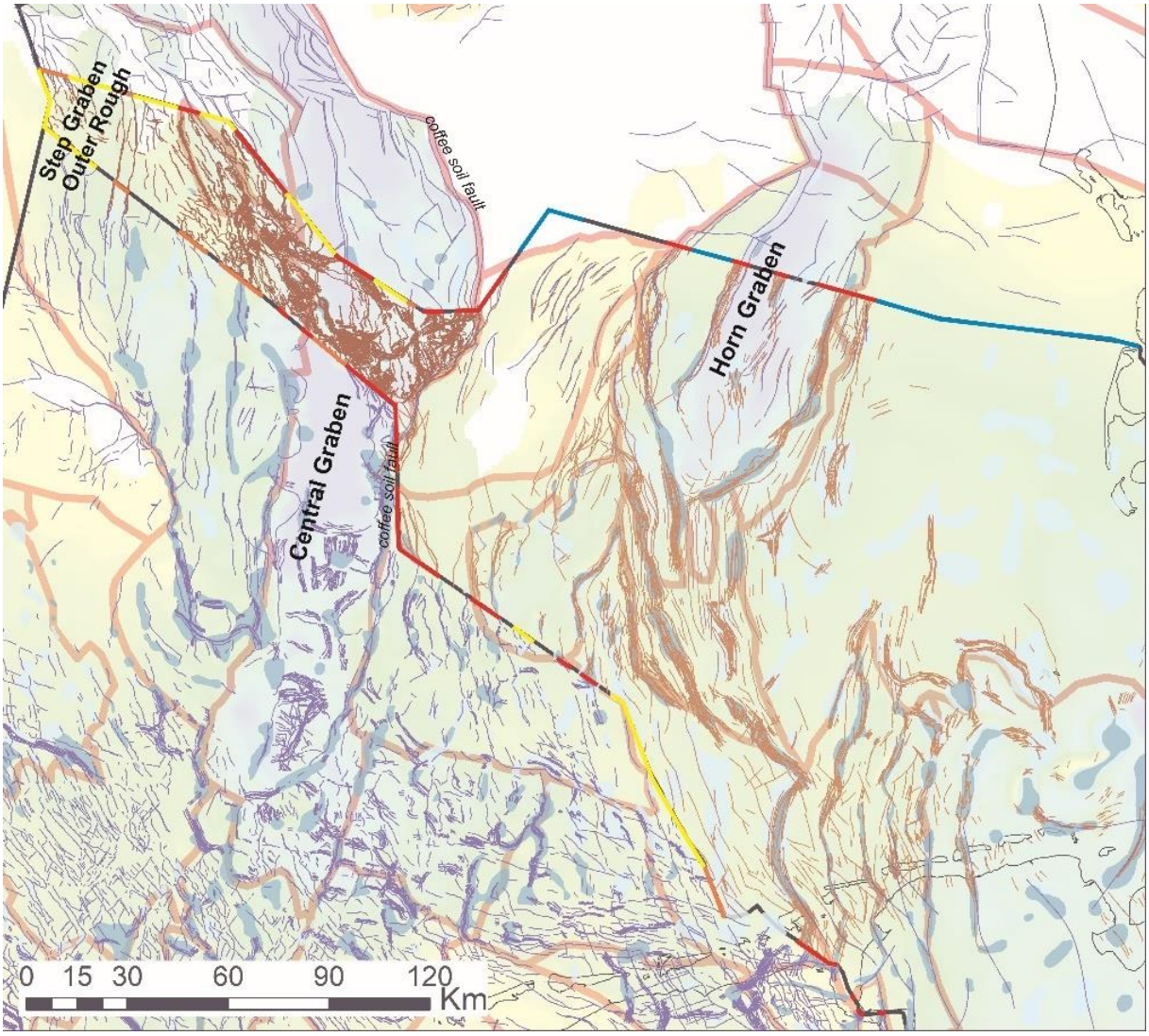

Figure 18 (see next page for description)

Figure 18 (previous page): Fault lineaments in Dutch, German and Danish North Sea provided for the HIKE project shown together with the Base Zechstein. The fault interpretations have a different degree of detail and generalization. For the German Entenschnabel, a high detailed fault analysis with offset outlines for 13 horizons exist. In contrast, only generalized fault lineaments of major faults are freely available for the Danish Sector. Along the border the different colors of the border-line highlight areas of different structural complexity across the borders. Very high structural complexity (red), high structural complexity (orange), moderate complexity (yellow), low complexity (blue).

Due to the large amount of structures whose consistent modeling requires cross-border harmonization (Figure 18) as well as the challenges in harmonizing existing structural interpretations and creating cross-border 3D structural models in depth (e.g. described in Malz et al., 2021), the project partners GEUS, BGR & TNO agreed to test at first possible approaches for fault harmonization using the example of the probably most prominent fault zone in the southern and central North Sea, the Coffee Soil Fault, also known as the Schillgrund Fault in the German and Dutch North Sea. This fault zone, hereafter referred to as the Coffee Soil Fault System (CSFS), delineates the eastern boundary of the North Sea Central Graben (Figure 19; Appendix A & E), a 500 km long, N-S trending half-graben straddling the Dutch, German and Danish, as well as the British and Norwegian offshore sectors. The region selected for fault harmonization covers thereby a c. 80 km long section in the middle segment of the Central Graben, which crosses the border region (the Entenschnabel) of the three partners involved (Figures 19 & 22). In addition to this, the segment of the fault zone chosen is of particularly interest, because fundamental characteristics of the Central Graben change in this region (e.g. halotectonics, inversion tectonics, strike and dip of main faults, depth of horizons) and a fault harmonization may contribute to a better overall understanding of the structural development of the entire rift structure.

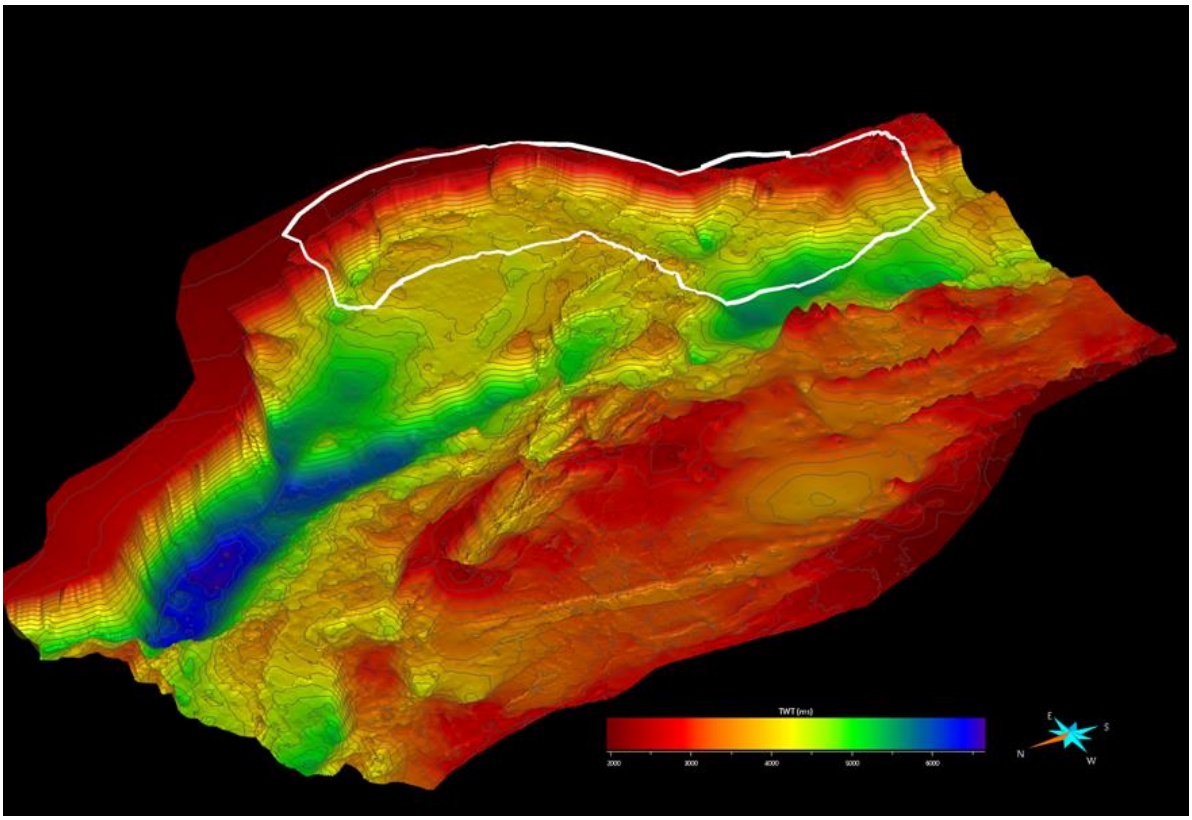

Figure 19: 3D view from NW on the middle segment of the North Sea Central Graben. Shown is the color-coded Top Pre-Zechstein within the time domain (Deliverable D3.6) and the white outline of the fault modeling study area.

3.2.2 Existing fault interpretations and models

A regional all-encompassing fault modeling in an overview scale has not yet been done for the CSFS in the study region. In general, detailed fault interpretations and a generalized structural model with tessellated fault surfaces existed only for the German offshore sector at the beginning of the work of WP3. These data were compiled within the framework of the GPDN project (German acronym for “Geo-scientific Potentials of the German North Sea”; Reinhardt et al., 2010). As part of this project, a detailed seismic mapping study has been carried out by the BGR in the northwestern part of the German North Sea, also referred to as the Entenschnabel (Arfai et al., 2014). Seismic mapping was done here for the first time and results were subsequently transferred into a detailed structural model. For this 155 km x 30 km area in the northwestern most part of the German North Sea sector, 13 seismic horizons, c. 800 faults and more than 20 salt diapirs were interpreted in a high level of detail (Figure 20a) based mainly on 3D seismic data. Due to the high structural complexity and associated challenges in the modeling process, a generalization (c. 300 faults and simplified salt structures) of the structural pattern became necessary (Figure 20b).

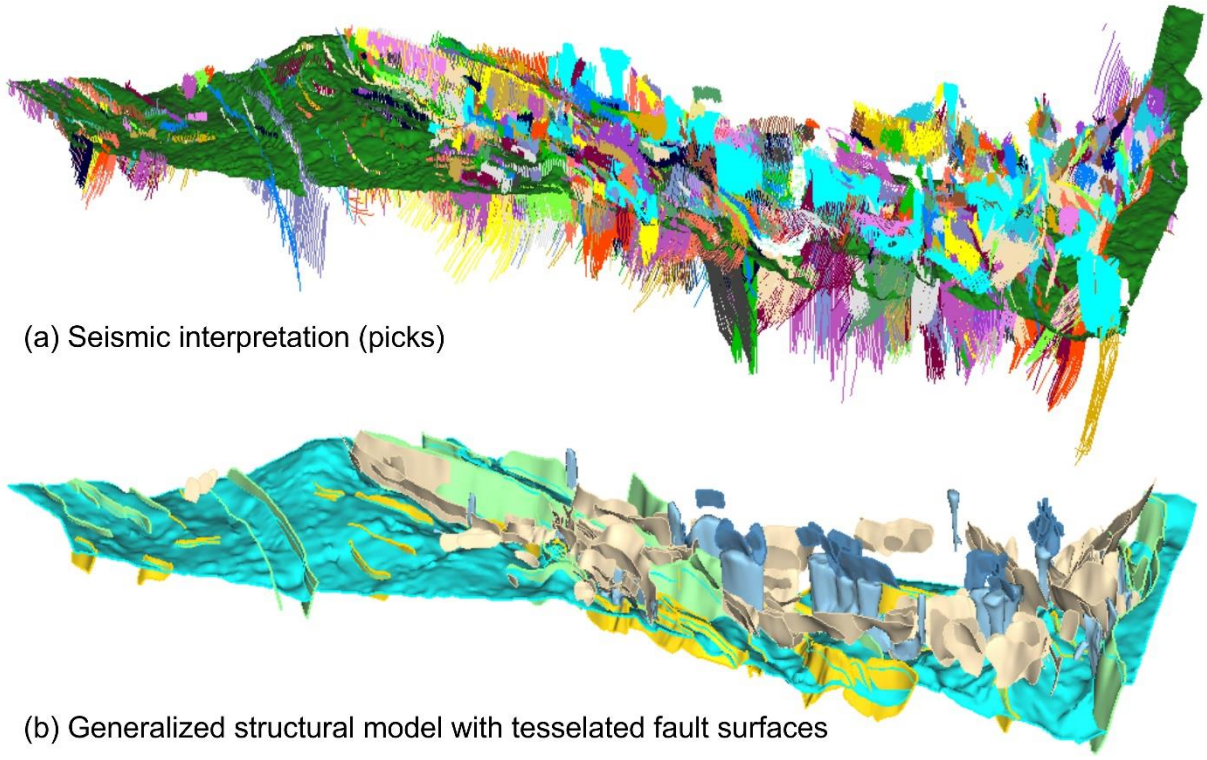

Figure 20: (a) Detailed seismic interpretation data (Arfai et al., 2014) and (b) derived structural model of the German Entenschnabel area (GPDN). The model shows a strongly deformed part of the Central Graben and surrounding areas. Halotectonics, a multiphase rift evolution as well as inversion tectonics resulted in a complex structural pattern of intersecting and interleaving structures. The model was developed with SKUA-GOCAD. (Legend for the structural model: Green faults = faults connecting basement and Mesozoic cover; yellow faults = basement faults; dark blue = faults in the top or related to diapirs and diapiric growth; beige faults = faults only traceable within the Mesozoic to Cenozoic overburden; light blue = diapirs).

No comparable fault interpretations and models were publicly available for the adjacent Dutch and Danish North Sea sectors. As described early, in the Dutch and Danish horizon models that served as input for the harmonized Entenschnabel model (Chapter 3.1), only major faults, i.e., faults with large offsets and faults that are important for the definition of structural elements, are usually considered. Therefore, their horizons partly coincide with fault planes and also locally e.g. with salt dome flanks (see e.g. Figures 31-33).

In the course of developing a Structural Framework (SF) for the Southern and Central North Sea (Chapter 4), interpretations derived from map compilations (typical formats: e.g. georeferenced images, polyline or point shapes/vector) were also evaluated as input data for the fault modeling study. However, such data are typically subject to strong generalization and cannot unambiguously translate into 3D by means of received interpretative concepts, e.g. to close data gaps. That it is even difficult to use the appropriate data for the creation of a consistent SF where structural borders have to be defined is clearly shown in Figures A-1 to A-6 of Appendix A. For example, Figure A-1 shows the spread of fault interpretations of the CSFS from over-regional structural maps. The fault lineaments of the individual studies are sometimes more than 30 km apart. By specifying additional information on how the displayed lineaments were defined (hanging wall or footwall cut-off, reference horizon) the fuzziness in the designation in a map can be limited, sometimes significantly, for a selected structure but not completely (Figure A-2). Beside this, geological conceptual ideas about faults have also a massive influence on the map representation of a fault. For example, in Cartwright (1987) & Wride (1995), among others, Transfer Zones are assumed (Figure A-4) to segment the CSFS, significantly influencing the orientation of the main fault. Other interpretations does not include these Transfer Zones. If all interpretations and generalizations are displayed scale-independently on a map, it becomes visible that, at least for the example presented here, a majority of interpretations and generalizations gather in one zone (Figure A-3). The wide of this zone is slightly smaller as of over-regional studies (Figure A-1). However, the remaining fuzziness also indicates that other factors prevent a discrete boundary designation between structural domains. Figures A-5 & A-6 show further that a higher detail of the underlying interpretations does not necessarily allow a clearer designation of structural boundaries. However, this often makes the conceptual approaches behind determinations more visible. For example, in Figure A-6 it becomes visible that the definition of the boundary between structural domains in this region is related to the course of the footwall cut-off at the base of the Zechstein. In summary, for the sake of simplicity, it must also be assumed in the here presented literature/map study (Appendix A) that the respective fault interpretations presented are unambiguous in themselves with respect to the basic data used, but generally not suitable to support the planned fault modeling study.

3.2.3 Fault interpretation / modeling – Working steps

The detailed fault interpretations made by the BGR in the area of the German Entenschnabel (Figure 20a) during the GPDN project served as a starting point for the planned cross-border fault modeling study. In this context, however, only fault interpretations (fault sticks in TWT) located within the fault model area of WP3 (Figure 22) were taken into account. These data were checked roughly for their geological plausibility and, if necessary, revised based on the available seismic data in the German sector. Subsequently, an attempt was made to extend the interpretations made in the time domain into the Danish and Dutch North Sea sectors. For this purpose, only seismic data available in BGR's own seismic database were used. The corresponding fault interpretations were then depth converted with a seismic velocity volume, which was modeled without salt structures down to the base of the Triassic (Figure 6b). Interpretations of prominent basement faults were subsequently modeled in the depth domain as fault surfaces in SKUA-GOCAD. The revised and into the neighboring countries extended German fault interpretations are provided with Deliverable 3.8 as fault sticks (in TWT & Depth) as well as in part as modeled fault surfaces (in Depth; Figure 22).

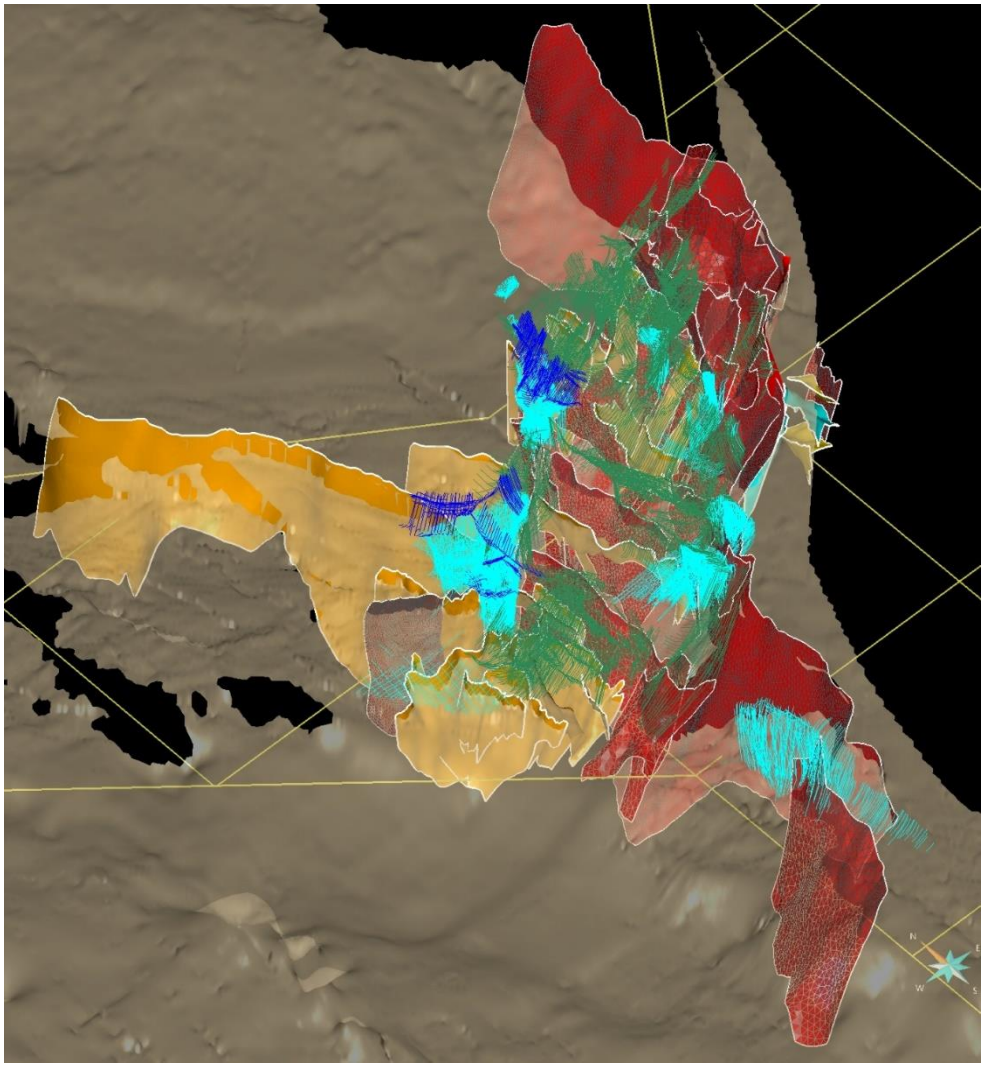

Figure 21: Detailed fault interpretations and modeled fault surfaces of the German segment of the CSFS and adjacent areas. The Central Graben and its eastern boundary, the CSFS, shows here a complex structural pattern of intersecting and interleaving structures. The data seen are available as fault sticks (in TWT & Depth) and modeled surfaces (in Depth; Chapter 5).

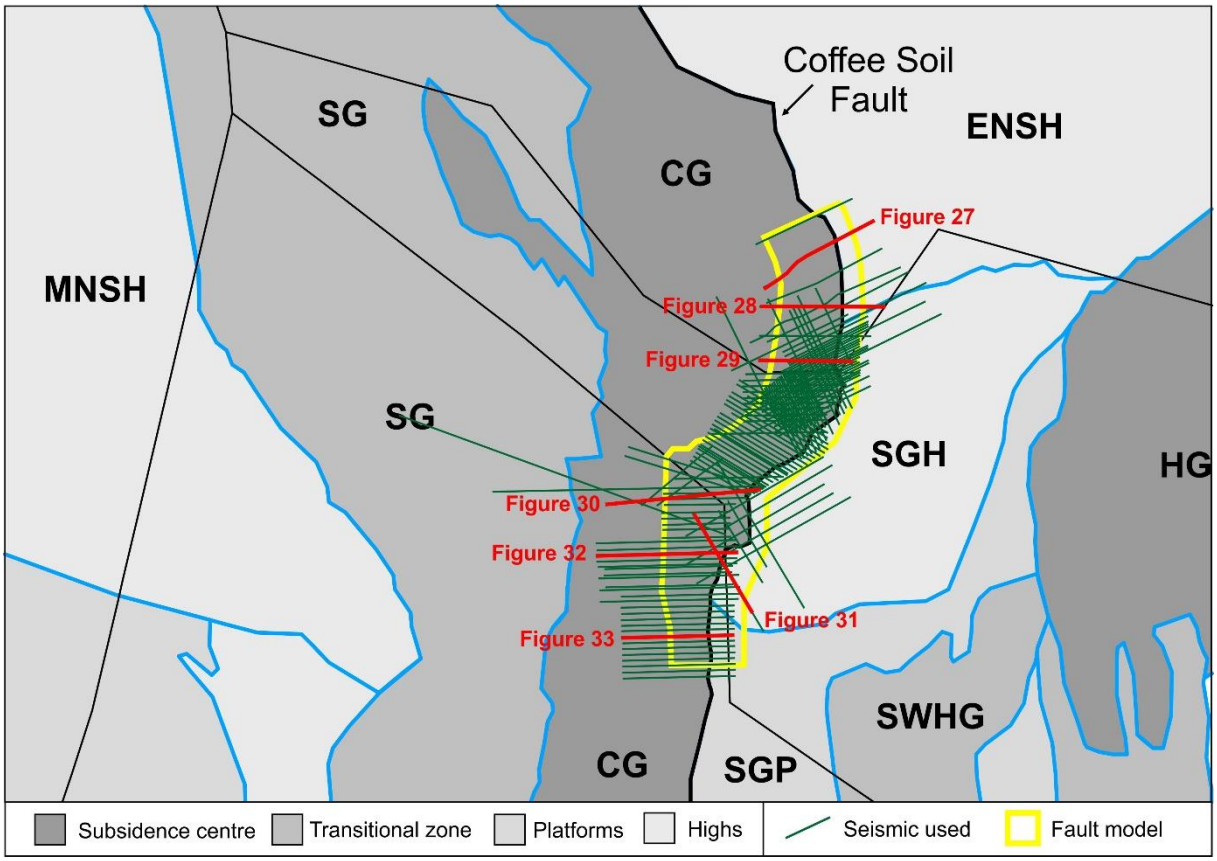

Figure 22: Structural element map showing the location of the fault model area and seismic data used to compile the generalized model of the CSFZ. The red lines indicate the position of seismic lines shown in Chapter 3.2.4.

Building on the fault interpretations shown in Figure 21, in a next step it was intended to interpret the general structure of the CSFS in the remaining parts of the fault model area as well. For this purpose, selected seismic lines were provided by the project partners for the Danish and Dutch parts of the investigated fault segment. However, due to the complex structure of the region, several more seismic lines had to be added to the initially provided data to ensure a consistent interpretation of the fault zone. These additional lines were taken from BGR's own seismic database. The corresponding seismic lines, shown in Figure 22, were converted to depth using a seismic velocity volume modeled without salt structures (Figure 6b). During the subsequent interpretation of the seismic sections, it turned out that the CSFS can only be consistently represented in higher levels of detail by a large number of faults. A detailed fault interpretation required for this purpose, however, was not feasible due to the limited time frame of the project. Another limiting factor has been the limited availability of data in certain parts of the model area (Figure 23). For example, in the northern part of the Danish model area only a few seismic lines were available for interpretation. Another critical region is the Dutch-German cross-border region. This complex region, characterized by a distinct change in strike direction and structural style of the fault system, is covered only by a few seismic lines which partly clearly contradict each other in the favored interpretation. Furthermore, seismic data generally do not cover the easternmost limit of the working area. There, the eastern limit of the fault system can only be covered in approximation (Figure 23).

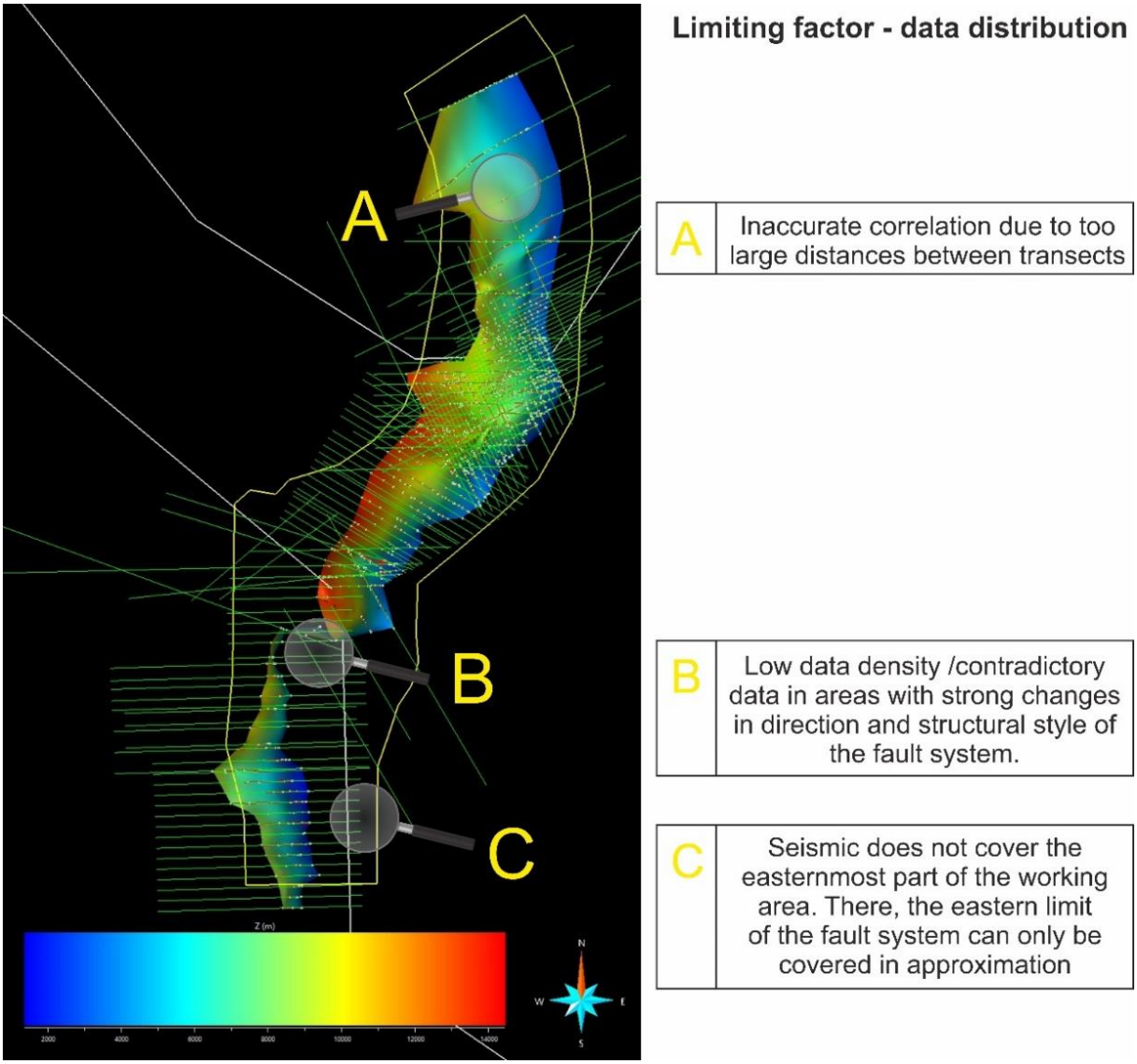

Figure 23: Fault model area and seismic data used to compile the generalized fault model. The color-coded surface shows thereby the western limit of the so called CSFS "core zone". Regions with sparse data coverage are indicated by the magnifying glasses (A to C).

Aside from the sparse data coverage in certain areas of the model region (Figure 23), the main reason why detailed fault interpretation and modeling was omitted in the adjacent areas away from the interpretation shown in Figure 21 was the tight time frame of the project. Instead of a detailed fault interpretation, the remaining study time focused on determining the extent of the fault system and the uncertainties in interpreting this region. For this purpose, the westernmost as well as the easternmost limit of a so-called "Fault System core zone" was mapped based on the seismic data shown in Figure 22. The limits of this "core zone" each represent possible generalized fault model solutions of the fault system as one fault plane. In some cases, they coincide with identified faults (e.g. Figures 31 & 32), but they can also represent only generalized solutions. The zone between the limits often but not always corresponds to an area in which the seismic quality decreases strongly and thus the interpretational bias increases (e.g. Figure 33). The "core zone" includes generally all subparallel faults that are aligned to the main strike direction of the fault system. Large faults branching off from the main

fault zone, e.g., a prominent splay fault in the Dutch offshore sector that probably continues toward the Johannes Graben (Appendix G), where it forms the northern boundary of the Dutch Central Graben subsidence center, are not covered by the “core zone”. The mapped limits of this "Fault System core zone" are shown in Figures 24 and 25, and the general characteristics of this zone are described in the following subchapter and illustrated by several seismic sections (Figures 27-33).

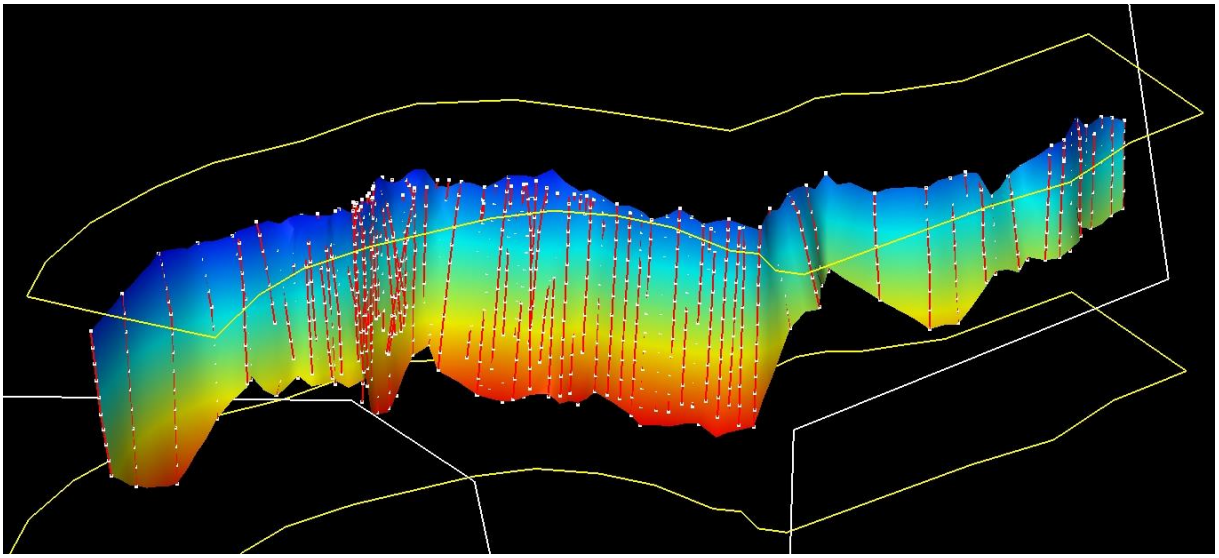

Figure 24: View on the fault model area showing the modeled surface of the eastern limit of the CSFS “core zone”. The underlying interpretations here for are shown as fault sticks.

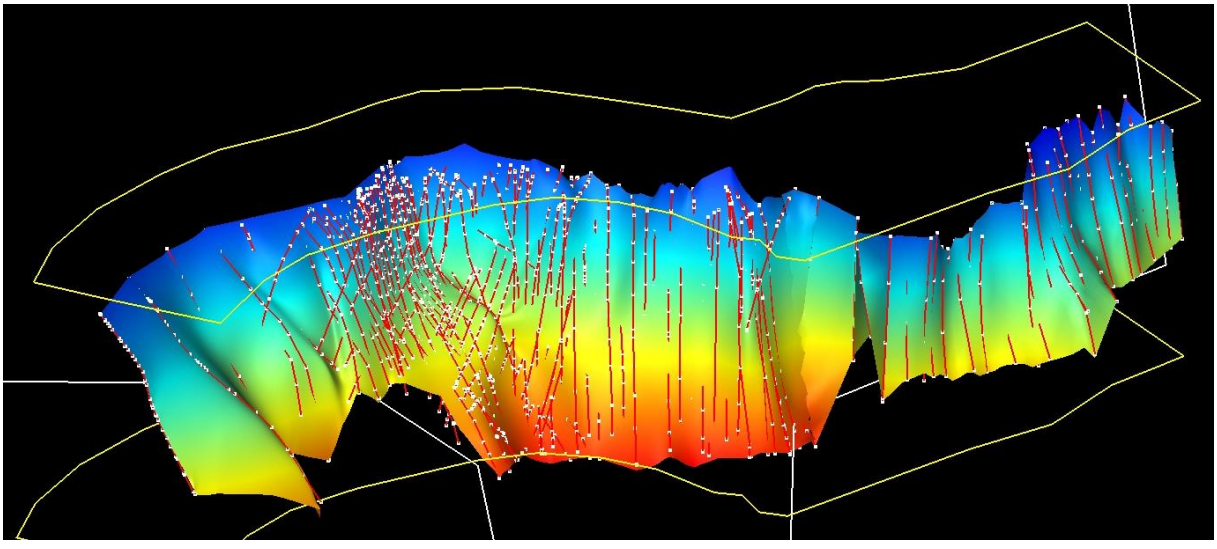

Figure 25: View on the fault model area showing the modeled surface of the western limit of the CSFS “core zone”. The underlying interpretations here for are shown as fault sticks.

3.2.4 Fault model overview

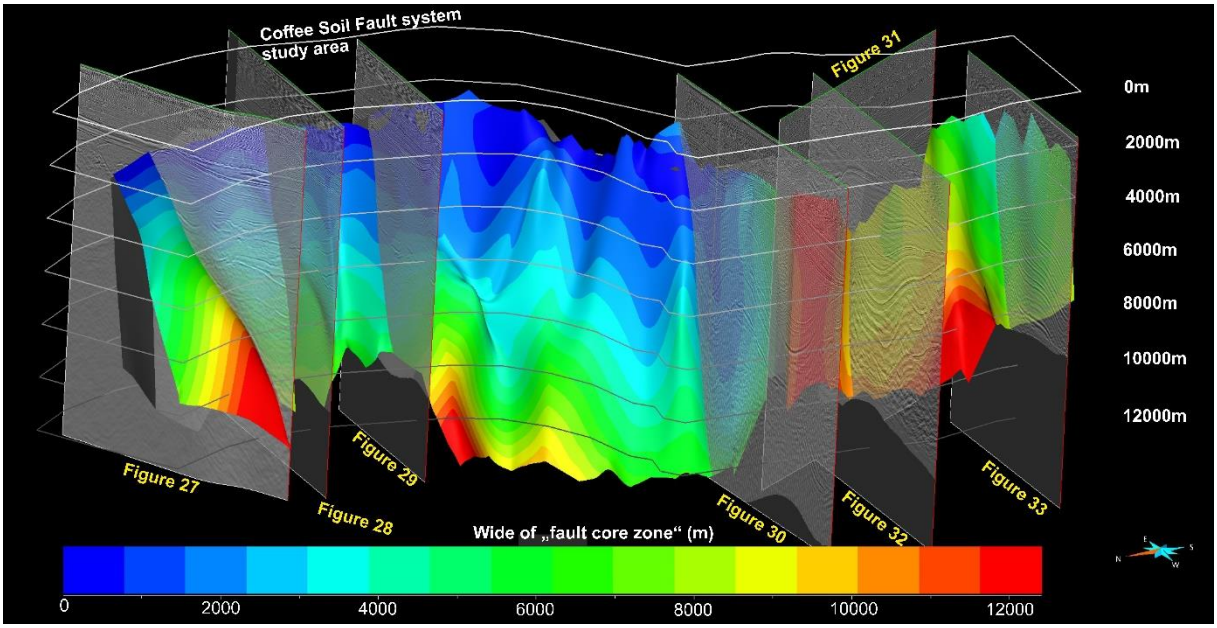

Figure 26: View from NW on the modeled western limit of the CSFS "core zone". The color of the modeled surface illustrates the wide of the "fault core zone". In general, the zone becomes increasingly wider towards the Dutch segment of the CSFS and with depth. Further shown are the position of the seismic sections presented in Figures 27-33.

As described above, the "core zone" of the CSFS is defined by a western and an eastern limit, which were modeled as surfaces in SKUA-GOCAD. The western limit of this zone is shown in Figure 26. Projected onto this surface is the horizontal extent of the so-called „Fault System core zone". In general, the zone becomes increasingly wider towards the Dutch segment of the CSFS and with depth. The widening trend is also evident in the seismic sections presented below (Figures 27-33), which also reveal the complex structure within the "core zone". The width of the "core zone" as interpreted in WP3 roughly agrees thereby with the spreading of existing fault interpretations compiled for the CFSZ in the study region in Appendix A (Figure A-1). As with our model, the CSFS shows here also a clear widening trend towards the Dutch segment of the CSFS and a clear delineation of the Central Graben and Schillgrund High structural domains becomes more and more difficult as the CSFS affects large portions of both structural domains (see e.g. Figure 40 and Thöle & Jähne-Klingberg, 2021). This is also one of the reasons why the representations of CSFS in the map references of this region are so widely spread (Appendix A – Figure A-1).

The general characteristics of the studied CSFS segment is presented below along several seismic sections. Shown is here also the defined "core zone" of the CSFS as well as in certain seismic sections (Figures 30-32) the detailed fault interpretation conducted along the German segment of the fault system and adjacent parts of the Dutch offshore.

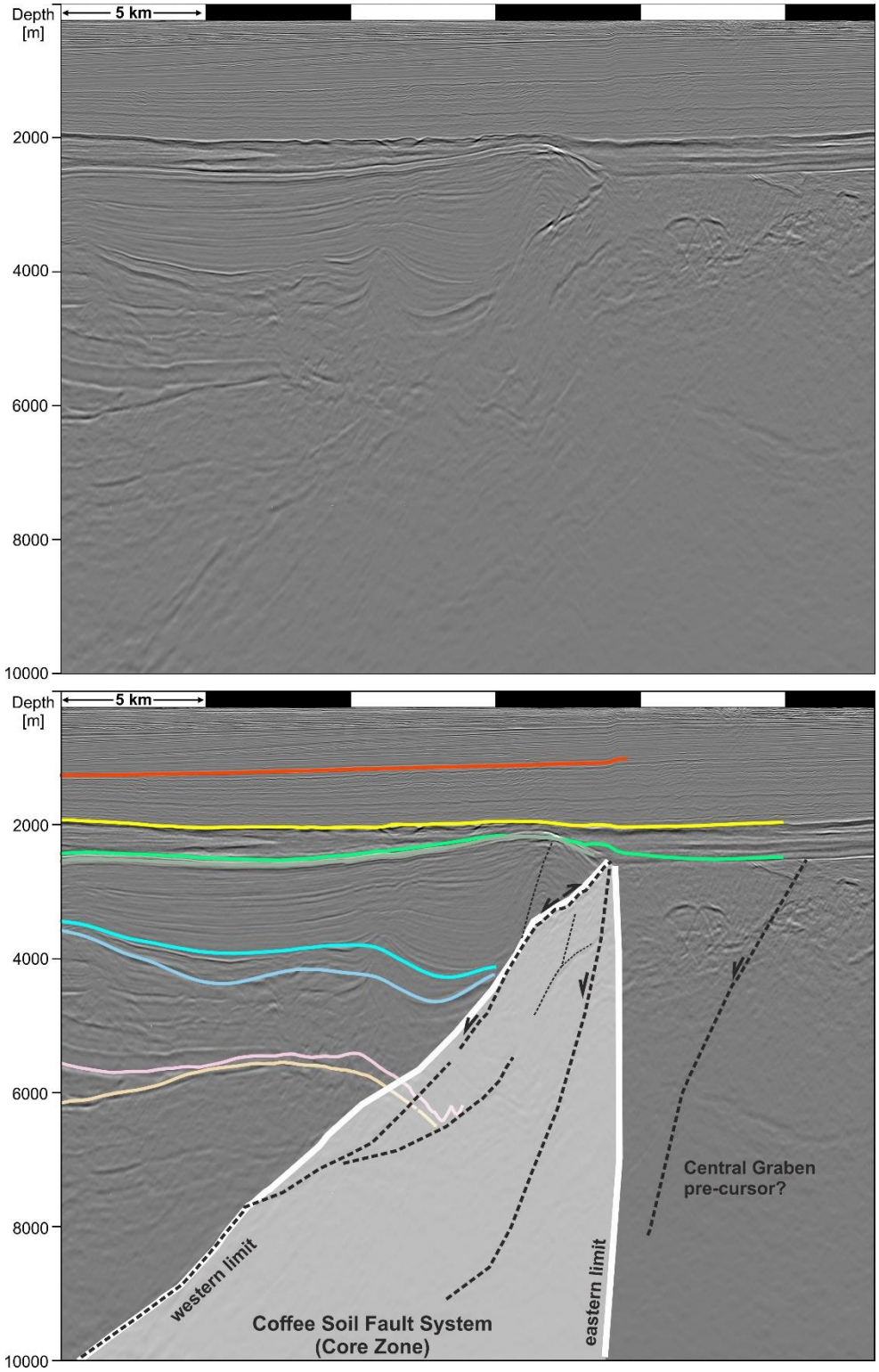

Figure 27: SW-NE oriented depth converted seismic section across the Danish segment of the CSFS (see Figures 22 or 26 for location). Shown in the lower image are the seismic horizons of the harmonized Entenschnabel horizon model (Chapter 3.1) as well as the CSFS "core zone" with its eastern and western limits. Structural inversion is evident along the western limit of the core zone by anticlinal uplift and a faulted flexure. The hanging wall anticline of the Pre-Zechstein indicates further a ramp flat or a strongly listric geometry of the major faults of the CSFS and the footwall basement of the Eastern North Sea High shows presumably Pre-Zechstein pre-cursor structures of the Central Graben (CG) or an early Pre-Jurassic rift stage.

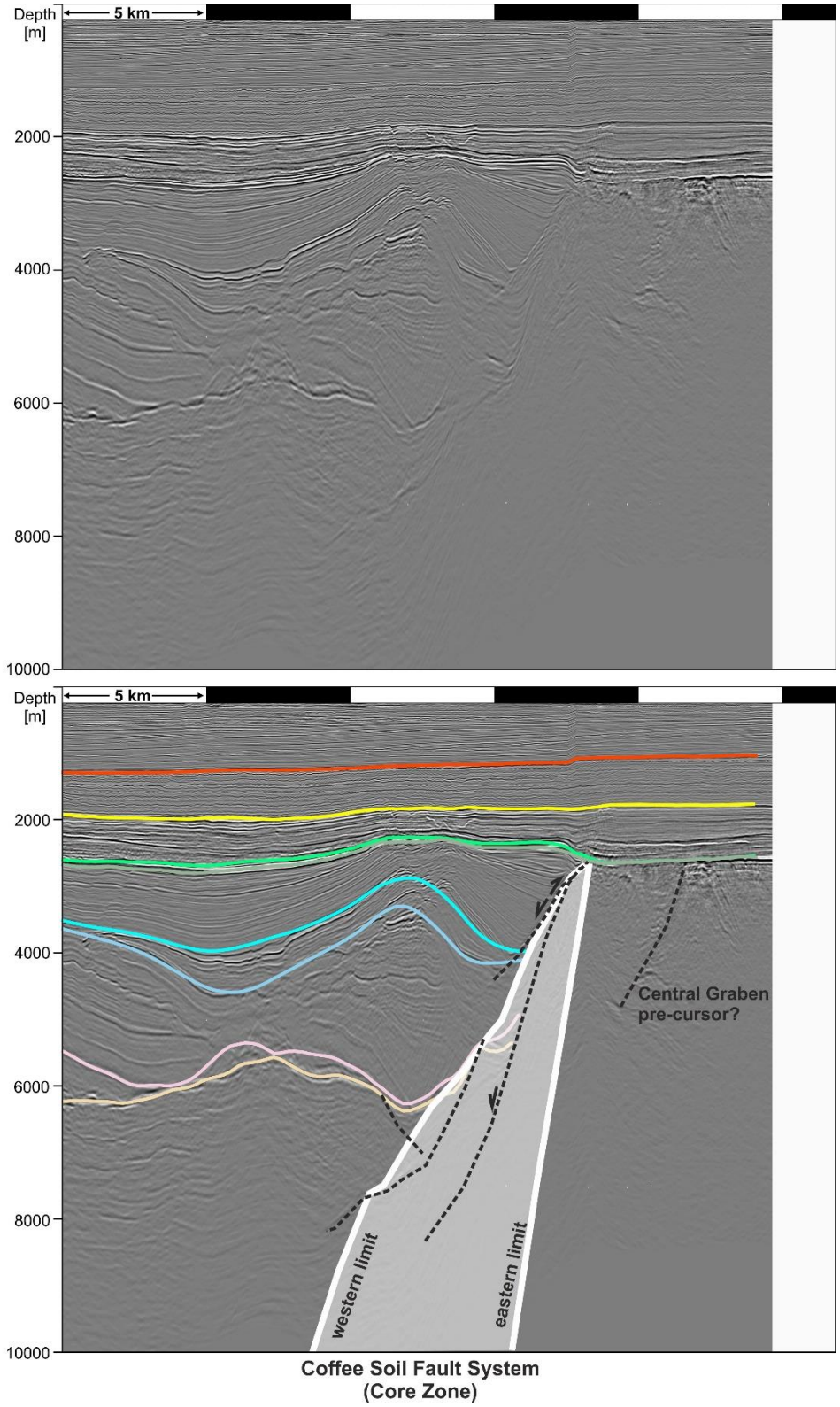

Figure 28: W-E oriented depth converted seismic section across the Danish segment of the CSFS (see Figures 22 or 26 for location). Shown in the lower image are the seismic horizons of the harmonized Entenschnabel horizon model (Chapter 3.1) as well as the CSFS "core zone" with its eastern and western limits. Structural inversion is evident along the western limit of the zone by broad anticlinal uplift. The geometry of the basement faults are less listric compared to the faults seen towards the north in Figure 27, but a distinct roll-over is present in the Mesozoic overburden. The footwall basement of the ENSH shows presumably Pre-Zechstein pre-cursor structures of the CG.

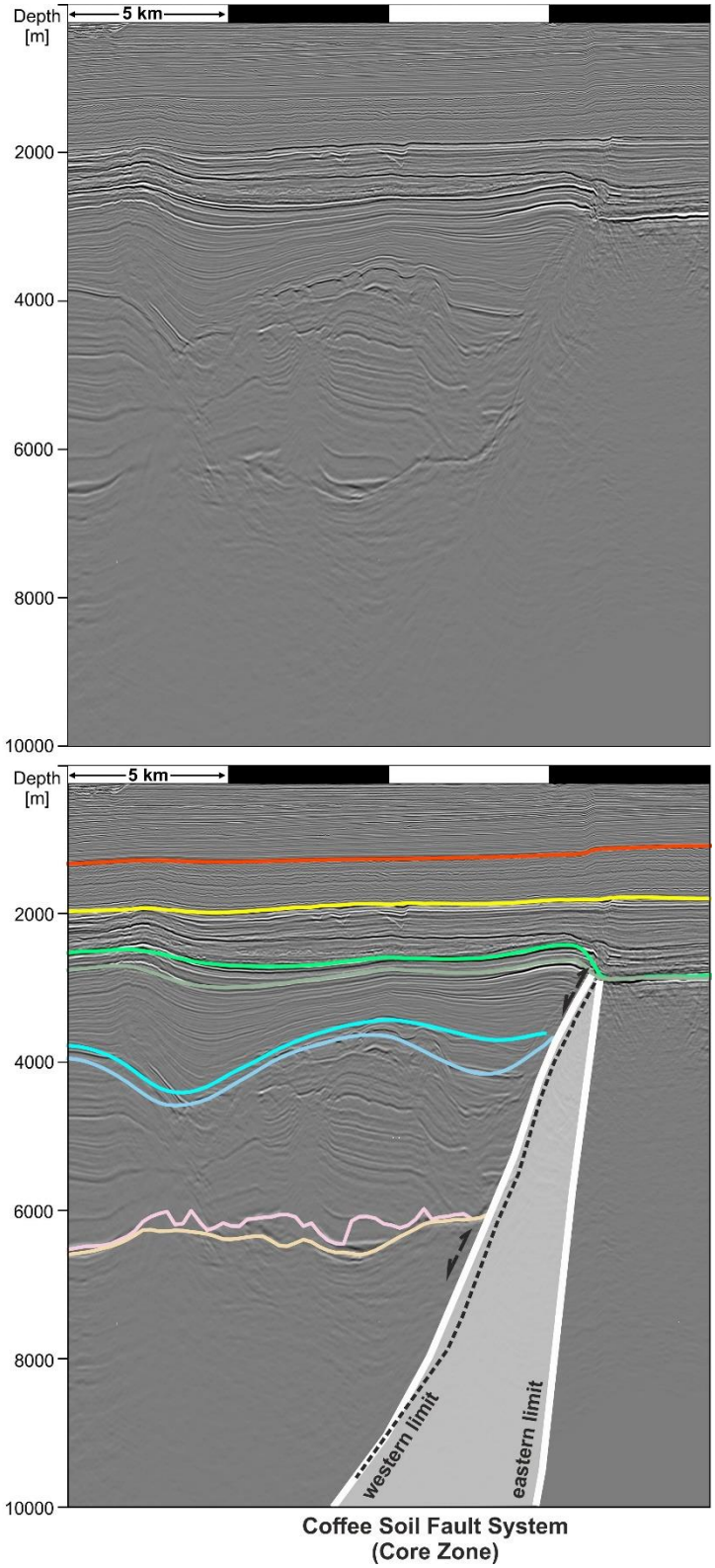

Figure 29 W-E oriented depth converted seismic section across the Danish segment of the CSFS (see Figures 22 or 26 for location). Shown in the lower image are the seismic horizons of the harmonized Entenschnabel horizon model (Chapter 3.1) as well as the CSFS "core zone" with its eastern and western limits. Indications for structural inversion are present in top of the CSFS "core zone" (faulted flexure), but also within the Pre-Zechstein basement. The geometry of the basement faults are less listric compared to the faults seen towards the north in Figures 27 and 28, but a distinct roll-over is present in the Mesozoic overburden. The CSFS has possibly only one prominent basement fault in this section.

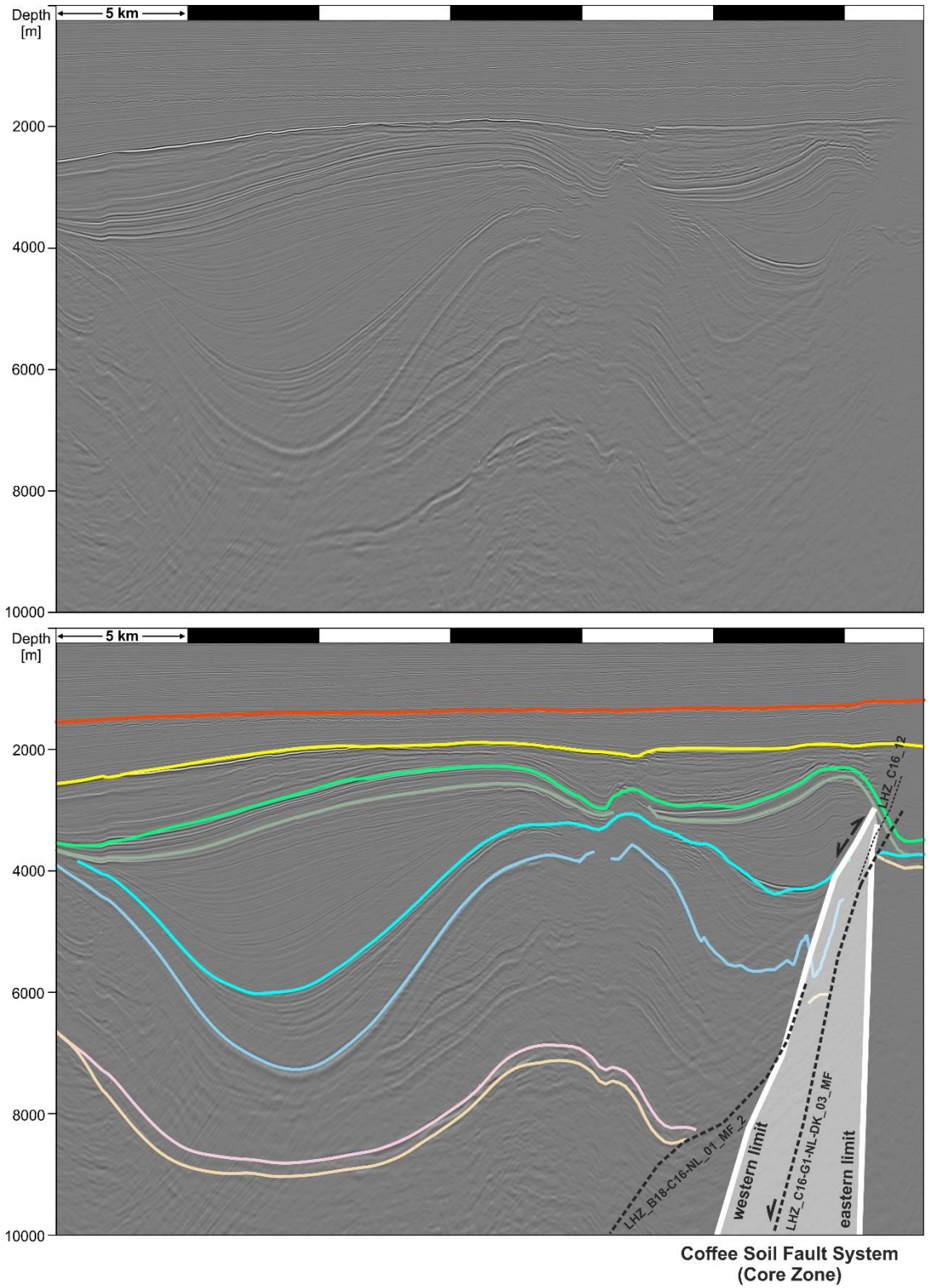

Figure 30: W-E oriented depth converted seismic section across the Dutch/German segment of the CSFS (see Figures 22 or 26 for location). Shown in the lower image are the seismic horizons of the harmonized Entenschnabel horizon model (Chapter 3.1) as well as the CSFS "core zone" with its eastern and western limits. Strong structural inversion along the CSFS "core zone" is evident by faulted flexure and high amplitude anticline in the top, but also steep anticlinal uplift within the Pre-Zechstein basement. Less listric fault geometry compared to the North and only low expression of thin-skinned tectonics along the fault zone (soft-linked style to thick-skinned style). Possibly only two prominent basement faults in this section. These two cryptically named faults are part of the detailed fault model shown in Figure 21 (fault models are available; see Chapter 5).

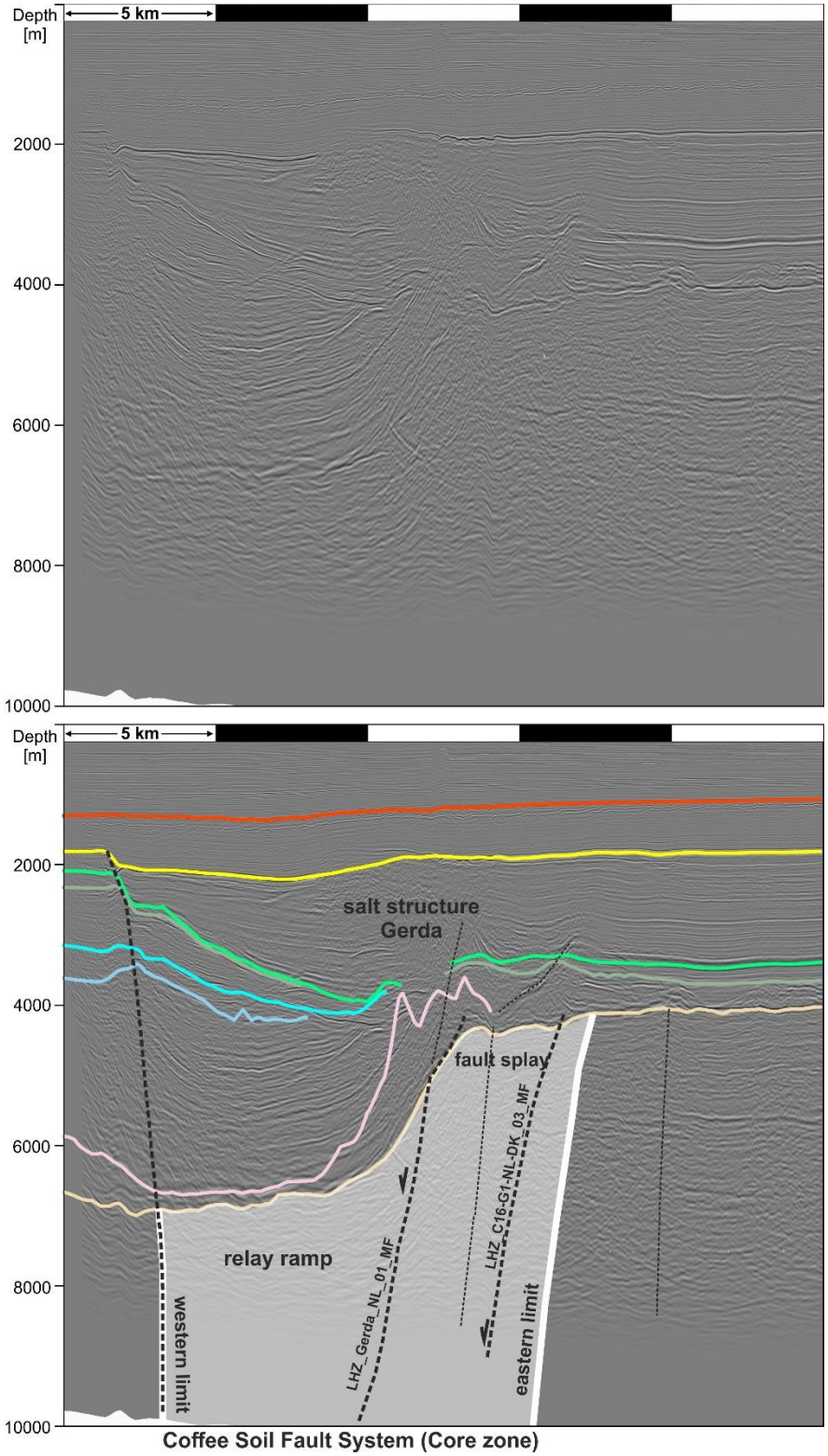

Figure 31: NW-SE oriented depth converted seismic section across the Dutch/German segment of the CSFS (see Figures 22 or 26 for location). Shown in the lower image are the seismic horizons of the harmonized Entenschnabel horizon model (Chapter 3.1) as well as the CSFS "core zone" with its eastern and western limits. Compared to adjacent areas to the north a decrease in structural inversion can be observed, probably buffered by deformation of the salt structure Gerda. No listric geometry of the basement faults. The region covered by the seismic section shows generally a wide "core zone" with faults of similar offsets (broad relay ramp dissected by several faults). The distribution of the fault offsets varies greatly from section to section in this region, forming a complex fault zone with frequently changing lateral geometry. The seismic section shown is generally difficult to interpret as aligned at an acute angle to the strike of the CSFS.

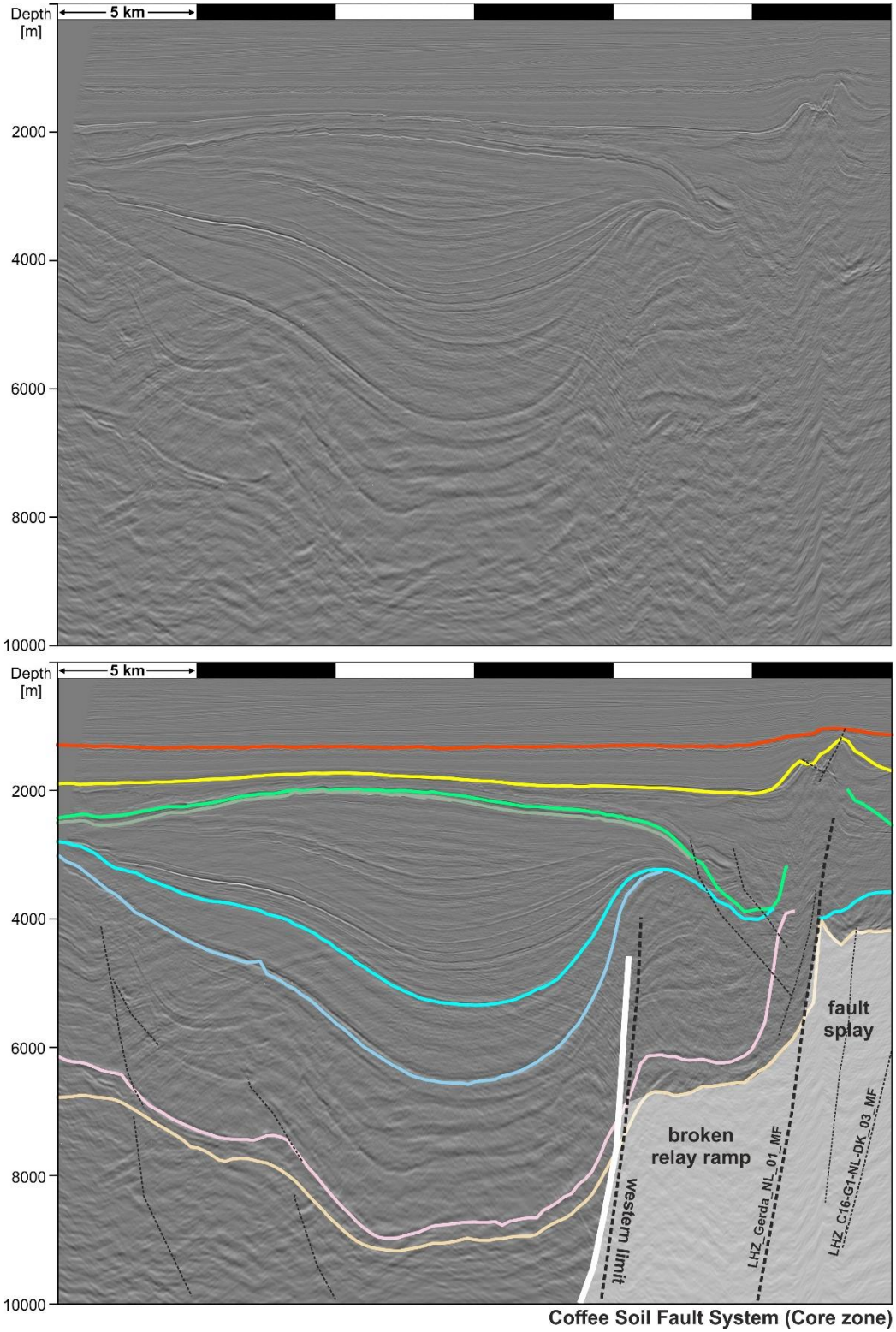

Figure 32: W-E oriented depth converted seismic section across the Dutch/German segment of the CSFS (see Figures 22 or 26 for location). Shown in the lower image are the seismic horizons of the harmonized Entenschnabel horizon model (Chapter 3.1) as well as the western limit of the CSFS "core zone". The eastern limit of the fault system, as here, is often not covered in the region by the seismic data (see also Figure 23). Presumably only minor Late Cretaceous structural inversion along the fault system. The main proportion of the fault offset of the CSFS is accumulated within this transect along two main faults. In general, no significant listric geometry of the basement faults.

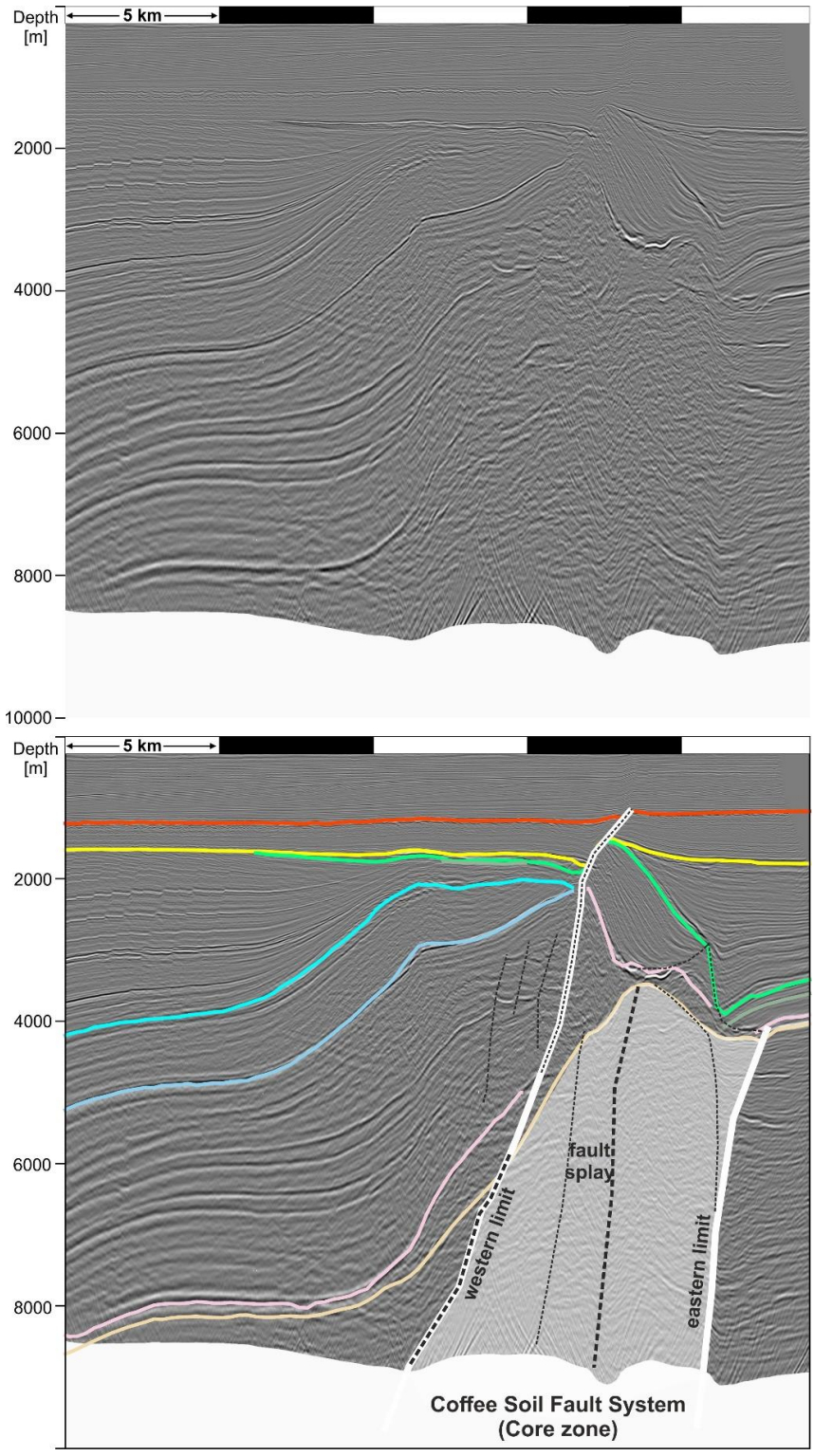

Figure 33: W-E oriented depth converted seismic section across the Dutch/German segment of the CSFS (see Figures 22 or 26 for location). Shown in the lower image are the seismic horizons of the harmonized Entenschnabel horizon model (Chapter 3.1) as well as the CSFS "core zone" with its eastern and western limits. The CSFS forms here a strongly faulted block which is seismically poorly imaged. No significant Late Cretaceous inversion along the fault system. The main proportion of the fault offset of the CSFS is accumulated within this transect along two main faults. In general, less listric component of the basement faults (thick-skinned to soft-linked style in the Mesozoic overburden). Rift-raft-like salt structure (Penge et al., 1999) is visible within the top of the CSFS.

3.2.5 Summary and outlook

As can be clearly seen from the detailed interpretation of the German CSFS segment and adjacent areas (Figure 21), the CSFS shows generally in the study area a complex structural pattern of intersecting and interleaving structures. Owing to this complex structure and the limited time frame of the project, a more detailed fault interpretation and modeling as presented here was not feasible. To achieve a more detailed and consistent fault model, it is generally mandatory to include also kinematic analysis and structural restoration of the CSFS into the modeling process. Only then can faults be modeled in a geological conclusive manner, since the “core zone” of the CSFS is subject to massive interpretational bias. Moreover, a detailed cross-border fault interpretation can only be achieved by providing more seismic data. For follow-up projects where cross-border fault modeling is sought, 3D seismic should be provided by the project partners if available. This would allow a more detailed fault interpretation than is possible with individual 2D seismic lines. Even with access to further high-resolution seismic data, however, uncertainties will still remain in fault models along such a complex fault system. Therefore, more efforts should be generally made in future fault modeling studies to capture and visualize uncertainties in interpretations (e.g. Zehner et al, 2019).

4 STRUCTURAL FRAMEWORK (NL-GER-DK North Sea)

4.1 Introduction

Within WP3, a Structural Framework (SF) was compiled for the Dutch, German and Danish North Sea and adjacent areas based on existing map and grid data (Figure 1). The need of a cross-border uniformly defined SF in terms of nomenclature, semantics, but also scale-independent unambiguous location of structural boundaries became obvious already with the beginning of the work of WP3. In a narrow sense, a SF can be considered as a consistent subdivision of the subsurface into structural domains, each of which has certain unique tectonostratigraphic histories or shows a distinct picture in its subsurface structure and geometry. In many cases, this kind of SF allows to explain changes in lithological distributions, petrophysical properties of rocks, as well as different fluid compositions, temperature distributions, and pressure states in the subsurface. An improved understanding of such interrelationships, referred to as Geomanifestations in the GeoEra research project GeoConnect³d, was also vital for various harmonization efforts in WP3, and therefore an attempt was made to develop a consistent SF for the study area.

One of the harmonization efforts of WP3 was the cross-border harmonization and modeling of the parameter seismic velocity (Deliverables 3.2 & 3.7). This parameter depends on a variety of influencing variables, of which lithology and burial depth are among the most important. These parameters, in turn, are a direct consequence of the overall tectonostratigraphic development of a region, and thus a SF may help to better understand regional differences in the seismic velocity. Deliverable 3.3, on the other hand, aimed to produce harmonized regional tectonostratigraphic charts for different structural elements in the North Sea. For some structural boundaries, however, clear definitions are lacking so far or there are uncertainties in their delimitation, which means that in more detailed studies in transitional areas, an assignment of the respective tectonostratigraphic history to a location cannot always be clearly assigned without a consistent SF. In Deliverable 3.4, the lithological and facial distribution was correlated between wells along two exemplary correlation profiles for the Jurassic and the Rotliegend. For a better understanding of changes in distributional pattern, it is also helpful to link them to a superordinate SF and the associated tectonostratigraphic history. Developing a harmonized seismic stratigraphy, as presented in Deliverable 3.5, also benefits from the definition of a SF, as seismic amplitude and other seismic parameters are strongly influenced by rheological parameters whose changes, as mentioned above, often coincide with boundaries in the higher-level SF.

In order to put the available geophysical base data and the derived parameters into the right context and thus to be able to evaluate them consistently, the partners in WP3 decided on a cross-border re-categorization and designation of structural domains of the deep subsurface of the German, Dutch and Danish North Sea and adjacent areas. The extent of the study area corresponds roughly to the red polygon in Figure 1, which represent the extent of WP3's transnational velocity model. The compiled SF extends thus from West to East over more than 400 km, and from South to North over c. 330 km. For this over-regional categorization approach 29 structural domains were defined (Figure 1).

4.2 Harmonization workflow & status of analysis

Due to the limited access to seismic data in the Danish and British North Sea sector, but also to adapt the work to the tight time frame of the project, the SF was developed in a first step based on a large number of map references and available grid data, which were merged into one data set (Figure 34a-e). The references used are listed and categorized within Appendix B according to their importance as a base for defining the borders of the SF and their relevance concerning the nomenclature and semantic used. Furthermore, the overview breaks down the references used into their specific content and regions referred to.

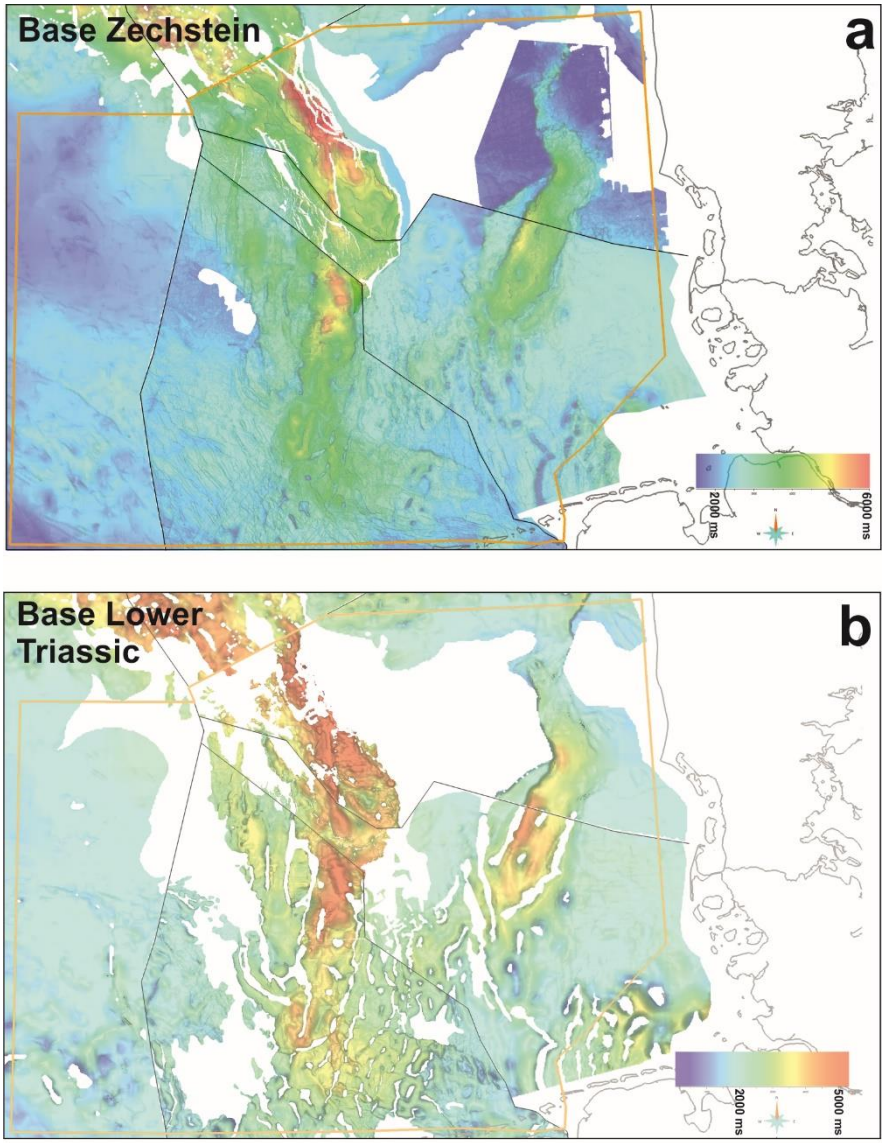

Figure 34 (continues on the next page): Seismic Travel Time [in ms] for different seismic horizons of the North Sea deeper subsurface. The maps are a compilations of over-regional (PGS Reservoir, 2006) and more detailed grid data of the geological national authorities of BGR, TNO & GEUS. The here presented grids have not yet been harmonized. However, discrepancies in this overview scale are only noticeable in a few places (e.g. Figure 34d). The grids from the Base Zechstein to the Base Cenozoic show further that the representation of structural patterns strongly depends on the respective reference level.

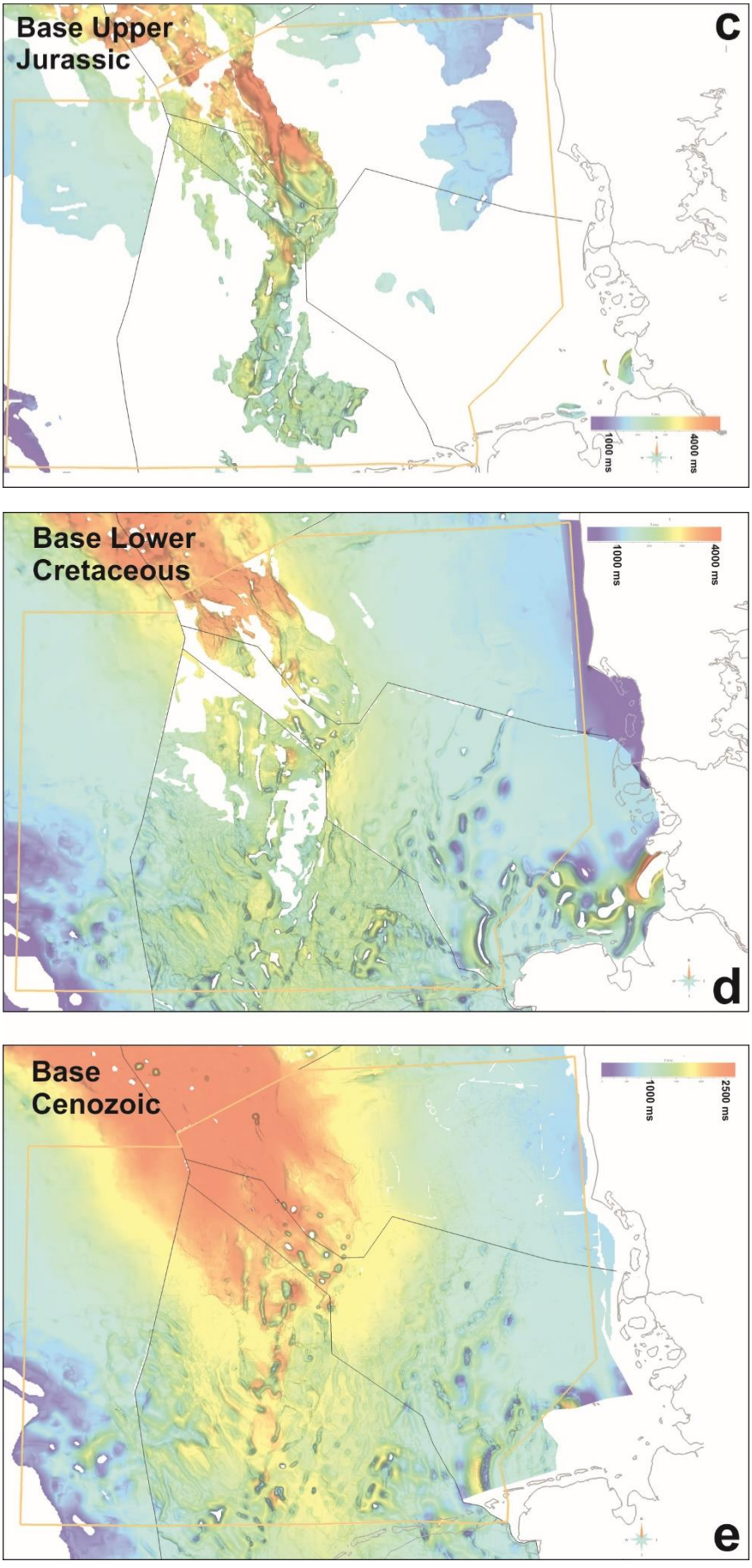

Figure 34 (see previous page for description).

After data compilation, the next step was to determine constrains and necessary definitions for defining structural domains in the same manner over the whole study area. In the course of this, the individual structural domains were classified according to their tectonostratigraphic most prominent and longest effective structural style from the Zechstein to the Late Cretaceous. The used categorization is: subsidence centre, transitional zone, platform or high (Figures 1 & 35). This does not preclude the possibility that these structural domains may also have temporarily adopted contrasting structural styles and structural positions during the Mesozoic.

Complementary to the selection of the Late Paleozoic to Late Mesozoic period as a general base for the SF, it was further necessary to determine a certain stratigraphic horizon to which the definition of the SF should generally refer. In the area of the North Sea this is of special importance, because due to halotectonic, especially of the Zechstein salinar, the structural style of the Pre-Zechstein and Post-Zechstein differ partly considerably. Ten Veen et al. (2012) discuss the influence of primary salt thickness on the resulting structural style (thin- or thick-skinned) of the Post-Salinar sedimentary cover. Because of the often strong masking effect of halotectonics, we decided to define the presented over-regional SF based on the depth of the Zechstein (or Top Pre-Zechstein). But in order to integrate existing structural definitions, compromises were also made in some cases. Thus, various structural domains in the study region, such as the Central Graben or the East North Sea High, were also defined according to distributional pattern of stratigraphic units. Therefore, the definition of boundaries based on the structure of the base Zechstein was made only where no boundaries between structural areas have been shown in published maps so far. Since the compilation presented here refers to published maps whose definition of structures is often ambiguous, this inconsistency in the definition of structural domains is also integral to the SF compiled.

Following the creation of a draft SF, the established structural boundaries were reviewed by the partners of GEUS and TNO for their offshore areas to ensure consistency. This review was based on regional horizon maps, but in particular also on seismic data. It turned out that in many places there are clear discrepancies between the proposals of the draft SF and the regional and local structural knowledge of the partners. A map section of the study area shown in Figure 35 indicates which structural boundaries can be reliably defined so far and which cannot be delineated with certainty. The reasons for the uncertain limits of structural domains can be manifold and includes, for example, different concept in defining structural borders (basement structures vs. distribution pattern; Figure 37). Furthermore, some boundaries can be generally difficult to define due to e.g. diffuse trends in distributional patterns or no clear basement structures (Figures 38 & 40). In addition to these conceptual uncertainties, technical uncertainties and limitations may also prevent a precise designation of SF boundaries. The reasons mentioned as well as other factors which may affect the delineation of structural boundaries are briefly summarized in Chapter 4.3.

Most of these problems concerning the precise delineation of structural boundaries can only be resolved by detailed reinterpretation based on seismic data and harmonized subsurface models, as well as integration of stratigraphic and lithofacies information into the models, and/or by time-consuming local studies. However, as this was not possible for the entire region due to time constraints of the project, the SF presented here should be considered as an important first step towards a more consistent SF of the Southern and Central North Sea on which future work can build on.

Since it was not possible to create a consistent SF for the entire region within the framework of the project, special attention was paid to introduce interested readers to the problem and providing them with the tools to work through this topic themselves. This goal is achieved by providing various digital products (Chapter 5) and comprehensive supplemental information on the region's SF in the Appendix to this report as well as in an additional report (Thöle & Jähne-Klingberg, 2021) that present an overview of structural elements of the southern Central and southern North Sea. Based on an interactive user interface, this report provides a quick insight into existing interpretive uncertainties and conceptual vagueness through a variety of seismic profiles that cross the individual structural domains and their boundaries. In addition to this, the general challenges in defining structural domains and building consistent structural frameworks for the area of the southern and central North Sea are briefly highlighted in the following chapter.

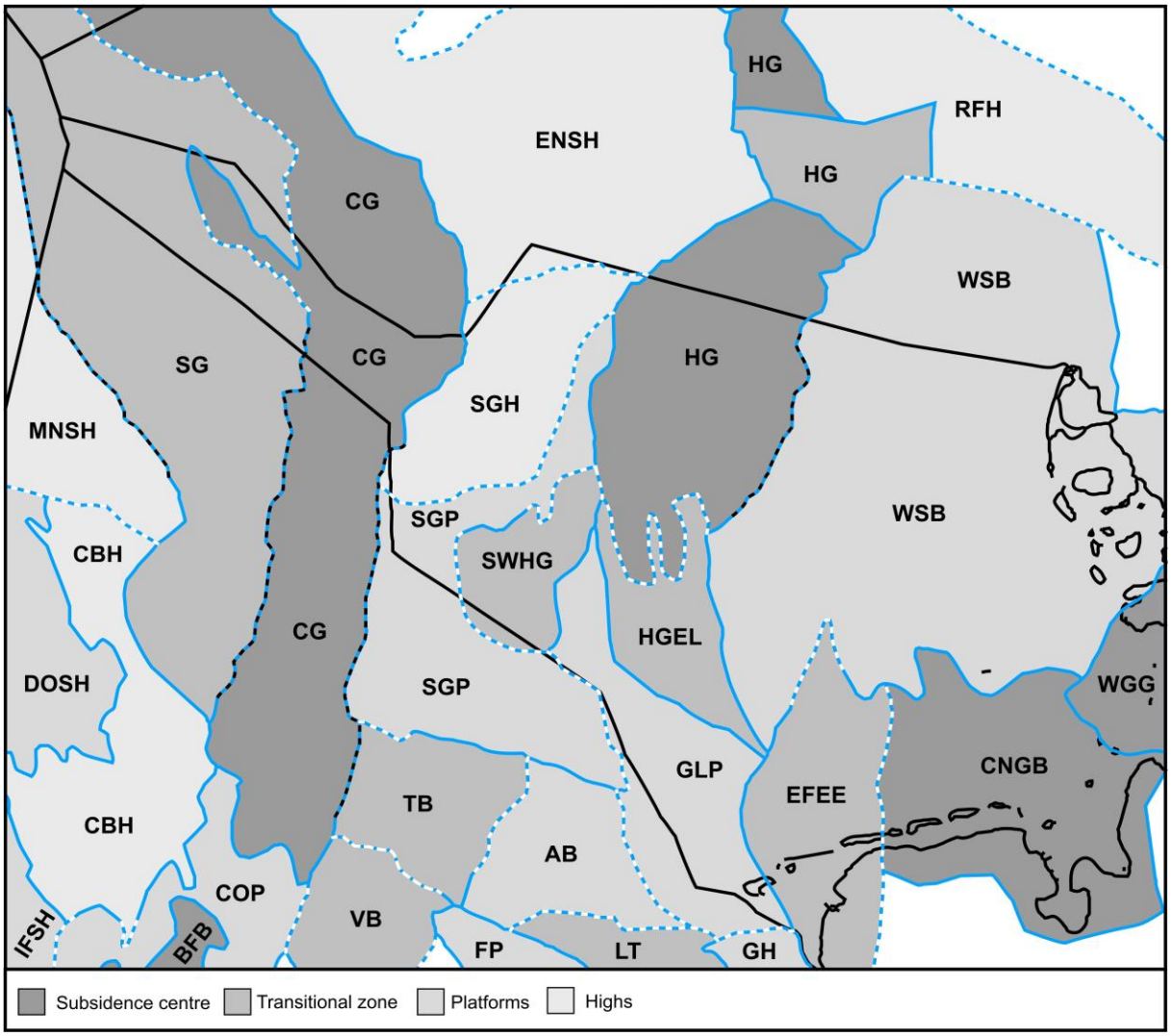

Figure 35: Preliminary map of main structural elements in the area of the Dutch, German and Danish North Sea Sectors. Obvious uncertain limits of structural elements which were under review in the project are indicated by dashed lines. Blue-black dashed lines: uncertain limits due to differing concepts in defining the boundaries, e.g. according to basement structures or distributional pattern (Figure 37). Blue-white dashed lines: boundaries difficult to define due to e.g. diffuse trends in distributional patterns or no clear basement structures. See Figure 1 for abbreviations of main structural elements.

4.3 Challenges in building a consistent SF for the study area

Building a SF generally involves the challenge to represent three-dimensional subsurface structures consistently within a map view. In a highly structured area such as the Southern and Central North Sea (Figure 18), this is particularly difficult, as shown earlier by the compilation of available fault interpretations for the eastern main fault of the Northern Central Graben (Coffee Soil Fault System) in Appendix A. Due to different degrees of detail and the different concepts behind the available fault interpretations, a consistent harmonization of derived fault lineaments and models is hardly possible or can only be guaranteed by strong generalization. Therefore, cross-border harmonization of faults in detail as well as the definition of a consistent SF of this region is only possible through prior harmonization work on seismic stratigraphic concepts (D3.5; Thöle et al., 2020), on time interpretations of prominent seismic horizons (D3.6; Thöle et al., 2021) and on the velocity model (D3.7; Doornenbal et al., 2021) of the study region as well as detailed cross-border fault interpretation studies (e.g. Chapter 3.2).

In the course of this study, a comprehensive discussion of all possible inconsistencies and uncertainties arising in the designation of structural domains was not possible. However, a brief summary of possible challenges and uncertainties in the delineation of SF boundaries is given below. This is followed by a brief outlook on the implementation of a cross-scale SF using the German Entenschnabel as an example. Individual aspects of this local multi-scale SF are clarified in large-format overviews in the Appendix C-G.

4.3.1 Challenges and uncertainties in the designation of structural domains.

Today's determining structural pattern of a region is mostly the result of a multitude of tectonic events, which in Western Europe and within the North Sea cover a period of more than 400 Mio years (e.g. Doornenbal & Stevenson, 2010). In the further structural development, the structures of previous deformation events are often overprinted (rotated, folded, overturned, segmented) during subsequent events. However, there are always zones of weakness that can be reactivated over a long period of time (Appendix E). Because of differences in stress orientation, the structural style as well as rheological and fluid conditions, pre-existing faults/structures are often only reactivated in parts, so that with each further deformation event the structural fabric of these long-living fault zones becomes more and more difficult to understand. The Central Graben and the Coffee-soil fault are examples of complex structures where it is difficult to consistently represent all important structures and their borders across multiple scales in a SF based on polylines in map-view (Appendix & Chapter 3.2). Uncertainties in the designation of an SF that are related to the complexity of structures or are a consequence of increased interpretational bias, due to often insufficient informative value of the base data in these faulted areas, are only one group of ambiguities in the definition of structural boundaries. Depending on the selected database, technical uncertainties and limitations may also prevent a precise designation of SF boundaries. Furthermore, ambiguities of a SF can also arise because underlying concepts are inconsistent or cannot be applied equally over the entire area of the study region. In the following section, these aspects are briefly described.

4.3.1.1 *Technical ambiguities & limitations:*

Technical uncertainties and limitations refer, on the one hand, to inaccuracies caused by insufficient data density or data quality as well as uncertainties in data processing, digitalization, georeferencing and representation of data on a map. On the other hand, this point also includes ambiguities resulting from what can be meaningfully represented at all in different scales. This is ultimately an unnecessary question in freely zoomable and scalable 3D models. However, even today a large part of geoscientific analysis work is still carried out on the basis of 2D maps in GIS-Systems. Thus, the question of how to consistently map as much 3D information as possible in 2D and make it analyzable is still relevant today. The ambiguities of mapped 2D fault information are comprehensively illustrated by the example of the Coffee Soil Fault in the Appendix A. Other examples are:

- Level of detail strongly decreases with depth as data density and resolution decrease. The consequence could be that the importance of some pre-existing deep structures cannot be properly assessed. If the SF is related to deep seated structures, this should be attributed with a sufficient spatial bias.

- Structures with a low dip or important listric faults with high horizontal offsets: For representation as one lineament/polyline in map view this faults must be strongly generalized. Therefore, it is probably also useful to show boundaries between structural domains themselves as polygons, quasi as a structural zone - at least in detailed views.

- Misties between different geophysical datasets and ambiguities in the reference level of wells and seismic. These inaccuracies are more relevant at detailed scales and in reservoir studies

- Since most structural investigations in sedimentary basins are based on seismic data, the seismic processing and the uncertainty of the underlying seismic velocity model play a significant role in the consistency of interpretations based on these data.

4.3.1.2 *Fault related "allocation uncertainty":*

This portion of the methodological vagueness includes the conceptual allocation mismatch of the structural domain border which is related to the given fault geometries. In addition, especially in strongly faulted areas, the decrease in seismic resolution also increases interpretational bias. Several examples of this category of uncertainty are highlighted in Thöle & Jähne-Klingberg (2021). Other examples for this kind of uncertainty are:

- Listric main faults with often high horizontal offsets: Determination whether hanging wall or footwall cut-offs are presented within the SF. From this follows that the respective wide fault zone and its individual faults would be assigned to different structural domains.

- A high interpretational bias in areas of high structural complexity and with less or contradictory base data: The borders of the SF needs to be attributed with a spatial bias and an uncertainty of interpretation.

- Figure 36 shows a very simplified case. Complex structures that have been reactivated several times over the geological history, also with different meanings, often do not

show horizon cut-offs that can be clearly interpreted (inverted fault zones or wrench tectonics.

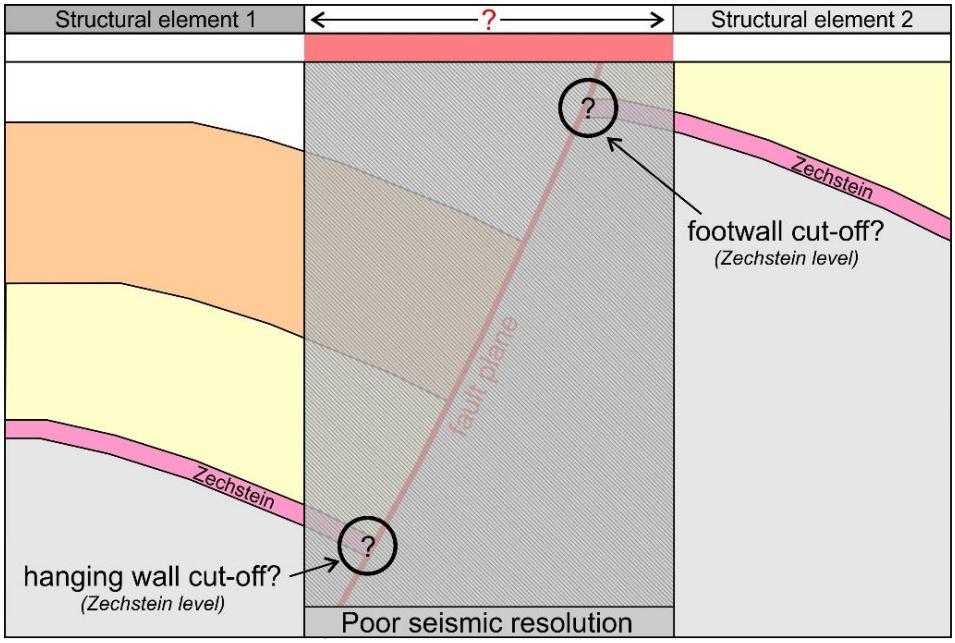

Figure 36: Sketch showing typical ambiguities in defining a SF border based on uncertain fault interpretations, summarized under the term "allocation uncertainty" introduced here.

4.3.1.3 Conceptional uncertainties/ambiguities:

Conceptional uncertainties result from the fact that in a study region the underlying concepts and assumptions are usually not applied uniformly over the entire area. Here, it is relatively clear that with the size of the working region or the structural complexity of a region, the "conceptional uncertainty" also increases. In Chapter 4.2, it was discussed that compromises in the designation of structure domains had to be made in order to implement existing designations based on other concepts in the own implementation of a SF which, however, increases the conceptual fuzziness in the end. Several examples of this type of uncertainty are highlighted in Thöle & Jähne-Klingberg (2021). Other examples for this kind of uncertainty are:

- Different structural styles, geometries & orientations in different structural levels (Pre-Zechstein Basement, Mesozoic cover, Tertiary cover), because of different degree of thick-skinned and thin-skinned tectonics caused by halotectonics or detachment tectonics. For consistent representation in map view one structural level must be defined as base for categorization for the whole study area.

- Level of detail strongly decreases with depth or when erosion events destroy the signs of past deformation events. The consequence is that the importance of some pre-existing structures or their underlying development history cannot be properly assessed: borders of the SF needs to be attributed with a spatial bias and an uncertainty of interpretation in such cases.

- What is the base for designation of the SF: lithological, thickness & facial trends or faults: In some regions, there is not the one fault or fault system that forms the boundary between structural domains (Figures 38 & 40). However, there are obvious changes in

thickness, lithology, or facies of certain stratigraphic units in partial 10's of km wide zones that suggest a different structural genesis of these regions.

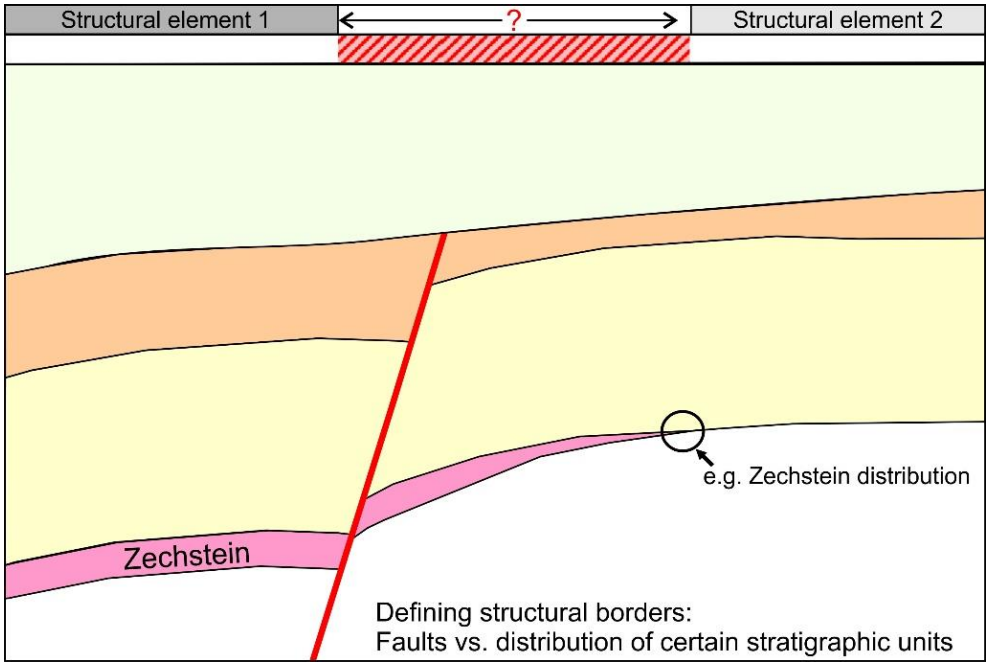

Figure 37: Sketch showing a typical case of "conceptional uncertainty" in defining a SF border on the base of stratigraphic distributional pattern or faults with characteristic to be determined uncertainly.

- Sometimes a transition between two structural domains to be distinguished is characterized by zones sometimes 10's of km wide with faults of the same genesis, kinematics, and offsets (Figure 38).

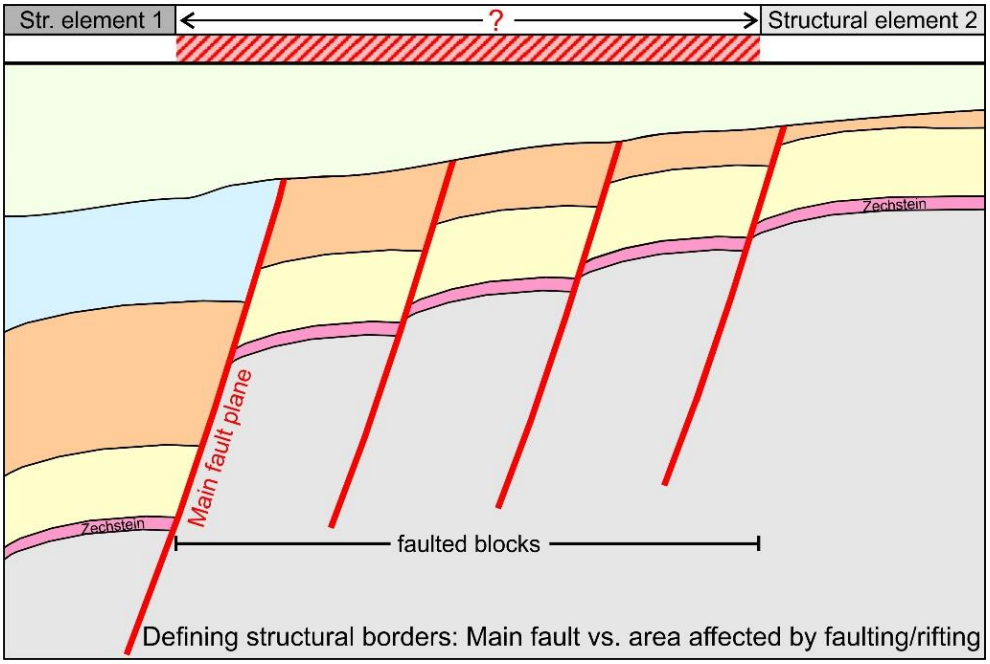

Figure 38: Sketch showing a typical case of "conceptional uncertainty" in defining a SF border in transitional areas with wide zones of faulted blocks with same offsets and kinematics.

4.3.2 Two examples of conceptional uncertainty in the study area

4.3.2.1 The East North Sea High and adjacent areas

As previously mentioned, the SF presented here was related to the structure at the base of Zechstein and, in exceptions, also at the base of other Mesozoic horizons (e.g. Upper Jurassic). However, some structural highs, such as the Mid North Sea High or even the East North Sea High, cannot be subdivided more precisely with respect to the top Pre-Zechstein area or younger horizons. Also because there is an economic interest in the Pre-Zechstein of this region, therefore, a structural subdivision based on the Pre-Zechstein has tended to establish itself in this region. Brackenridge et al. (2020) use a Wheeler diagram along a seismic transect to show very clearly that the Mesozoic overburden contains few structures that would be distinguishable from one another or that deeply incisive erosional events have eroded much of the Mesozoic succession. In contrast, Arsenikos et al. (2015), among others, show a detailed structural subdivision of this regions based on the structure of the Paleozoic basement.

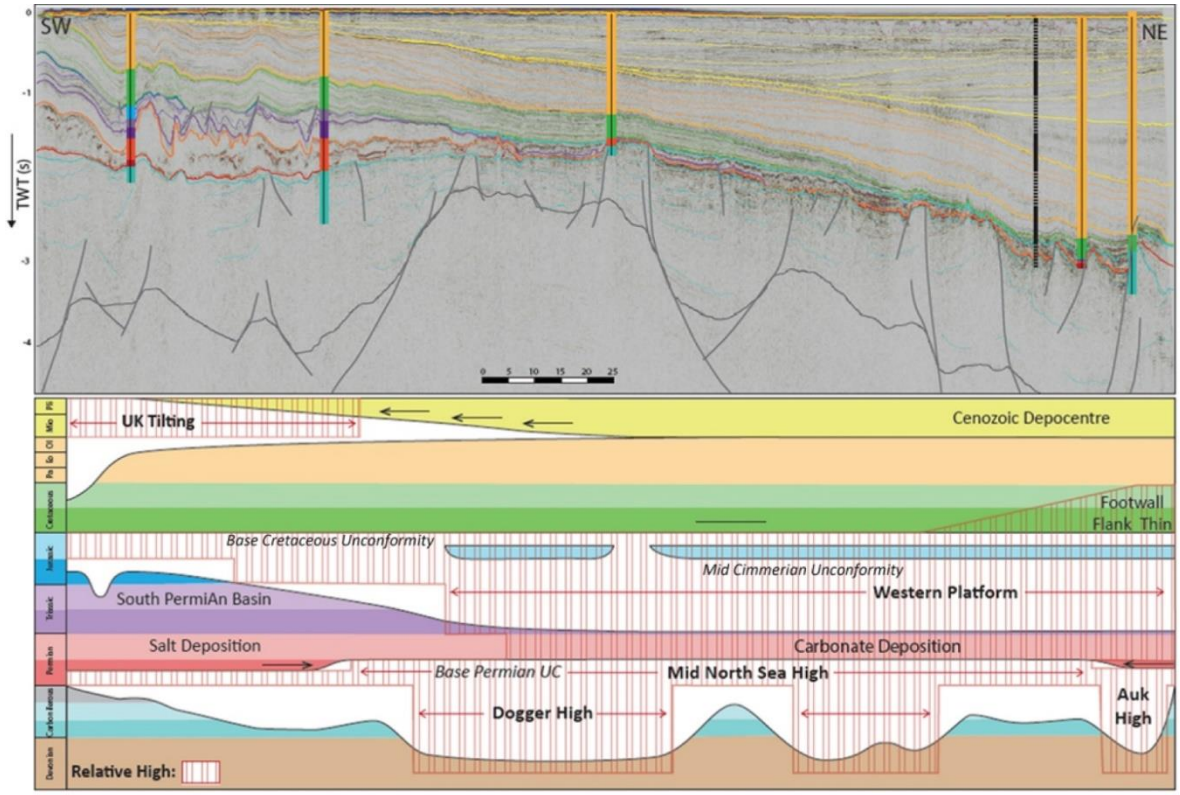

Figure 39: Interpreted SW-NE seismic section (OGA 2015_L18) with a wheeler diagram on the base of seismic interpretation taken from Brackenridge et al. (2020).

4.3.2.2 The southern Coffee Soil/ Schillgrund Fault within the Dutch offshore

As sketchily indicated in Figure 38, the fault offset between a basin and adjacent highs and platforms can be distributed over broad zones. In these zones, faults of the same kinematics, with the same dip and similar offset magnitudes are often found. In the current version of the SF, the boundary between the Central Graben & Schillgrund Platform/Terschelling Basin structural domains runs along the westernmost of these faults (Figure 40). In principle, these rotated fault blocks could still be counted as part of the Central Graben from the point of view of their structural development and kinematics. However, in the Netherlands the structure domain Central Graben is defined by the distribution of thick Jurassic which does not always correspond to the fault characteristics at the base Zechstein.

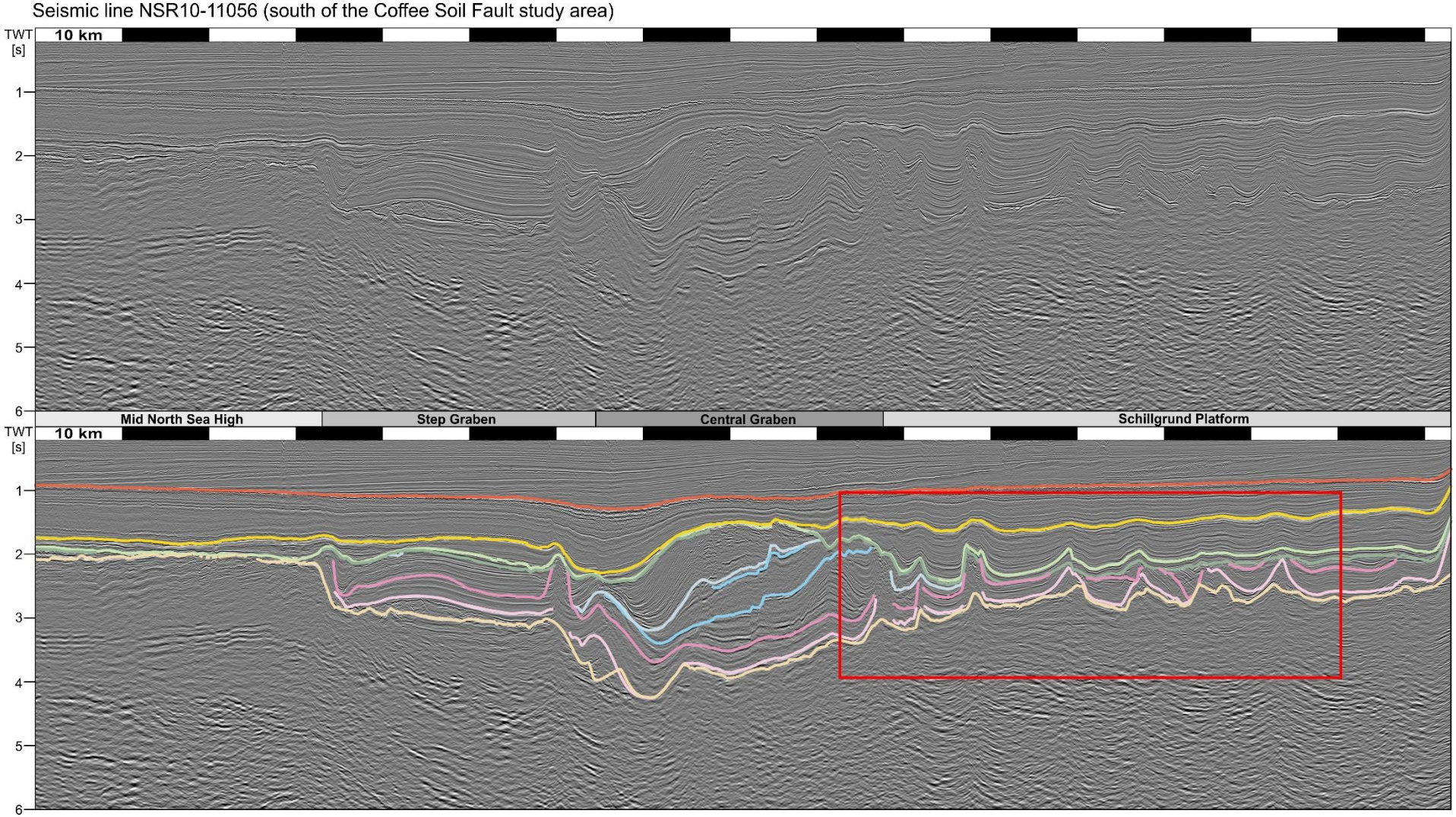

Figure 40: Seismic section across the eastern flank of the Dutch Central Graben. In the bottom picture the seismic section is overlaid by DGM-DEEP V5 grids. The red rectangle show the area with in sub-chapter 4.3.2.2 discussed "conceptional uncertainty"

4.4 Outlook: Developing a multi-scale SF – an example from the German Entenschnabel

The previous chapters focused almost exclusively on the implementation and ambiguities/uncertainties of an over-regional SF in the area of the Danish, German and Dutch North Sea. For the future, however, it would be desirable to implement a cross-scale SF for this region. Currently, however, the existing fault data, compiled in the HIKE database (Figure 18), are not sufficient for a cross-border harmonization of structures at detailed scales. This also indicates that a consistent cross-scale and cross-boundary designation of a SF, as was done in the GeoConnect³d R2R study (van Daele et al., 2021) using some faults of the Roer Valley – Rhine rehion as example, is not yet possible for the whole study area with the currently available fault interpretations. Fault data interpreted in the course of former BGR projects within the German Entenschnabel (GPDN 2009-2013 / TUNB 2014-2021), however, allow us to implement a consistent cross-scale SF as an example. Individual aspects of this multi-scale SF are clarified in large-format overviews in the Appendix:

Appendix C: This overview slide compares different scale representations of similar structure overviews using the same example of the German Entenschnabel. This overview is intended to give a feeling for the level of detail that should be chosen for the subdivision of the structure domains, the representation of faults and the naming of the structures in order to ultimately maintain readability at each scale. The Entenschnabel covers parts of the Central Graben, the Step Graben and in the most SE of the Schillgrund High. In the supra-regional scale the Step Graben and Central Graben could be defined together as the Central Graben, as the Step Graben and its structural features ultimately represent the strongly rifted half-graben shoulder of the Central Graben.

Appendix D: This overview slide gives an overview of 1st & 2nd order structural features in the German Entenschnabel area. In addition, it is made clear how many map sheets would have to be produced in order to be able to depict the structure image to scale.

Appendix E: Based on several illustrations and short descriptions, basic information on structural development, tectonostratigraphy and structural style in the German Entenschnabel is presented. The understanding of the regional geological basics presented here is the basis for creating a consistent SF of the region.

Appendix F: In this overview, the structures of the region are broken down and assigned to different scales of representation according to their extent and importance. The structures of the Entenschnabel were first comprehensively and coherently presented by Wride (1995). Therefore, the naming of individual structures was often adopted from Wride (1995), even if the structures in the draft presented here are partly presented in a different context. This kind of categorisation of individual structural features is a first proof of concept.

Appendix G: This overview shows the location of the structures categorised in Appendix E. Due to the large number of structures and limitations in the presentation, three overviews were prepared, each representing the following structure groups: Structural low's/grabens; highs & transitional areas; faults & linear structural features.

4.5 Links & synergies with HIKE & GeoConnect³d

The GeoERA research projects HIKE and GeoConnect³d as well as the study presented here address a similar topic field with overlapping tasks. The HIKE project has as its main goal a cataloguing of fault data in a database and an integration of a variety of additional fault information using a unified semantic concept. In this context, fault data from the Dutch, German and Danish North Sea were also integrated (Figure 18, 3DGEO-EU WP5). However, these data were not available until later in the course of the work in WP3, which meant that it was not possible to validate and adapt the SF presented here to these data. Clearly, these are synergy potentials for the future between the continued development of a SF in the region of North Sea and the integration of consistent fault data with additional information into the HIKE fault database.

The basic concepts for the creation and visualization of a multi-scale SF were developed within the GeoConnect 3D project, also with the participation of BGR and TNO. These concepts were adapted and partially implemented for the study area in the North Sea as part of BGR's work for GeoConnect 3D (WP2). However, since there was a stronger link between the work on the North Sea SF and the work in the 3D-GEO-EU WP3, and other work e.g. on geomanifestations were not implemented, this study could not be published as a pilot region in the GeoConnect³d product canon. However, since the definition of a SF presented here on exclusively published maps and grid data, as well as its validation with a dense network of geophysical data, is a particularly unique feature of this study, there is a clear added value from the results presented here, especially when evaluating uncertainties of a SF. Another difference is that the pilot areas presented in GeoConnect³d are strongly related to surface geology. This is not the case in the North Sea. The deeper subsurface of the central and southern North Sea is covered by partly thick Quaternary and Tertiary sediments. The Tertiary and Quaternary forms a broad northward dipping basin structure which appears hardly differentiated in itself (Figure 34e). This structure is fundamentally different from the underlying Mesozoic (Figure 34b-d) and Late Paleozoic (Figure 34a) successions which represent a strongly structured basin system (Appendix E). The Paleozoic basement, in turn, consists largely of a rifted passive shelf and, in the south, of outliers of a Variscan foreland basin. In addition, Late Paleozoic volcanic rocks are also included in this sequence. This complex overlap of structures cannot be consistently represented in one SF without producing overlaps. Thus, the structural pattern of the Mesozoic was predominantly used to define the structural domains in the North Sea area. In contrast, SF in the GeoConnect³d onshore pilot regions predominantly relate to structural patterns of the surface geology. Thus, the SF in the R2R pilot study (van Daele et al., 2021) is significantly defined by Variscan basement patterns, covered by Mesozoic basin and platform sediments as well as Tertiary rifting. Since the study presented here is entirely in the center of a sedimentary basin and different epochs do not have to be represent equally in the designation of structural domains and also different geomanifestations would be of importance for the offshore, there are inevitably also differences in the creation of the Structural Framework's of these fundamentally different regions. When in the future hopefully area-wide Structural Framework's have been created according to the principles of GeoConnect³d, a harmonization of these individual model concepts will certainly become necessary, since regional peculiarities of the geology always make compromises in the implementation of a generalized SF-approach necessary. Thus, these regional SF's will certainly differ even if only in details at first. Only by harmonizing the differences in the approaches and definitions of existing and future regional SF, which are not yet obvious in the pilot study stage, the long-term goal of a consistent multi-scale SF for the whole of Europe can be achieved.

5 PROVIDED DIGITAL PRODUCTS

Table 4: Overview of digital products provided with Deliverable 3.8. The seismic velocity volumes generated are only available on request.

<table>
<tr><th colspan="4">Provided digital data</th><th>Data format</th><th>Region covered</th></tr>
<tr><td rowspan="6">Time-to-depth conversion</td><td rowspan="2">Input data</td><td colspan="2">V0-K_velocity grids + Vint grid
Velocity data compiled for the transnational velocity model in D3.7 (Doornenbal et al., 2021)</td><td>CPS3</td><td>(UK)-NL-GER-DK Offshore sectors</td></tr>
<tr><td colspan="2">Closed horizon grids in TWT
Entenschnabel (ES) horizon model</td><td>Incl. salt stuctures
Excl. salt structures</td><td>CPS3</td><td rowspan="6">Entenschnabel (ES) region</td></tr>
<tr><td rowspan="3">Final product</td><td colspan="2">Seismic velocity volumes with average velocities
Available on request</td><td>Incl. salt stuctures
Excl. salt structures</td><td>SEGYs</td></tr>
<tr><td colspan="3">Please contact: Hauke.Thoele@bgr.de or Fabian.Jaehne-Klingber@bgr.de</td></tr>
<tr><td rowspan="4">Harmonized depth models</td><td rowspan="2">ES horizon model</td><td colspan="2">Open horizon grids in m</td><td rowspan="3">Z-MAP / CPS3</td></tr>
<tr><td colspan="2">Closed horizon grids in m</td><td>Incl. salt stuctures
Excl. salt structures</td></tr>
<tr><td rowspan="2">CSF model</td><td>Input data</td><td>Detailed fault interpretation in TWT & TVD
Starting point for cross-border fault modeling</td><td rowspan="2">DXF / GOCAD TSURF (.ts) & PLINE (.pl)</td><td>German segment of the Coffee Soil Fault and adjacent areas</td></tr>
<tr><td colspan="2">Generalized fault model in TVD
incl. uncertainties</td><td>Cross-border segment of the Coffee Soil Fault</td></tr>
<tr><td colspan="2" rowspan="2">Structural Framework</td><td colspan="2">Structural Framework (UK)-NL-GER-DK North Sea</td><td>shapefile</td><td rowspan="2">(UK)-NL-GER-DK Offshore sectors</td></tr>
<tr><td colspan="2">Supporting document to Deliverable 3.8:
“Discovery of structural elements and their uncertain limits in the southern and central North Sea”.</td><td>Interactive PDF</td></tr>
</table>

6 ACKNOWLEDGMENT

We thank Emerson for providing Paradigm Software Package licenses via the Academic Software Program (https://www.pdgm.com/affiliations/academic-software-programs/) to support the national geological services in their non-profit work for the public and education. This will enable BGR to develop a variety of digital products on the subsurface and make them available. The digital products created and presented in Chapters 2 & 3 using Paradigm Suite and SKUA-GOCAD can be freely reused under the condition of referencing our products.

Finally, the authors would like to thank Stefan Knopf (BGR) for his excellent and devoted coordination of the 3DGEO-EU project. Only because of your support we were able to put all our efforts into our products.

7 REFERENCES

7.1 Report

Andsbjerg, J. & Dybkjær, K. (2003): Sequence stratigraphy of the Jurassic of the Danish Central Graben. Geological Survey of Denmark and Greenland Bulletin, 1: pp. 265-300.

Arfai & Jähne-Klingberg (2013): Depth & Thickness maps German Entenschnabel. https://www.gpdn.de/?pId=1591#p1591

Arfai, J., Jähne, F., Lutz, R., Franke, D., Gaedicke, C. & Kley, J. (2014): Late Palaeozoic to Early Cenozoic geological evolution of the northwestern German North Sea (Entenschnabel): New results and insights. Netherlands Journal of Geosciences, 93, 04: pp. 147-174. DOI:doi:10.1017/njg.2014.22

Arsenikos, S., Quinn, M.F., Pharaoh, T., Sankey, M and Monaghan, A.A. (2015): Seismic interpretation and generation of key depth structure surfaces within the Devonian and Carboniferous of the Central North Sea, Quadrants 25 – 44 area. British Geological Survey Commissioned Report, CR/15/118. 67pp.

Baldschuhn, R., Binot, F., Fleig, S. & Kockel, F. (2001): Geotektonischer Atlas von Nordwest-Deutschland und dem deutschen Nordsee-Sektor. (Geologisches Jahrbuch). Vol. A: p. 88 S. mit 3 CD ROMs; Hannover (Schweizerbart´sche Verlagsbuchhandlung).

Bouroullec, R., Verreussel, R., Boxem, T., de Bruin, G., Zijp, M., Janssen, N., Kerstholt-Boegehold, S., Munsterman, D. and Kőrösi, D. (2016): COMMA Project – Understanding Jurassic Sands of the Complex Margins of the eastern part of the Terschelling Basin during the Upper Jurassic and Lowermost Cretaceous. TNO report 2016 R11341, 124pp.

Bouroullec, R., Verreussel, R., Geel, K., Munsterman, D., de Bruin, G., Zijp, M., Janssen, N., Millán, I. and Boxem, T. (2016): FOCUS – Upper Jurassic Sandstones: Detailed sedimentary facies analyses, correlation and stratigraphic architectures of hydrocarbon bearing shoreface complexes in the Dutch offshore. TNO report, 274pp.

Britze, P., Japsen, P. and Andersen, C., (1995a): Danish Central Graben : "Base Cretaceous" and the Cromer Knoll Group : (two-way traveltime and depth, interval velocity and isochore). Kortserie / Danmarks Geologiske Undersøgelse ; 49. DGU, København

Britze, P., Japsen, P. and Andersen, C., (1995b). Danish Central Graben : "Base Upper Jurassic" and the Upper Jurassic : (two-way traveltimes and depth interval velocity and isochore). Kortserie / Danmarks Geologiske Undersøgelse ; 50. DGU, København.

Brackenridge, R.E., Underhill, J.R., Jamieson, R. & Bell, A. (2020): Structural and stratigraphic evolution of the Mid North Sea High region of the UK Continental Shelf. Petroleum Geoscience: pp. petgeo2019-076. DOI:10.1144/petgeo2019-076

Brennand, T.P., Hoorn, B. Van and James, K.H. (1990): Historical review of North Sea exploration. Introduction to the Petroleum Geology of the North Sea, K.W. Glennie (ed.), 1-33. Blackwell Scientific Publications, Oxford.

Cartwright, J.A. (1987): Transverse structural zones in continental rifts - an example from the Danish sector of the North Sea. (In: BROOKS & GLENNIE (Eds.): Petroleum Geology of North West Europe). pp. 441-452; London (Graham Trotman).

Cloetingh, S., Van Wees, J.-D., (2005): Strength reversal in Europe's intraplate lithosphere: Transition from basin inversion to lithospheric folding. Geology 33, 285-288.

de Bruin, G., Bouroullec, R., Geel, K., Fattah, A.R., van Hoof, T., Pluymaekers, M., van den Belt, F., Vandeweijer, V. & Zijp, M. (2015): New petroleum plays in the Dutch Northern Offshore, Report R10920, 104 p., TNO, Utrecht.

Doornenbal, J.C. & Stevenson, A.G. (2010): Petroleum Geological Atlas of the Southern Permian Basin Area. 341 p.; Houten (EAGE Publications b.v. Houten).

Doornenbal, H., den Dulk, M., Thöle, H., Jähne-Klingberg, F., Britze, P. & Jakobsen, F. (2021): Deliverable 3.7 – A harmonized cross-border velocity model. GEOERA 3DGEO-EU; 3D Geomodeling for Europe; project number GeoE.171.005., Report, 33 p.

Evans, D.J., Graham, C., Armour, A. & Bathurst, P. (2003): The Millennium Atlas: Petroleum geology of the central and northern North Sea. 390 p.; London (The Geological Society).

Groß, U., (1986): Gaspotential Deutsche Nordsee – Die regionale Verteilung der seismischen Anfangsgeschwindigkeiten in der Deutschen Nordsee. Bundesanstalt für Geowissenschaften und Rohstoffe (BGR), Hannover, pp. 58.

Japsen, P., (1993): Influence of lithology and Neogene uplift on seismic velocities in Denmark: implications for depth conversion of maps. American Association of PetroleumGeologists Bulletin 77, No.2: 194-211.

Japsen, P., Britze, P. & Andersen, C. (2003): Middle Jurassic to Early Cretaceous-Lower Cretaceous of the Danish Central Graben: structural framework and nomenclature. In: Ineson, J.R. & Surlyk, F. (eds) The Jurassic of Denmark and Greenland. Geological Survey of Denmark and Greenland Bulletin, 1, pp. 233–246.

Jürgens, U., Schöneich, H., (1989): Darstellung und Benennung der Salzstrukturen in der Deutschen Nordsee. Erdöl, Erdgas, Kohle, Petrochem. 105, 10 - 11, 11 Abb.

Kley, J., (2018): Timing and spatial patterns of Cretaceous and Cenozoic inversion in the Southern Permian Basin. Special Publication - Geological Society of London 469, 19-31.

Kley, J., Franzke, H.-J., Jähne, F., Krawczyk, C., Lohr, T., Reicherter, K., Scheck-Wenderoth, M., Sippel, J., Tanner, B., van Gent, H., (2008): Strain and Stress, in: Littke, R., Bayer, U., Gajewski, D., Nelskamp, S. (Eds.), Dynamics of Complex Intracontinental Basins, The Central European Basin System. Springer, Berlin, pp. 97-124.

Klinkby, L., Kristensen, L., Nielsen, E.B., Zinck-Jørgensen, K., Stemmerik, L., (2005): Mapping and characterization of thin chalk reservoirs using data integration: the Kraka Field, Danish North Sea. Petroleum Geoscience 11, 113-124.

Kombrink, H., Doornenbal, J.C., Duin, E.J.T., den Dulk, M., ten Veen, J.H. & Witmans, N. (2012): New insights into the geological structure of the Netherlands; results of a detailed mapping project. Netherlands Journal of Geosciences - Geologie en Mijnbouw, 91, 4: pp. 419-446. DOI:10.1017/S0016774600000329

Malz, A., Doornenbal, H., Müller, C.O., Wächter, J., Szynkaruk, E., Malolepszy, Z., Jahnke, C., Obst, K., Żuk, T., Toro, R., Izquierdo-Llavall, E., Casas, A.M., Ayala, C., Pueyo, E.L., Jähne-Klingberg, F. and Thöle, H. (2021): Deliverable 5.1 – Methods, bottlenecks, best practices and accompanying descriptions to faults in 3D models. GEOERA 3DGEO-EU; 3D Geomodeling for Europe; project number GeoE.171.005. Report, 67 p.

Møller, J.J. & Rasmussen, E.S. (2003): Middle Jurassic-Early Cretaceous rifting of the Danish Central Graben. (In: Ineson, J.R. & Surlyk, F. (Eds.): The Jurassic of Denmark and Greenland). Vol. 1. Geological Survey of Denmark and Greenland Bulletin: pp. 247-264; (Geological Survey of Denmark and Greenland Bulletin).

Naqi, M. (2016): Salt-influenced normal faulting related to salt-dissolution and extensional tectonics: 3D seismic analysis and 2D numerical modeling of the Salt Valley salt wall, Utah and Danish Central Graben, North Sea. PhD thesis, 168pp.

NOPEC (1988): North Sea Atlas - Major structural elements. map. [London] (NOPEC).

NPD (2019): Structure elements in the Norwegian Continental Shelf. Shape-File: https://www.npd.no/en/facts/geology/structure-elements/

Penge, J., Munns, J.W., Taylor, B. & Windle, T.M.F. (1999): Rift-raft tectonics: examples of gravitational tectonics from the Zechstein basins of northwest Europe. (In: Fleet, A.J. & Boldy, S.A.R. (Eds.): Petroleum Geology of Northwest Europe: Proceedings of the 5th Conference). pp. 201-213; London (The Geological Society).

Pharaoh, T.C., (1999): Palaeozoic terranes and their lithospheric boundaries within the Trans-European suture zone (TESZ); a review. Tectonophysics 314, 17-41.

PGS Reservoir (2006): North Sea Digital Atlas - Version 2.06 (NSDA-2.06), Industrial report 2003, PGS Reservoir, Berks, UK.

Reinhardt, L., Krüger, A. and Zeiler, M., 2010. Geopotenzial Deutsche Nordsee. Geowissenschaftliche Mitteilungen, 41: 6-16.

Robein, E., (2003): Velocities, Time-imaging and Depth-Imaging in Reflection Seismics. Principles and Methods, EAGE Publications b.v.

Schnabel, M., Noack, V., Ahlrichs, N. and Hübscher, Chr. (2021): A comprehensive model of seismic velocities for the Bay of Mecklenburg (Baltic Sea) at the North German Basin margin: implications for basin development. Geo-Marine Letters, https://doi.org/10.1007/s00367-021-00692-w

Smit, F.W.H., van Buchem, F.S.P., Holst, J.C., Lüthje, M., Anderskouv, K., Thibault, N., Buijs, G.J.A., Welch, M.J. & Stemmerik, L. (2018): Seismic geomorphology and origin of diagenetic geobodies in the Upper Cretaceous Chalk of the North Sea Basin (Danish Central Graben). Basin Research, 30, 5: pp. 895-925. DOI:10.1111/bre.12285

Stemmerik, L., Ineson, J.R. & Mitchell, J.G. (2000): Stratigraphy of the Rotliegend Group in the Danish part of the Northern Permian Basin, North Sea. Journal of the Geological Society, 157, 6: pp. 1127-1136. DOI:10.1144/jgs.157.6.1127

ten Veen, J.H., van Gessel, S.F. & den Dulk, M. (2012): Thin- and thick-skinned salt tectonics in the Netherlands; a quantitative approach. Netherlands Journal of Geosciences, 91, 04: pp. 447-464. DOI:doi:10.1017/S0016774600000330

ter Borgh, M.M., Jaarsma, B. & Rosendaal, E.A. (2019): Structural development of the northern Dutch offshore: Paleozoic to present. Geological Society, London, Special Publications, 471, 1: pp. 115-131. DOI:10.1144/sp471.4

The CRETSYS Project (2017): The Cretaceous Petroleum System in the Danish Central Graben. Data available through a dedicated web portal service provided by GEUS.

The PETSYS Project (2014): The Jurassic Petroleum System in the Danish Central Graben. Data available through a dedicated web portal service provided by GEUS.

Thöle, H., Jähne-Klingberg, F., Bense, F., Doornenbal, H., den Dulk, M. & Britze, P. (2019): Deliverable 3.1 - State of the Art Report. GEOERA 3DGEO-EU; 3D Geomodeling for Europe; project number GeoE.171.005. Report, 50 p.

Thöle, H., Jähne-Klingberg, F., Doornenbal, H., den Dulk, M., Britze, P. & Jakobsen, F. (2020): Deliverable 3.5 – Harmonized seismic stratigraphic concepts – A base for consistent structural interpretations. GEOERA 3DGEO-EU; 3D Geomodeling for Europe; project number GeoE.171.005. Report, 82 p.

Thöle, H., Jähne-Klingberg, F., Doornenbal, H., den Dulk, M., Britze, P. & Jakobsen, F. (2021): Deliverable 3.6 – Harmonized time model of the Entenschnabel region. GEOERA 3DGEO-EU; 3D Geomodeling for Europe; project number GeoE.171.005. Report, 45 p.

Thöle, H. and Jähne-Klingberg, F (2021): Supporting document to Deliverable 3.8 – Discovery of structural elements and their uncertain limits in the southern and central North Sea. GEOERA 3DGEO-EU; 3D Geomodeling for Europe; project number GeoE.171.005. Report, 94 p.

van Buchem, F.S.P., Smit, F.W.H., Buijs, G.J.A., Trudgill, B. & Larsen, P.-H. (2017): Tectonostratigraphic framework and depositional history of the Cretaceous–Danian succession of the Danish Central Graben (North Sea) – new light on a mature area. Geological Society, London, Petroleum Geology Conference series, 8, 1: pp. 9-46. DOI:10.1144/pgc8.24

Van Daele, J., Dirix, K., Ferket, H. & R., Barros (2021): Lessons Learnt from the R2R (Roer-to-Rhine) case. GeoERA GeoConnect^{3}D Deliverable 5.2c. Horizon 20020 grant agreement number 731166, 58pp.

van Dalfsen, W., Doornenbal, J.C., Dortland, S. and Gunnink, J.L., (2006): A comprehensive seismic velocity model for the Netherlands based on lithostratigraphic layers. Geologie en Mijnbouw. Netherlands Journal of Geosciences, 85(4): 277-292.

Vejbaek, O.V. and Britze, P., (1994): Top pre-Zechstein: (two-way traveltime and depth, interval velocity and isochore). Kortserie / Danmarks Geologiske Undersøgelse ; 45. Danmarks Geolog. Undersøgelse.

Wong, T.E., Batjes, D.A.J. & De Jager, J. (Eds.) (2007): Geology of the Netherlands. 354 p.; Amsterdam (Royal Netherlands Academy of Arts and Sciences).

Wride, V.C. (1995): Structural features and structural styles from the Five Countries Area of the North Sea Central Graben. First Break, 13: pp. 395-407, 14 Abb.

Zehner, B. (2019): Deliverable 4.1 – State of the art in uncertainty visualization. GEOERA 3DGEO-EU; 3D Geomodeling for Europe; project number GeoE.171.005.

Ziegler, P.A. (1990): Geological Atlas of Western and Central Europe, 2nd and completely revised edition. 2nd and completely revised edition ed.: 239 p.; The Hague, Netherlands (Shell International Petroleum Maatschappi B.V.).

Zwaan, F., (2018): Lower Cretaceous reservoir development in the North Sea Central Graben, and potential analogue settings in the Southern Permian Basin and South Viking Graben. Geological Society, London, Special Publications 469, 479-504.

7.2 Structural Framework compiled

7.2.1 Cross-border overview

Brennand, T.P., Hoorn, B. Van and James, K.H. (1990): Historical review of North Sea exploration. Introduction to the Petroleum Geology of the North Sea, K.W. Glennie (ed.), 1-33. Blackwell Scientific Publications, Oxford.

Doornenbal, J.C. & Stevenson, A.G. (2010): Petroleum Geological Atlas of the Southern Permian Basin Area. 341 p.; Houten (EAGE Publications b.v. Houten).

Evans, D.J., Graham, C., Armour, A. & Bathurst, P. (2003): The Millennium Atlas: Petroleum geology of the central and northern North Sea. 390 p.; London (The Geological Society).

Glennie, K W. (1984): Introduction to the petroleum geology of the North Sea. United States: N. p., 1984. Web.

Kombrink, H. & Patruno, S. (2020): The integration of public domain lithostratigraphic data into a series of cross-border North Sea well-penetration maps. Geological Society, London, Special Publications, 494: pp. SP494-2020-25. DOI:10.1144/sp494-2020-25

Lyngsie, S.B., Thybo, H. & Rasmussen, T.M. (2006): Regional geological and tectonic structures of the North Sea area from potential field modeling. Tectonophysics, 413, 3-4: pp. 147-170.

Maystrenko, Y., Olesen, O., Ebbing, J. & Nasuti, A. (2017): Deep structure of the northern North Sea and south-western Norway based on 3D density and magnetic modeling. NORWEGIAN JOURNAL OF GEOLOGY, 97: pp. 169-210. DOI:10.17850/njg97-3-01

NOPEC (1988): North Sea Atlas - Major structural elements. map. [London] (NOPEC).

Patruno, S., Kombrink, H. & Archer, S.G. (2021): Cross-border megasequence stratigraphy of the Northern, Central and Southern North Sea: a comparative tectono-stratigraphic synthesis. Geological Society, London, Special Publications, 494: pp. SP494-2020-228. DOI:10.1144/sp494-2020-228

PGS Reservoir (2006): North Sea Digital Atlas - Version 2.06 (NSDA-2.06), Industrial report 2003, PGS Reservoir, Berks, UK.

7.2.2 Danish offshore

Andsbjerg, J. & Dybkjær, K. (2003): Sequence stratigraphy of the Jurassic of the Danish Central Graben. Geological Survey of Denmark and Greenland Bulletin, 1: pp. 265-300.

Cartwright, J.A. (1987): Transverse structural zones in continental rifts - an example from the Danish sector of the North Sea. (In: BROOKS & GLENNIE (Eds.): Petroleum Geology of North West Europe). pp. 441-452; London (Graham Trotman).

Cartwright, J.A. (1989): The kinematics of inversion in the Danish Central Graben. Geological Society, London, Special Publications, 44, 1: pp. 153-175. DOI:10.1144/gsl.sp.1989.044.01.10

Cartwright, J. (1990): The structural evolution of the Ringkøbing-Fyn High. (In: Blundell, D.J. & Gibbs, A.D. (Eds.): Tectonic evolution of the North Sea Rifts). pp. 200–216; London (Clarendon Press).

Clausen, O.R. & Pedersen, P.K. (1999): Late Triassic structural evolution of the southern margin of the Ringkobing-Fyn High, Denmark. (In: Pedersen, P.K. (Ed.): Marine and Petroleum Geology).Vol. 16: pp. 653-665; United Kingdom (Elsevier : Oxford, United Kingdom).

Duffy, O.B., Gawthorpe, R.L., Docherty, M. & Brocklehurst, S.H. (2013): Mobile evaporite controls on the structural style and evolution of rift basins: Danish Central Graben, North Sea. Basin Research, 25, 3: pp. 310-330.

Hansen, T.H., Clausen, O.R. & Andresen, K.J. (2021): Thick- and thin-skinned basin inversion in the Danish Central Graben, North Sea – the role of deep evaporites and basement kinematics. Solid Earth, 12, 8: pp. 1719-1747. DOI:10.5194/se-12-1719-2021

Jakobsen, F., Ineson, J.R., Kristensen, L. & Stemmerik, L. (2004): Characterization and zonation of a marly chalk reservoir: the Lower Cretaceous Valdemar Field of the Danish Central Graben. Petroleum Geoscience, 10, 1: pp. 21-33. DOI:10.1144/1354-079303-584

Jarsve, E.M., Maast, T.E., Gabrielsen, R.H., Faleide, J.I., Nystuen, J.P. & Sassier, C. (2014): Seismic stratigraphic subdivision of the Triassic succession in the Central North Sea; integrating seismic reflection and well data. Journal of the Geological Society. DOI:10.1144/jgs2013-056

Javed, M.A. (2012): Late Carboniferous-Early Permian structural development of the Ringkøbing-Fyn High and adjacent Norwegian-Danish Basin. Department of Geosciences, Master Thesis, Petroleumsgeologi og petroleumsgeofysikk [102]: p. 97; University of Oslo.

Kilhams, B., Stevanovic, S. & Nicolai, C. (2018): The 'Buntsandstein' gas play of the Horn Graben (German and Danish offshore): dry well analysis and remaining hydrocarbon potential. Geological Society, London, Special Publications, 469. DOI:10.1144/sp469.5

Klinkby, L., Balling, N. & J. Liboriussen (1997): A deep seismic reflection line in the Danish Central Graben. Bulletin of the Geological Society of Denmark, 44.

Møller, J.J. & Rasmussen, E.S. (2003): Middle Jurassic-Early Cretaceous rifting of the Danish Central Graben. (In: Ineson, J.R. & Surlyk, F. (Eds.): The Jurassic of Denmark and Greenland). Vol. 1. Geological Survey of Denmark and Greenland Bulletin: pp. 247-264; (Geological Survey of Denmark and Greenland Bulletin).

Petersen, H., Andsbjerg, J., Bojesen-Koefoed, J., Nytoft, H. & Rosenberg, P. (1998): Petroleum potential and depositional environments of Middle Jurassic coals and non-marine deposits, Danish Central Graben, with special reference to the S??gne Basin. Geol. Denm. Surv. Bull., 36.

Petersen, H.I., Nielsen, L.H., Bojesen-Koefoed, J.A., Mathiesen, A., Kristensen, L. & Dalhoff, F. (2008): Evaluation of the quality, thermal maturity and distribution of potential source rocks in the Danish part of the Norwegian–Danish Basin. Geological Survey of Denmark and Greenland Bulletin, 16: p. 27.

Petersen, H.I. & Jakobsen, F.C. (2021): Lithostratigraphic definition of the Upper Jurassic – lowermost Cretaceous (upper Volgian–Ryazanian) organic-rich and oil-prone Mandal Formation in the Danish Central Graben, North Sea. Marine and Petroleum Geology, 129: p. 105116. DOI:https://doi.org/10.1016/j.marpetgeo.2021.105116

Scheck, M., Thybo, H., Lassen, A., Abramovitz, T. & Laigle, M. (2002): Basement structure in the southern North Sea, offshore Denmark, based on seismic interpretation. Geological Society, London, Special Publications, 201, 1: pp. 311-326. DOI:10.1144/gsl.Sp.2002.201.01.15

Smit, F.W.H., van Buchem, F.S.P., Holst, J.C., Lüthje, M., Anderskouv, K., Thibault, N., Buijs, G.J.A., Welch, M.J. & Stemmerik, L. (2018): Seismic geomorphology and origin of diagenetic geobodies in the Upper Cretaceous Chalk of the North Sea Basin (Danish Central Graben). Basin Research, 30, 5: pp. 895-925. DOI:10.1111/bre.12285

Thybo, H. (2001): Crustal structure along the EGT profile across the Tornquist Fan interpreted from seismic, gravity and magnetic data. Tectonophysics, 334: pp. 155-190.

van Buchem, F.S.P., Smit, F.W.H., Buijs, G.J.A., Trudgill, B. & Larsen, P.-H. (2017): Tectonostratigraphic framework and depositional history of the Cretaceous–Danian succession of the Danish Central Graben (North Sea) – new light on a mature area. Geological Society, London, Petroleum Geology Conference series, 8, 1: pp. 9-46. DOI:10.1144/pgc8.24

Vejbaek, O.V. (1990): The Horn Graben and its relationship to the Oslo Graben and the Danish Basin. Tectonophysics, 178: pp. 29-49, 18 Abb.

Vejbaek, O.V. & Britze, P. (1994): Geological map of Denmark 1: 750 000, Top pre-Zechstein (two-way traveltime and depth). Ministry of Environment and Energy (DGU) Map series No. 45: pp. 1-3, 5 maps.

Vejbaek, O.V. (1997): Dybe strukturer i danske sedimentaere bassiner. Geologisk Tidsskrift, 4: p. 31.

Vejbaek, O.V. & Andersen, C. (2002): Post Mid-Cretaceous Inversion Tectonics in the Danish Central Graben – regionally synchronous tectonic events? Bulletin of the Geological Society of Denmark, 49: pp. 139-144.

Wride, V.C. (1995): Structural features and structural styles from the Five Countries Area of the North Sea Central Graben. First Break, 13: pp. 395-407, 14 Abb.

7.2.3 German offshore

Arfai & Jähne-Klingberg (2013): Depth & Thickness maps German Entenschnabel. https://www.gpdn.de/?pId=1591#p1591

Arfai, J., Jähne, F., Lutz, R., Franke, D., Gaedicke, C. & Kley, J. (2014): Late Palaeozoic to Early Cenozoic geological evolution of the northwestern German North Sea (Entenschnabel): New results and insights. Netherlands Journal of Geosciences, 93, 04: pp. 147-174. DOI:doi:10.1017/njg.2014.22

Baldschuhn, R., Binot, F., Fleig, S. & Kockel, F. (2001): Geotektonischer Atlas von Nordwest-Deutschland und dem deutschen Nordsee-Sektor. (Geologisches Jahrbuch). Vol. A: p. 88 S. mit 3 CD ROMs; Hannover (Schweizerbart´sche Verlagsbuchhandlung).

Best, G., Kockel, F. & Schöneich, H. (1983): Geological history of the southern Horn Graben. Geologie en Mijnbouw. Netherlands Journal of Geosciences, 62: pp. 25-33. DOI:10.1007/978-94-009-5532-5_2

Brückner-Röhling, S., Forsbach, H. & Kockel, F. (2005): The structural development of the German North Sea sector during the Tertiary and the Quaternary. Zeitschrift der Deutschen Gesellschaft für Geowissenschaften 156: pp. 341-355.

Jähne-Klingberg, F., Wolf, M., Steuer, S., Bense, F., Kaufmann, D. & Weitkamp, A. (2014): Speicherpotenziale Deutsche Nordsee. BGR. Geopotenzial Deutsche Nordsee: p. 110; Hannover.

Jürgens, U. & Schöneich, H. (1989): Darstellung und Benennung der Salzstrukturen in der Deutschen Nordsee. - Erdöl, Erdgas, Kohle, Petrochem., 105,1,: 10 - 11, 1 Abb.; Hamburg

Kilhams, B., Stevanovic, S. & Nicolai, C. (2018): The 'Buntsandstein' gas play of the Horn Graben (German and Danish offshore): dry well analysis and remaining hydrocarbon potential. Geological Society, London, Special Publications, 469. DOI:10.1144/sp469.5

Kockel, F., Baldschuhn, R., Best, G., Binot, F., Frisch, U., Groß, U., Jürgens, U., Röhling, H.-G. & Sattler-Kosinowski, S. (1991): Gaspotential Deutsche Nordsee - Structural Geology of the German North Sea Sector. Bundesanstalt für Geowissenschaften und Rohstoffe (BGR), Abschlussbericht ed.; Hannover.

Kockel, F. (1995): Structural and palaeogeographical development of the German North Sea sector. (In: Bender, F., Jacobshagen, V. & Lüttig, G. (Eds.): Beiträge zur regionalen Geologie der Erde). Vol. 26: p. 96; Berlin, Stuttgart (Gebrüder Bornträger).

TUNB (2020): The project "Potenziale des unterirdischen Speicher- und Wirtschaftsraumes im Norddeutschen Becken" - Structural model of the North German Basin

Wride, V.C. (1995): Structural features and structural styles from the Five Countries Area of the North Sea Central Graben. First Break, 13: pp. 395-407, 14 Abb.

7.2.4 Dutch offshore

Bouroullec, R., Verreussel, R.M.C.H., Geel, C.R., de Bruin, G., Zijp, M.H.A.A., Kőrösi, D., Munsterman, D.K., Janssen, N.M.M. & Kerstholt-Boegehold, S.J. (2018): Tectonostratigraphy of a rift basin affected by salt tectonics: synrift Middle Jurassic–Lower Cretaceous Dutch Central Graben, Terschelling Basin and neighbouring platforms, Dutch offshore. Geological Society, London, Special Publications, 469, 1: pp. 269-303. DOI:10.1144/sp469.22

DGM-deep V5 (2019): Two Way Time, Timethickness, Depth and Thickness grids of the Netherlands on- and offshore. https://www.nlog.nl/en/dgm-deep-v5-and-offshore

Duin, E.J.T., Doornenbal, J.C., Rijkers, R.H.B., Verbeek, J.W. and Wong, T.E. (2006): Subsurface structure of the Netherlands – results of recent onshore and offshore mapping. Netherlands Journal of Geosciences, 85(4): 245-276.

Geluk, M.C. (2007a): Permian. In: T.E. Wong, D.A.J. Batjes and J. de Jager (Editors), Geology of the Netherlands. Royal Netherlands Academy of Arts and Sciences, Amsterdam, pp. 63-84.

Geluk, M.C. (2007b): Triassic. In: T.E. Wong, D.A.J. Batjes and J. de Jager (Editors), Geology of the Netherlands. Royal Netherlands Academy of Arts and Sciences, Amsterdam, pp. 85-106.

Jeremiah, J., Duxbury, S. & Rawson, P. (2010): Lower Cretaceous of the southern North Sea Basins: reservoir distribution within a sequence stratigraphic framework. Netherlands Journal of Geosciences - Geologie en Mijnbouw, 89, 3-4: pp. 203-237.

Kombrink, H., Doornenbal, J.C., Duin, E.J.T., den Dulk, M., ten Veen, J.H. & Witmans, N. (2012): New insights into the geological structure of the Netherlands; results of a detailed mapping project. Netherlands Journal of Geosciences - Geologie en Mijnbouw, 91, 4: pp. 419-446. DOI:10.1017/S0016774600000329

ten Veen, J.H., van Gessel, S.F. & den Dulk, M. (2012): Thin- and thick-skinned salt tectonics in the Netherlands; a quantitative approach. Netherlands Journal of Geosciences, 91, 04: pp. 447-464. DOI:doi:10.1017/S0016774600000330

ter Borgh, M.M., Jaarsma, B. & Rosendaal, E.A. (2019): Structural development of the northern Dutch offshore: Paleozoic to present. Geological Society, London, Special Publications, 471, 1: pp. 115-131. DOI:10.1144/sp471.4

van der Molen, A.S. (2004): Sedimentary development, seismic stratigraphy and burial compaction of the Chalk Group in the Netherlands North Sea area. Dissertation, Utrecht University Faculty of Geosciences.

van Wijhe, D.H. (1987): Structural evolution of inverted basins in the Dutch offshore. Tectonophysics, 137, 1-4: pp. 171-175, 179-181, 185-187, 191-210, 213-219.

van Winden, M., de Jager, J., Jaarsma, B. & Bouroullec, R. (2018): New insights into salt tectonics in the northern Dutch offshore: a framework for hydrocarbon exploration. Geological Society, London, Special Publications, 469. DOI:10.1144/sp469.9

Wong, T.E., Batjes, D.A.J. & De Jager, J. (Eds.) (2007): Geology of the Netherlands. 354 p.; Amsterdam (Royal Netherlands Academy of Arts and Sciences).

Wride, V.C. (1995): Structural features and structural styles from the Five Countries Area of the North Sea Central Graben. First Break, 13: pp. 395-407, 14 Abb.

7.2.5 British offshore

Arsenikos, S., Quinn, M.F., Pharaoh, T., Sankey, M and Monaghan, A.A. (2015): Seismic interpretation and generation of key depth structure surfaces within the Devonian and Carboniferous of the Central North Sea, Quadrants 25 – 44 area. British Geological Survey Commissioned Report, CR/15/118. 67pp.

Arsenikos, S., Quinn, M., Kimbell, G., Williamson, P., Pharaoh, T., Leslie, G. & Monaghan, A. (2018): Structural development of the Devono-Carboniferous plays of the UK North Sea. Geological Society, London, Special Publications, 471, 1: pp. 65-90. DOI:10.1144/sp471.3

BGS (1985): Map 1: Pre-Permian Geology of the United Kingdom (south). Map 2." Contours on the top of the pre-Permian surface of the United Kingdom (south`). Scale 1:1000000. British Geological Survey.

Brackenridge, R.E., Jamieson, R. & J.R., Underhill (2018): Controls on the structure, stratigraphy and Prospectivity of the Mid North Sea High. Presentation PESGB/ Geological Society Collaboration Showcase, PETEX Tues 27th Nov 2018

Brackenridge, R.E., Underhill, J.R., Jamieson, R. & Bell, A. (2020): Structural and stratigraphic evolution of the Mid North Sea High region of the UK Continental Shelf. Petroleum Geoscience: pp. petgeo2019-076. DOI:10.1144/petgeo2019-076

Corfield, S., Moore, J., Bamford, M., Barnwell, A. & P. Barnard (2017): Hydrocarbon plays of the Mid North Sea High: an integrated seismic and basin modeling study. GWL - Geoscience Wales presentation. http://geoscience.wales/wp-content/uploads/2017/03/GWL-Talk-Jan-2017-for-website.pdf (last access 11.10.2021)

Coward, M.P. & Stewart, S.A (1995): Synthesis of salt tectonics in the southern North Sea, UK. Marine and Petroleum Geology, 12, 5: pp. 457-475.

GECO (1989): Tectonic Map of the North Sea and adjacent onshore areas. Scale 1 : 1 000 000.

George, G.T. & Berry, J.K. (1997): Permian (Upper Rotliegend) synsedimentary tectonics, basin development and palaeogeography of the southern North Sea. Geological Society, London, Special Publications, 123, 1: pp. 31-61. DOI:10.1144/gsl.Sp.1997.123.01.04

Grant, R.J., Underhill, J.R., Hernández-Casado, J., Jamieson, R.J. & Williams, R.M. (2019a): The evolution of the Dowsing Graben System: implications for petroleum prospectivity in the UK Southern North Sea. Petroleum Geoscience, 27, 1: pp. petgeo2018-064. DOI:10.1144/petgeo2018-064

Grant, R.J., Underhill, J.R., Hernández-Casado, J., Barker, S.M. & Jamieson, R.J. (2019b): Upper Permian Zechstein Supergroup carbonate-evaporite platform palaeomorphology in the UK Southern North Sea. Marine and Petroleum Geology, 100: pp. 484-518. DOI:https://doi.org/10.1016/j.marpetgeo.2017.11.029

Grant, R.J., Booth, M.G., Underhill, J.R. & Bell, A. (2020): Structural evolution of the Breagh area: implications for carboniferous prospectivity of the Mid North Sea High, Southern North Sea. Petroleum Geoscience, 26, 2: pp. 174-203. DOI:10.1144/petgeo2019-100

Haarhoff, M.Q., Hughes, F., Heath-Clarke, M., Harrison, D., Taylor, C., Ware, D.L., Emms, G.G. & Mortimer, A. (2018): The history of hydrocarbon exploration and development in North Yorkshire. Geological Society, London, Special Publications, 465, 1: pp. 119-136. DOI:10.1144/sp465.12

Monaghan, A.A., Arsenikos, S., Quinn, M.F., Johnson, K.R., Vincent, C.J., Vane, C.H., Kim, A.W., Uguna, C.N., Hannis, S.D., Gent, C.M.A., Millward, D., Kearsey, T.I. & Williamson, J.P. (2017): Carboniferous petroleum systems around the Mid North Sea High, UK. Marine and Petroleum Geology, 88: pp. 282-302. DOI:https://doi.org/10.1016/j.marpetgeo.2017.08.019

Oil & Gas Authority: https://www.ogauthority.co.uk/

Patruno, S., Reid, W., Jackson, C.A.-L. & Davies, C. (2018): New insights into the unexploited reservoir potential of the Mid North Sea High (UKCS quadrants 35–38 and 41–43): a newly described intra-Zechstein sulphate–carbonate platform complex. Geological Society, London, Petroleum Geology Conference

Sharp, R., Adam, J., Scarselli, N. & Morse, S. (2016): Thick vs thin-skinned deformation of the Sole Pit High (UK Southern North Sea Basin) and its impact on the evolution of supra-salt prospectivity. Extended Abstract - Geol. Soc. London Conference: Mesozoic Resource Potential in the Southern Permian Basin, September 2016

Stewart, S.A. (2007): Salt tectonics in the North Sea Basin: a structural style template for seismic interpreters. (In: Ries, A.C., Butler, R.W.H. & Graham, R.H. (Eds.): Deformation of the Continental Crust: The Legacy of Mike Coward). 272: pp. 361-396; London (Geological Society Special Publication).

Tectonic Map of Britain (1996). Tectonic map of Britain, Ireland and adjacent areas. Sheet 1. 1:1 500 000 series. Published 1996. Print code 96/5000 Map Viewer: https://largeimages.bgs.ac.uk/iip/mapsportal.html?id=1004599

UK National Data Repository: https://ndr.ogauthority.co.uk/

Van Hoorn, B. (1987): Structural evolution, timing and tectonic style of the Sole Pit inversion. Tectonophysics, 137, 1-4: pp. 239-284. DOI:10.1016/0040-1951(87)90322-2

Wride, V.C. (1995): Structural features and structural styles from the Five Countries Area of the North Sea Central Graben. First Break, 13: pp. 395-407, 14 Abb.

8 APPENDIXES

8.1 Appendix A: Uncertainties in definition of Structural Framework domain borders – the example of the Northern Coffee Soil fault / Schillgrund Fault system

Fig. A-1
spread of fault-interpretation of the Coffee Soil Fault / Schillgrund Fault from over-regional structural maps

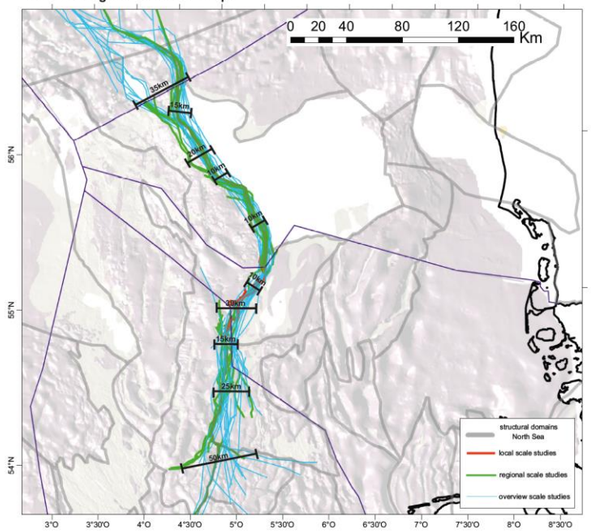

Fig. A-2
spread of hanging wall & footwall interpretation of the Coffee Soil Fault / Schillgrund Fault from over-regional structural maps

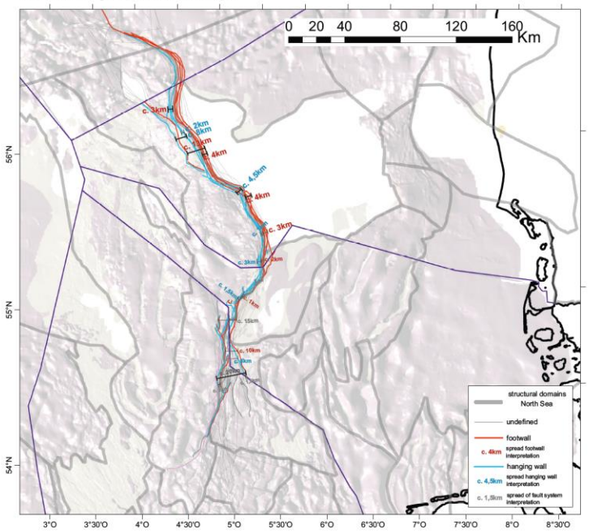

Fig. A-3
spread of fault-interpretation of the Coffee Soil Fault / Schillgrund Fault:
comparison of all scales of studies for the Danish Central Graben

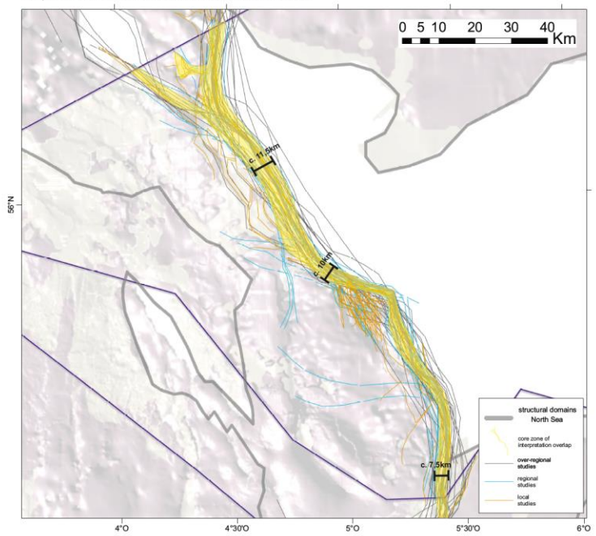

References:

Fig. A-1 & A-2 (A-3): used over-regional fault maps Central Graben

- NOPEC (1988)
- Jürgens & Schöneich (1989)
- Brennand et al. (1990)
- Ziegler (1990)
- Pharaoh (1999)
- Evans et al. (2003)
- Cloetingh et al. (2005)
- PGS Reservoir (2006)
- Kley et al. in Littke et al. (2008)
- Doornenbal & Stevenson (2010)
- Kombrink et al. (2012)
- TNO Focus - Bouroullec et al. (2016b)
- Zwaan (2018)
- NPD (2019)

Fig. A-1 & A-2 (A6-3): used regional fault maps Central Graben

GER:
- Baldschuhn et al. (2001)
- Arfai et al. (2014)

NL:
- Wong (2007)
- TNO - Bruin et al. (2015)
- TNO COMMM - Bouroullec et al. (2016a)
- ter Borgh et al. (2019)
- HIKE fault data - the Netherlands (2021)

cross-border:
- Evans et al. (2003)
- PGS Reservoir (2006)
- Kombrink et al. (2012)

Fig. A-4 & A-3: used regional fault maps Danish Central Graben

- Cartwright (1987)
- Andsbjerg & Dybkjaer (2003)
- Japsen et al. (2003)
- Møller, J.J. & Rasmussen, E.S. (2003)
- Klinkby et al. (2005) after Britze et al. (1995)
- Nøjd (2016) after Sundsbo & Megson (1993)
- van Buchem et al. (2017) after Japsen et al. (2003)
- Smit et al. (2018)

Fig. A-5 & A6-3 : used local fault maps & data Danish Central Graben

GEUS: Post Chalk fault shape
GEUS: Chalk Group fault shape

GEUS - Cretsys Project (2017): Top Chalk
GEUS - Cretsys Project (2017): Base Chalk
GEUS - Cretsys Project (2017): BCU

DGU map serie no. 49: Lower Cretaceous Cromer Knoll Group
DGU map serie no. 50: Upper Jurassic
DGU map serie no. 45: Top Pre-Zechstein

GEUS - Petsys Project: BCU faults
GEUS - Petsys Project: Volgian faults
GEUS - Petsys Project: Kimmeridgian faults
GEUS - Petsys Project: Top Middle Jurassic faults
GEUS - Petsys Project: Base Jurassic/Top Triassic faults

Fig. A-4
spread of hanging wall & footwall interpretation of the Coffee Soil Fault / Schillgrund Fault from regional structural maps

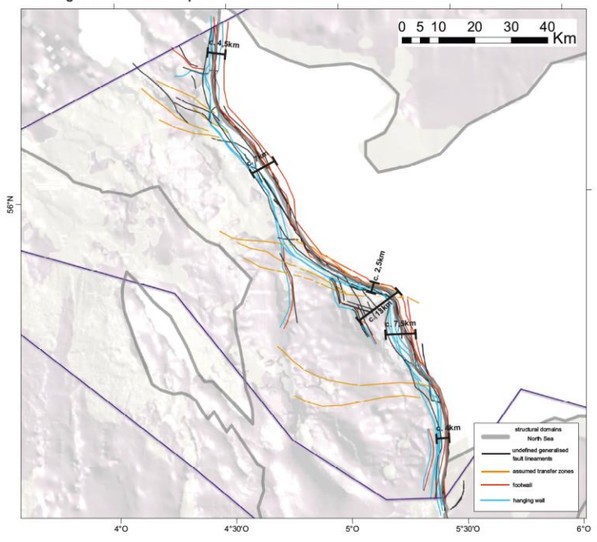

Fig. A-5
spread of interpretation of the Coffee Soil Fault / Schillgrund Fault from regional to local fault data

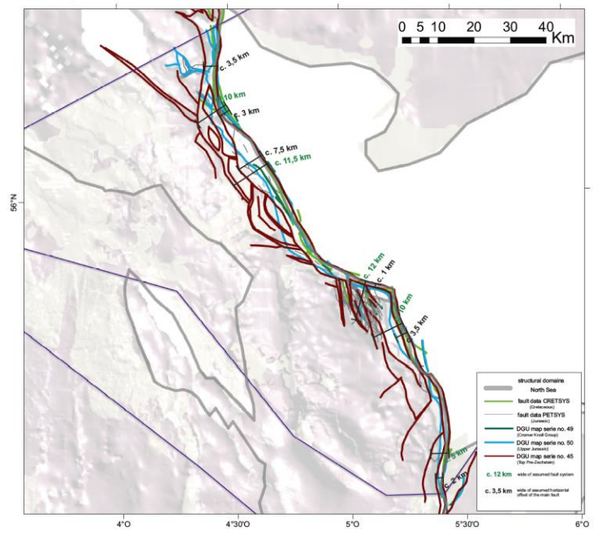

Fig. A-6
hanging wall & footwall interpretation of the Coffee Soil Fault / Schillgrund Fault based on different horizons (on the example of the German Entenschnabel)

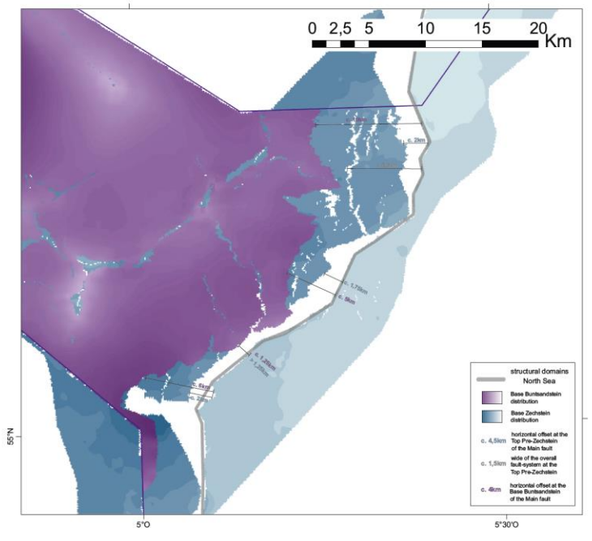

Fig. A-6: used local fault map & data German Central Graben

Arfai et al. (2014)
Arfai & Jähne-Klingberg (2014)

Figure Caption:

Figure A6.1 to A6.5 show the differences of fault interpretations of the Coffee Soil fault from several References which describe the structure in different scales. The background show a grid-compilation of the Base Zechstein (beige) and Base Triassic (baby pink). The figures each highlight different aspects of conceptual fuzziness & structural uncertainty. Figure A-6 illustrates the geologic conceptual challenges in defining a structural domain boundary that exist independent of an excellent interpretive base, using the Schillgrund fault in the German section of the Central Graben as an example.

8.2 Appendix B: Analysis of References for a Structural Framework of the central and southern North Sea

structural overview maps	short Reference	importance of Reference or Data Source for development of Post-Permian multi-scale Structural Framework of the DK, GER, NL North Sea area	GRIDS or maps (Depth, Traveltime or Thickness Maps)	structural map (detailed/local scale)	structural map (regional scale)	structural map (overview scale)	section maps & seismic / geological sections	Main focus of the study
cross-border overview								
	Glennie (1984)	middle	no	no	no	yes	yes/both	North Sea overview
	NOPEC (1988)	middle	no	no	no	yes	no	North Sea overview
	Brennand et al. (1990)	high	no	no	no	yes	no	North Sea overview
	Evans et al. (2003)	high	maps	yes	yes	yes	yes/both	Central to Northern North Sea (UK, NO, DK)
	Lyngsie et al. (2006)	high	no	no	no	yes	no	North Sea overview: potential field data
	Maystrenko et al. (2017)	middle	no	no	no	yes	no	North Sea overview: potential field data
	Kombrink & Patruno (2020)	low	no	no	no	yes	no	North Sea overview
	Patruno et al. (2021)	middle	no	no	no	yes	yes/both	North Sea overview
	Doornenbal & Stevenson (2010)	high	digital data & maps	yes	yes	yes	yes/both	Southern Permian Basin
	PGS Reservoir (2006)	high	digital data & maps	no	no	yes	no	North Sea overview
DK								
	Cartwright (1987)	high	maps	no	yes	no	yes/both	Danish Central Graben
	Cartwright (1989)	high	maps (Upper Cretaceous)	no	yes	no	yes/both	Danish Central Graben
	Cartwright (1990)	middle	?	no	yes	?	?	Ringkøbing-Fyn High
	Vejbaek (1990)	middle	maps (Top Pre-Zechstein)	no	?	yes	geological profiles	Danish Horn Graben and surrounding
	Vejbaek & Britze (1994)	high	maps (Top Pre-Zechstein)	no	no	yes	no	national scale Danish offshore
	Wride (1995)	high	no	no	yes	?	yes/both	Entenschnabel
	Klinkby et al. (1997)	low	no	no	yes	no	yes	Danish Central Graben
	Vejbaek (1997)	high	maps (Top-Pre-Zechstein)	no	yes	yes	yes/both	national scale Danish offshore
	Petersen et al. (1998)	low	no	no	yes	no	no	Danish Central Graben
	Clausen & Pedersen (1999)	middle	no	no	no	no	yes	Ringkøbing-Fyn High
	Thybo (2001)	low	no	no	no	yes	yes	eastern North Sea: deep refraction seismic
	Scheck et al. (2002)	middle	map (TWT near basement reflection)	no	no	no	yes	East North Sea High & Horn Graben
	Vejbaek, O.V. & Andersen, C. (2002)	high	maps (Cretaceous)	no	yes	no	yes/both	Danish Central Graben
	Andsbjerg, J. & Dybkjær, K. (2003)	middle	maps (Jurassic)	no	yes	no	no	Danish Central Graben
	Møller & Rasmussen (2003)	middle	maps (Jurassic)	no	yes	no	yes/both	Danish Central Graben
	Jakobsen et al. (2004)	low	map (Cretaceous)	yes	yes	no	no	Danish Central Graben
	Petersen et al. (2008)	low	map (Base Zechstein)	no	yes	yes	geological profiles	national scale Denmark
	Javed (2012)	high	maps (NoDaB & ENSH)	no	yes	no	yes	East North Sea High - Ringkøbing-Fyn High
	Duffy et al. (2013)	middle	maps	yes	yes	no	yes/both	Danish Central Graben: salt tectonics
	Jarsve et al. (2014)	low	maps (Triassic)	no	yes	yes	yes	Danish-Norwegian Basin
	van Buchem et al. (2018)	high	maps (Cretaceous)	no	yes	no	yes	Danish Central Graben
	Kilhams et al. (2018)	middle	map (Buntsandstein)	no	yes	yes	yes/both	Horn Graben & surrounding
	Smit et al. (2018)	low	no	no	yes	no	yes	Danish Central Graben: Chalk
	Hansen et al. (2021)	middle	maps	yes	yes	no	yes/both	Danish Central Graben
	Petersen & Jakobsen (2021)	low	maps	no	yes	no	yes	Danish Central Graben: Jurassic & Cretaceous

PART 1 of 3

structural overview maps	short Reference	importance of Reference or Data Source for development of Post-Permian multi-scale Structural Framework of the DK, GER, NL North Sea area	GRIDS or maps (Depth, Traveltime or Thickness Maps)	structural map (detailed/local scale)	structural map (regional scale)	structural map (overview scale)	section maps & seismic / geological sections	Main focus of the study
GER								
	Best et al. (1983)	low	no	no	yes	no	geological profiles	Horn Graben and surrounding
	Jürgens, U. & Schöneich, H. (1989)	high	no	no	yes	no	no	Central German North Sea
	Kockel et al. (1991)	low	no	no	yes	no	no	Central German North Sea
	Kockel (1995)	middle	no	no	yes	no	no	Central German North Sea (without Entenschnabel)
	Wride (1995)	high	no	no	yes	no	yes	Entenschnabel
	Baldschuhn et al. (2001)	high	digital data & maps (Zechstein - Tertiary)	no	yes	yes	geological profiles	Central German North Sea & western North German Basin
	Brückner-Röhling et al. (2005)	low	maps (Tertiary)	no	yes	no	no	Central German North Sea (without Entenschnabel)
	Arfai et al. (2014)	high	maps (Zechstein - Tertiary)	no	yes	no	geological profiles	Entenschnabel
	Jähne-Klingberg et al. (2014)	middle	maps	yes	yes	no	yes	Central German North Sea
	Kilhams et al. (2018)	middle	map (Buntsandstein)	no	yes	yes	yes/both	Horn Graben & surrounding
	Arfai & Jähne-Klingberg (2013)	high	digital data (Zechstein - Tertiary)	no	no	no	no	Entenschnabel
	TUNB (2020)	middle	digital data (Zechstein - Tertiary)	no	no	no	no	North German Basin & German Entenschnabel
NL								
	Van Wijhe (1987)	high	no	no	no	yes	no	Dutch offshore and surrounding
	Wride (1995)	high	no	no	yes	?	yes/both	Entenschnabel
	van der Molen (2004)	middle	maps (Chalk Group)	no	no	yes	yes	Dutch offshore: Chalk
	Geluk (2007)	middle	no	no	no	yes	no	Dutch on- & offshore
	Geluk (2007)	middle	maps (Triassic)	no	no	yes	yes	Dutch on- & offshore
	Wong et al. (2007)	middle	maps	yes	yes	yes	yes/both	Dutch on- & offshore
	Jeremiah et al. (2010)	low	no	no	yes	no	yes	Dutch offshore and surrounding: Lower Cretaceous
	Kombrink et al. (2012)	middle	maps	no	yes	yes	no	Dutch offshore
	ten Veen et al. (2012)	middle	no	no	yes	yes	yes	the Netherlands (Focus offshore)
	van Winden et al. (2018)	low	map (Top Zechstein Group)	no	yes	no	yes/both	northern Dutch offshore (Central Graben region and surrounding)
	Bouroullec et al. (2018)	low	?	no	yes	no	yes	Dutch northern offshore: Jurassic - Lower Cretaceous
	ter Borgh et al. (2019)	high	no	no	yes	no	yes	Dutch offshore (Step Graben & Central Graben)
	Duin et al. (2006)	high	digital data & maps	no	no	yes	geological profiles	Dutch on- & offshore
	DGM-deep V5 (2019)	high	digital data (Zechstein - Tertiary)	no	no	no	no	Dutch on- & offshore

PART 2 of 3

structural overview maps	short Reference	importance of Reference or Data Source for development of Post-Permian multi-scale Structural Framework of the DK, GER, NL North Sea area	GRIDS or maps (Depth, Traveltime or Thickness Maps)	structural map (detailed/local scale)	structural map (regional scale)	structural map (overview scale)	section maps & seismic / geological sections	Main focus of the study
UK								
	BGS (1985)	low	maps (Pre-Permian)	no	yes	no	no	Central British North Sea
	Van Hoorn (1987)	high	maps	no	yes	yes	yes	Southern North Sea
	GECO (1989)	low	no	no	no	?	no	British North Sea
	Coward & Stewart (1995)	middle	no	no	yes	no	yes	Silverpit Basin / Sole Pit Trough / Dowsing Fault Zone
	Tectonic Map of Britain (1996)	middle	no	no	yes	no	no	Tectonic Map of Britain on- & offshore
	George & Berry (1997)	middle	no	no	yes	no	no	Southern British North Sea
	Stewart (2007)	low	map (Zechstein)	no	yes	yes	yes	salt tectonics: British Southern and Central North Sea
	Underhill et al. (2009)	low	maps (detailed region)	yes	no	yes	yes/both	SE Sole Pit/ Cleaver Bank High/ Broad Fourteens Basin
	Arsenikos et al. (2015)	middle	maps (Pre-Permian)	no	yes	no	yes	Pre-Zechstein: Central British North Sea & Orcadian Basin
	Sharp et al. (2016)	low	no	no	yes	no	yes	Southern British North Sea
	Corfield et al. (2017)	low	no	no	yes	?	yes	Central British North Sea - Pre-Zechsteon structural Framework
	Monaghan et al. (2017)	low	no	no	no	yes	no	Pre-Zechstein: Central British North Sea
	Arsenikos et al. (2018)	low	maps (Pre-Permian)	no	yes	yes	yes/both	Pre-Zechstein: Central British North Sea & Orcadian Basin
	Brackenridge et al. (2018)	middle	maps	no	yes	no	yes	Central British North Sea overview
	Haarhoff et al. (2018)	low	no	no	no	yes	no	Pre-Zechstein Southern British North Sea
	Patruno et al. (2018)	low	maps (detailed region)	no	?	yes	yes/both	Zechstein - Central British North Sea
	Grant et al. (2019a)	high	maps (detailed region)	yes	yes	yes	yes/both	focus on Dowsing fault zone
	Grant et al. (2019b)	low	maps (detailed region)	yes	yes	yes	yes/both	focus on SW rim Sole Pit (Zechstein Layer)
	Patruno et al. (2019)	middle	maps	no	yes	yes	yes/both	Pre-Zechstein - Central British North Sea (partly Southern British North Sea)
	Brackenridge et al. (2020)	high	maps	no	yes	no	yes/both	Central British North Sea overview
	Grant et al. (2020)	high	maps (detailed region)	yes	yes	yes	yes/both	focus on Silverpit Basin
	Oil & Gas Authority	high	digital data	no	no	yes	yes	Gis Data & seismic, well datasets
	UK National Data Repository	high	digital data	no	no	yes	yes	geophysical data

PART 3 of 3

8.3 Appendix C: Top Pre-Zechstein structure represented in different scales

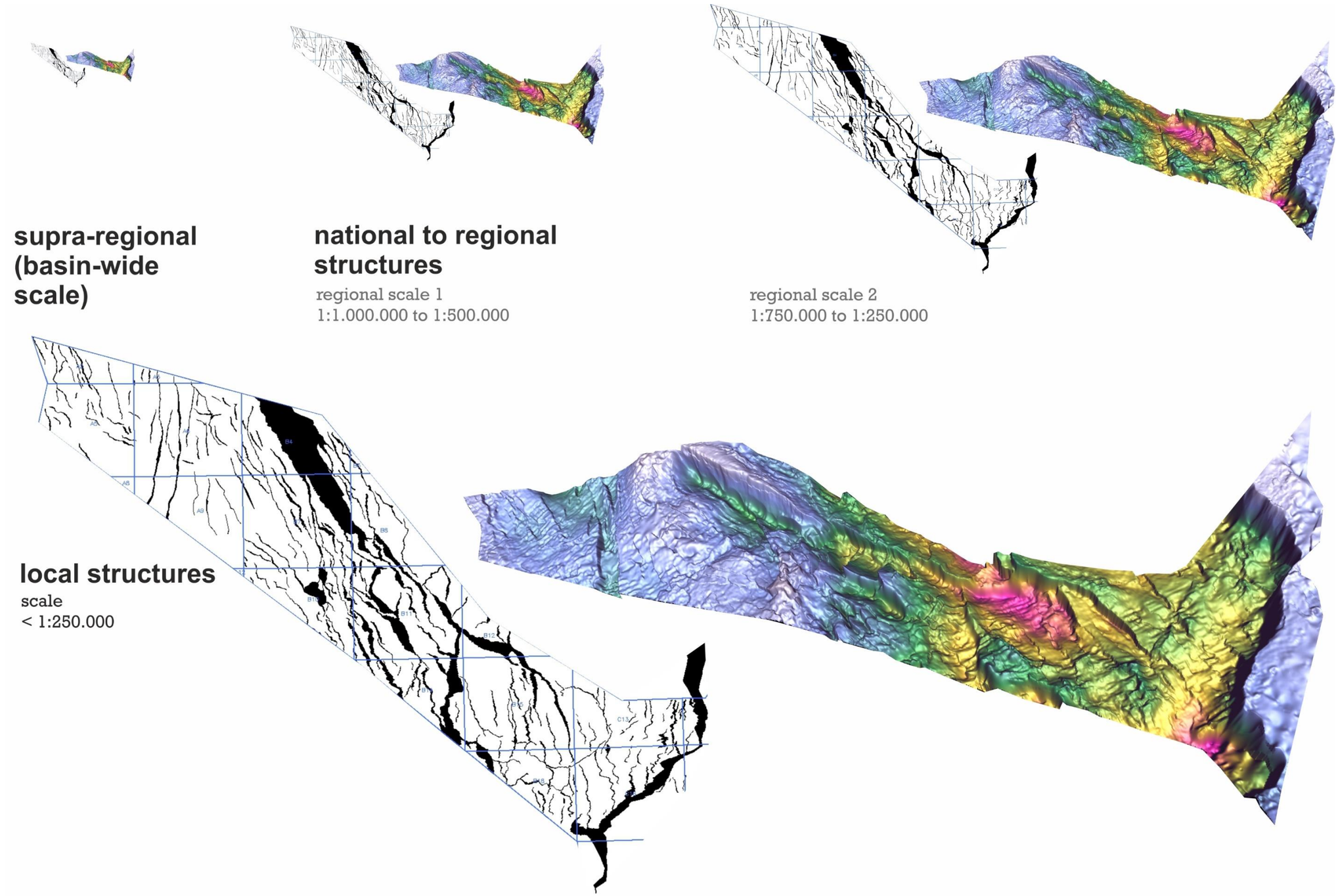

Top Pre-Zechstein fault map (2d view with fault offsets) & horizont map (Top Pre-Zechstein isometric view) in different scales

8.4 Appendix D: Structural Framework – comparison of different mapping scales – the example of the German Entenschnabel (based on Top Pre-Zechstein topography)

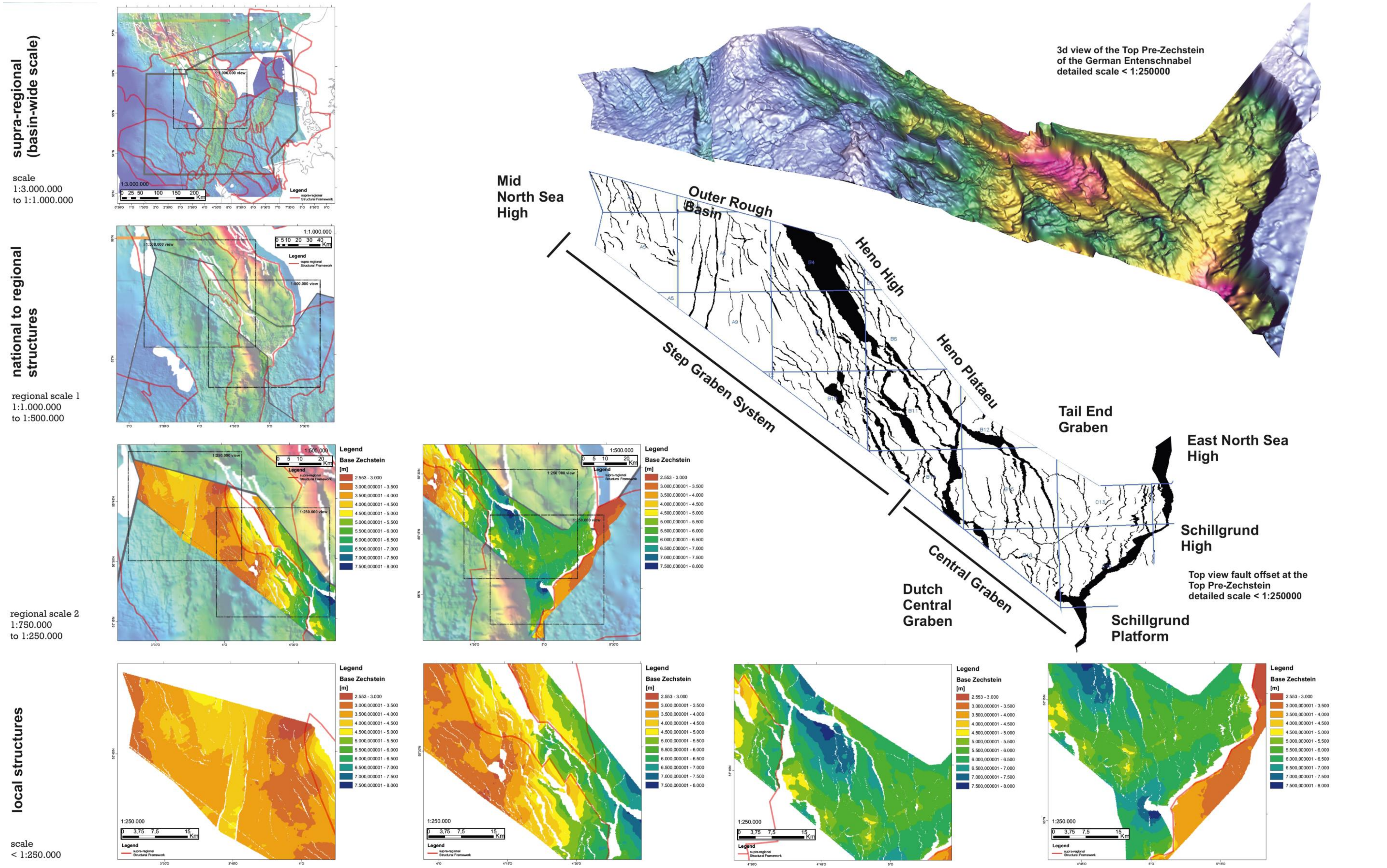

8.5 Appendix E: the structure & multiphase tectonic evolution of the North Sea Central Graben – the example of the German Entenschnabel

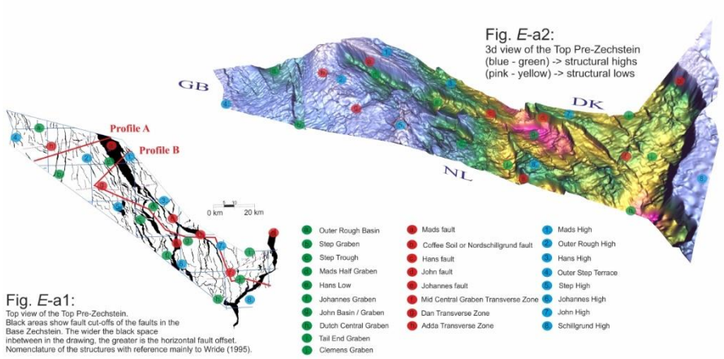

Fig. *E*-a2:
3d view of the Top Pre-Zechstein
(blue - green) -> structural highs
(pink - yellow) -> structural lows

Fig. *E*-a1:
Top view of the Top Pre-Zechstein.
Black areas show fault cut-offs of the faults in the Base Zechstein. The wider the black space inbetween in the drawing, the greater is the horizontal fault offset.
Nomenclature of the structures with reference mainly to Wilde (1995).

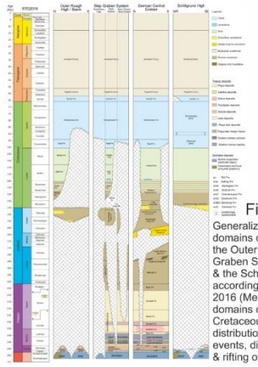

Fig. *E*-b:
Generalized lithostratigraphic charts of structural domains of the German Entenschnabel: the Outer Rough High/Basin, the Step Graben System, the German Central Graben & the Schillgrund High. Time scale and ages according to the Stratigraphic Table of Germany 2016 (Menning & Hendrich, 2016). The structural domains differ especially in the Triassic to Cretaceous development. Thus, thickness and facies distribution can be explained by a variety of erosional events, differential subsidence, salt tectonics & rifting of different intensity

Influence of mobilized Zechstein rock-salt on sedimentation and erosion in the overburden Mesozoic to Cenozoic rocks

Fig. *E*-c1:

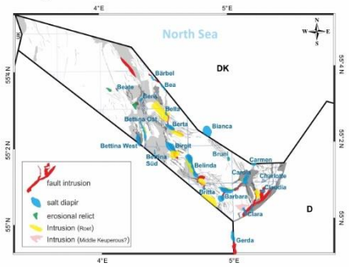

The Zechstein salt is a prominent detachment horizon in Western European basins. Under changing tectonic settings rock salt of the Zechstein was mobilized, provided that a pressure gradient existed. The related deformation of the overburden partly initialized diapirism. Salt withdrawal or inflow of rock-salt strongly affected, the subsidence or uplift pattern of the overburden sediments. Most of the salt structures in the study area (Fig. *E*-c1) are within the Central Graben structure (Central Graben & Step Graben domain). To the northwest, lower initial thicknesses of the Zechstein (Fig. *E*-c2) and a change in the rock lithology prevent the formation of salt diapirs and the use of the Zechstein as a detachment. There thick-skinned tectonic is the dominant structural style (Fig. *E*-d: Profile A). At the Outer Rough Basin, Mads High and on the Schillgrund High most of the Triassic to Jurassic sediments are eroded (Fig. *E*-e2). There Upper Jurassic sediments cover a deeply eroded Zechstein (Fig. *E*-e3).

Fig. *E*-c1: map of the Zechstein salt structures in the German Entenschnabel area. In addition to the salt structures, the fault patterns in the Keuper and Jurassic are also shown in summary form. In comparison with the fault patterns in the Top pre-Zechstein (Fig. *E*-a1), there are partly enormous differences as a result of varying degrees of thin-skinned or thick-skinned tectonics across the region.

Fig. *E*-c2: map of the German Entenschnabel with the Zechstein salt thickness

Fig. *E*-c2:

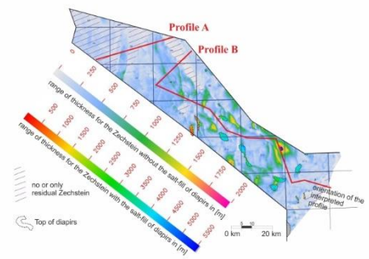

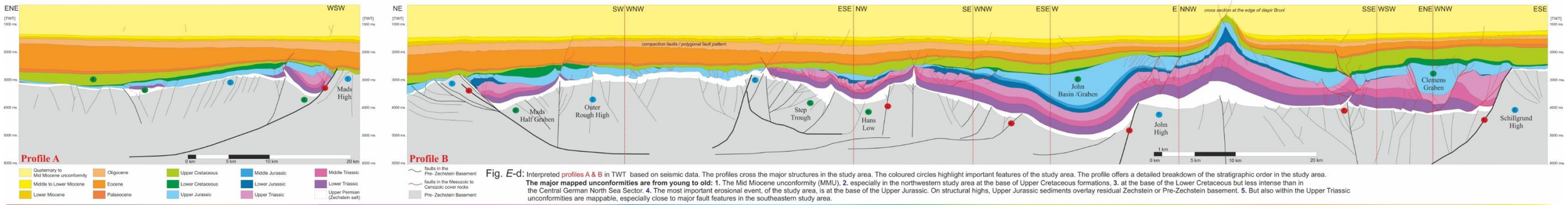

Fig. *E*-d: Interpreted profiles A & B in TWT based on seismic data. The profiles cross the major structures in the study area. The coloured circles highlight important features of the study area. The profile offers a detailed breakdown of the stratigraphic order in the study area.
The major mapped unconformities are from young to old: 1. The Mid Miocene unconformity (MMU), **2.** especially in the northwestern study area at the base of Upper Cretaceous formations, **3.** at the base of the Lower Cretaceous but less intense than in the Central German North Sea Sector. **4.** The most important erosional event, of the study area, is at the base of the Upper Jurassic. On structural highs, Upper Jurassic sediments overlay residual Zechstein or Pre-Zechstein basement. **5.** But also within the Upper Triassic unconformities are mappable, especially close to major fault features in the southeastern study area.

structural pre-cursor or pre-existing structural features of the region | **Initial rifting of the Central Graben during the Triassic** | **Reorganisation and reactivation of structures and a changing subsidence pattern in the Jurassic** | **Late Cretaceous to Palaeocene contraction with reactivation and structural inversion of structures** | **Increased subsidence of the North Sea Basin during the Palaeogene**

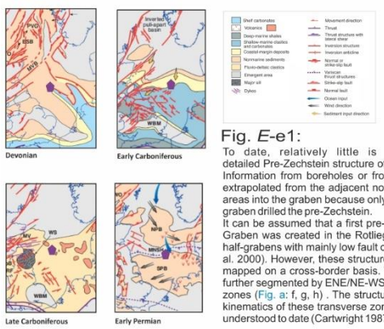

Fig. *E*-e1:
To date, relatively little is known about the detailed Pre-Zechstein structure of the Central Graben. Information from boreholes or from seismic is usually extrapolated from the adjacent not so deeply subsided areas into the graben because only few boreholes in the graben drilled the pre-Zechstein.
It can be assumed that a first pre-cursor of the Central Graben was created in the Rotliegend (small grabens/ half-grabens with mainly low fault offsets) (Stemmerik et al. 2000). However, these structures have not yet been mapped on a cross-border basis. The Pre-Zechstein is further segmented by ENE/NE-WSW/SW striking cross-zones (Fig. a: f, g, h) . The structural development and kinematics of these transverse zones is also not clearly understood to date (Cartwright 1987, Wride 1995).

Palinspastic maps of the North Sea for: Devonian times, Early Carboniferous times, Late Carboniferous times & Early Permian times (edited after Evans et al., 2003).

Fig. *E*-e2:
First extensional pulses took place in the Lower Triassic followed by several phases of rifting from the Middle to Late Triassic. The age of rifting phases can be defined by thickening of syn-tectonic Triassic towards the major fault zones (Fig. c).

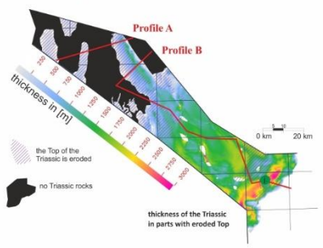

Fig. *E*-e3:
During the Upper Jurassic a major extensional phase took place in combination with extensive diapirism. Analyses of the distribution and the thicknesses of sediments in rim-synclines reveal that most of the salt structures inside the Central Graben had a main phase of growth during the Late Jurassic (Fig. *E*-c). Especially in the John Basin and in the Clemens Graben very thick Upper Jurassic strata is conserved as a result of high subsidence maybe caused by salt tectonic.

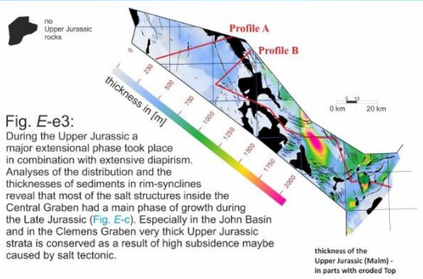

Fig. *E*-e4:
Greatest thicknesses of the Upper Cretaceous are reached on the eastern graben shoulder of the Central Graben along the Schillgrund High in the foreland of the inverted Nordschillgrund faultzone. The subsidence along this long-living Triassic to Jurassic structural high is not only controlled by thrusting along the Nordschillgrund fault (Fig. *E*.-a & *E*-d). The reason for the formation of a wide basin in the Upper Cretaceous on the Schillgrund High has to be investigated.

First results suggests that the greatest amount of contraction and inversion during the Late Cretaceous was accumulated along the eastern border fault of the Central Graben (Nordschillgrund fault or coffee soil fault).

The inversion or reactivation are related to pre-existing Triassic to Jurassic faults (zones of weakness) like the Clemens Graben (Fig. *E*-a & *E*-d ; j.) and the Mid Central Graben Transverse Zone (Fig. *E*-a & *E*-c; f.).

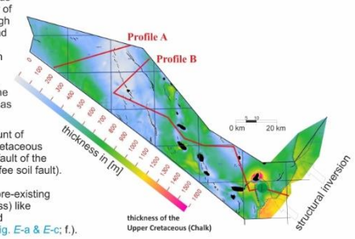

References:

Cartwright, J.A. (1987):
Transverse structural zones in continental rifts - an example from the Danish sector of the North Sea.
(In: BROOKS & GLENNIE (Eds.): Petroleum Geology of North West Europe). pp. 441-452; London (Graham Trotman).

Evans, D.J., Graham, C., Armour, A. & Bathurst, P. (2003):
The Millennium Atlas: Petroleum geology of the central. The Geological Society of London, 989 pp.

Stemmerik, L., Ineson, J.R. & Mitchell, J.G. (2000):
Stratigraphy of the Rotliegend Group in the Danish part of the Northern Permian Basin, North Sea. Journal of the Geological Society, 157, 6: pp. 1127-1136. DOI:10.1144/jgs.157.6.1127

Wride, V.C. (1995):
Structural features and structural styles from the Five Countries Area of the North Sea Central Graben. First Break, Vol 13, No 10.

Fig. *E*-e5: With the end of the Palaeocene, the inversion tectonic ended and the influence of the Atlantic rift increased. A change in the depositional trend towards the central North Sea developed. The region around the North Sea Dome, in the Jurassic and Lower Cretaceous an area of extensive uplift, changes to a region with high subsidence rates.

- some diapirs in the Central Graben are still active.
But for the most of them substantial movements of rock salt ceased in the Upper Cretaceous to Lower Palaeogene

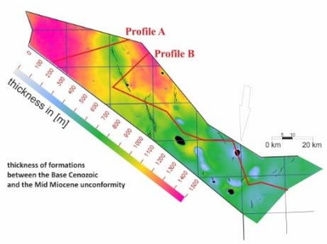

8.6 Appendix F: Structural Framework in different scales & nomenclature adapted to it – the example of the German Entenschnabel (based on Top Pre-Zechstein topography)

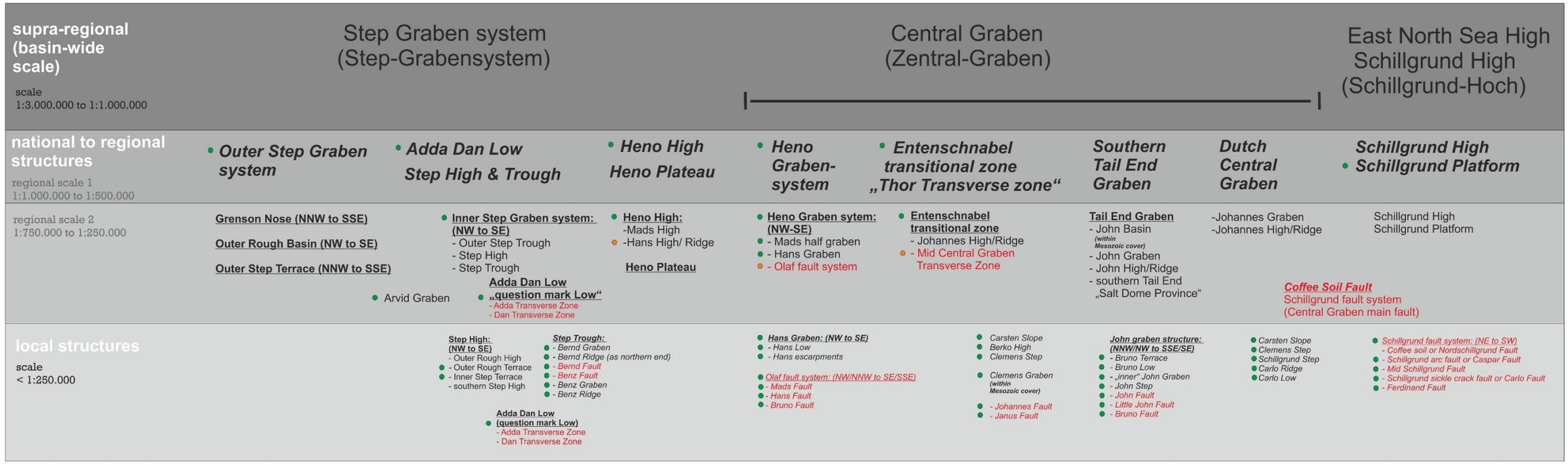

8.7 Appendix G: Nomenclature for a detail Structural Framework – the example of the German Entenschnabel